1985

An Anatomical and Physiological Investigation of the Infralimbic Region of the Rat Medial Frontal Cortex

Robert T. Terreberry
Loyola University Chicago

AN ANATOMICAL AND PHYSIOLOGICAL INVESTIGATION OF THE INFRALIMBIC REGION OF THE RAT MEDIAL FRONTAL CORTEX

by

Robert R. Terreberry

A Dissertation Submitted to the Faculty of the Graduate School of Loyola University of Chicago in Partial Fulfillment of the Requirements for the Degree of Doctor of Philosophy

October

1985

DEDICATION

To my family

ACKNOWLEDGMENTS

I would like to thank my advisor Dr. E.J. Neafsey for his support, guidance, enthusiasm and insight which made this work possible. I would also like to thank the other members of the dissertation committee, Dr. T.S. Gray, Dr. C.C.C. O'Morchoe, Dr. R.S. Swenson and Dr. R.D. Wurster for their helpful and critical evaluation of this dissertation work. Finally, I would like to thank all the faculty, staff and students of the Department of Anatomy of Loyola University Medical Center for their support and encouragement during my tenure in the department.

VITA

The author, Robert R. Terreberry, is the son of Robert G. and Bette Terreberry. He was born on May 20, 1958 in Chicago, Illinois.

His secondary education was obtained at Wheeling High School in Wheeling, Illinois, which he graduated from in June, 1976. In September of 1976 he entered Illinois Benedictine College in Lisle, Illinois and graduated with a Bachelor of Science degree in Biology in May of 1980. In August of 1980, he entered the Department of Anatomy of the Graduate School at Loyola University of Chicago. While ar Loyola, he received a Basic Science Fellowship and taught in the gross anatomy, histology and neuroscience courses. In 1984 he received a University Dissertation Fellowship. He is a member of the Society for Neuroscience, the American Association of Anatomists and the Society of Sigma XI.

In November of 1985, he will begin a post-doctoral fellowship in the Department of Anatomy of the University of California Los Angeles under the supervision of Dr. Ronald M. Harper.

TABLE OF CONTENTS

LIST OF ABBREVIATIONS

ac	anterior commissure
AC	anterior cingulate cortex
ACd	anterior cingulate cortex, dorsal division
ACv	anterior cingulate cortex, ventral division
AgM	agranular medial cortex
AM	anteromedial thalamic nucleus
AP	area postrema
AV	anteroventral thalamic nucleus
BLa	basolateral nucleus amygdala
BM	basomedial nucleus amygdala
CA1	field CA1 of Ammon's horn (hippocampus)
CA2	field CA2 of Ammon's horn (hippocampus)
CA3	field CA3 of Ammon's horn (hippocampus)
CC	corpus callosum
Ce	central nucleus amygdala
Cem	centromedial thalamic nucleus
CG	central gray
CL	centrolateral thalamic nucleus
CLi	caudal linear raphe nucleus
CP	cerebral peduncle
Cun	nucleus cuneiformis
Dk	nucleus Darkschewitsch
dlNTS	dorsolateral nucleus solitary tract
DMN	deep mesencephalic nucleus
DMN X	dorsal motor nucleus vagus
DPB	dorsal parabrachial nucleus
DPC	dorsal peduncular cortex
dPSR	dorsal parasolitarius region
DR	dorsal raphe
DTg	dorsal tegmental nucleus of Gudden
ECN	external cuneate nucleus
F	fornix
fc	fasciculus cuneatus
FR	fasciculus retroflexus
GN	nucleus gracilis
ic	internal capsule
IC	inferior colliculus
icp	inferior cerebellar peduncle
IL	infralimbic cortex
INC	interstitial nucleus Cajal
iNTS	interstitial nucleus solitary tract
INTS	intermediate nucleus solitary tract
IO	inferior olive
La	lateral nucleus amygdala
LC	locus coeruleus

LD	lateral dorsal thalamic nucleus
LDTg	lateral dorsal tegmental nucleus
LGD	lateral geniculate, dorsal
LGV	lateral geniculate, ventral
LH	lateral hypothalamus
LP	lateral posterior thalamic nucleus
LPO	lateral preoptic area
lPSR	lateral parasolitarius region
LR	lateral reticular nucleus
LV	lateral vestibular nucleus
mes 5	mesencephalic trigeminal nucleus
MD	mediodorsal thalamic nucleus
MGD	medial geniculate, dorsal
MGM	medial geniculate, magnocellular
MH	medial habenular nucleus
ml	medial lemniscus
MnR	median raphe nucleus
mNTS	medial nucleus solitary tract
MS	medial septum
mtt	mammillothalamic tract
mV	motor trigeminal nucleus
MV	medial vestibular nucleus
NA	nucleus ambiguus
NC	nucleus cuneatus
NTS	nucleus solitary tract
oc	optic chiasm
OT	optic tract
PBN	parabrachial nuclei
PC	posterior commissure
Pc	paracentral thalamic nucleus
Pf	parafascicular nucleus
PGi	paragigantocellular reticular nucleus
PL	prelimbic cortex
Pn	pontine nuclei
PnO	pontine reticular nucleus, oralis
PO	posterior thalamic nucleus
PrH	nucleus prepositus hypoglossi
PRT	pretectum
Pt	parataenial thalamic nucleus
pV	principal sensory trigeminal nucleus
PV	paraventricular thalamic nucleus
py	pyramidal tract
pyx	decussation pyramidal tract
R	thalamic reticular nucleus
Re	reuniens thalamic nucleus
Rh	rhomboid thalamic nucleus
RMg	nucleus raphe magnus

RN	red nucleus
RPn	nucleus raphe pontis
SC	superior colliculus
scp	superior cerebellar peduncle
SG	supragenículate nucleus
sm	stria medullaris
SM	submedius thalamic nucleus
SNc	substantia nigra, pars compacta
SNr	substantia nigra, pars reticulata
sPf	subparafascicular nucleus
spV	spinal trigeminal nucleus
SpVe	spinal vestibular nucleus
st	stria terminalis
Str	striatum
SV	superior vestibular nucleus
ts	solitary tract
tt	taenia tecta
VB	ventrobasal thalamic nucleus
VDBV	ventral division, vertical nucleus diagonal band
VL	ventrolateral thalamic nucleus
vlNTS	ventrolateral nucleus solitary tract
VM	ventromedial thalamic nucleus
vNTS	ventral nucleus solitary tract
VP	ventral pallidum
VPB	ventral parabrachial nucleus
vPSR	ventral parasolitarius region
VTA	ventral tegmental area
VII	facial motor nucleus
xscp	decussation superior cerebellar peduncle
XII	hypoglossal nucleus
ZI	zona incerta
3V	third ventricle
4V	fourth ventricle

LIST OF FIGURES

CHAPTER VI:

CHAPTER VII

LIST OF TABLES

CHAPTER I

INTRODUCTION

In 1937 James Papez proposed that "the cortex of the cingular gyrus may be looked on as the receptive region for the experiencing of emotion ... Radiation of the emotive process from the gyrus cinguli to other regions in the cerebral cortex would add emotional colouring to psychic processes." Papez theorized that the hypothalamus, the anterior thalamic nuclei, the gyrus cinguli, the hippocampus and their connections constituted a harmonious mechanism which could elaborate the functions of central emotion, the Papez circuit. MacLean (1952) broadened the concept of the Papez circuit to include additional structures and named the resulting complex the "limbic system." MacLean (1949) felt that certain aspects of the "limbic system" dealt not only with emotional states but with visceral functions as well. His concept of the limbic system as the "visceral brain" suggested an explanation of the commonly observed interaction between emotional states and visceral autonomic functions. Until recently, however, this concept of a "visceral brain" has been somewhat forgotten, perhaps due to interest in limbic system functions in learning and memory (Seifert, 1983). However, recent anatomical and physiological studies indicate that the cingulate cortex may well be a key component of the "visceral brain."

There have numerous studies done on the effects of electrical stimulation of the cingulate cortex on autonomic functions (see Kaada, 1951; 1960; Lofving, 1961; Hoff et al., 1963 for reviews). The types of responses seen after stimulation of the anterior cingulate cortex

(AC) ranged from alterations in cardiovascular functions, respiration and gastric motility to pupillary responses (see Kaada, 1960). Recently, several studies have shown that electrical stimulation of homologous regions of the rodent frontal cortex elicits a similar spectrum of autonomic responses (Burns et al., 1983; Terreberry and Neafsey, 1984; Burns and Wyss, 1985).

Until recently however, the possible neuroanatomical pathways by which these responses were mediated remained unknown. Studies by van der Kooy et al. (1982, 1984) and Terreberry and Neafsey (1983) have demonstrated a direct descending projection from the infralimbic (IL) and prelimbic (PL) region of the rat medial frontal cortex to the nucleus of the solitary tract in the dorsomedial medulla. Thus, an anatomical basis for these cortically-evoked responses may have been provided.

CHAPTER II

REVIEW OF LITERATURE

Central Visceral Control: A Brief Historical Review

The concept that metabolic, secretory, cardiovascular and other visceral as well as skeletal motor activities are integrated at various levels of the central nervous system, including the cerebral cortex, has been proposed for over one hundred years. The idea was first presented by Hughlings Jackson (1875) who expressed the conviction that not only are voluntary movements of the body represented in the cerebrum, but the movements of arteries and viscera as well. Within a few years of Jackson's observations, experiments studying higher regulation of cardiovascular activity in animals measured heart rate and arterial blood pressure changes evoked by electrical stimulation of exposed cortical surfaces. The first direct evidence that modification of autonomic function can originate from experimental electrical stimulation of the isocortex was provided almost simultaneously by Schiff (1875) and Danilewsky (1875). Schiff reported acceleration of the heart after stimulation of the cortex in dogs, and Danilewsky reported rises in arterial blood pressure with slowing of the heart after stimulating the cortex in the region around the suprasylvian sulcus in dogs. In spite of these results and the results of numerous other early investigators (see Hoff et al., 1963 for further review of early studies), the role of the cerebral cortex in the regulation of autonomic activity was by no means fully established, widely accepted or well understood. One criticism of these early studies was that the effects seen from cortical

stimulation may have been due to current spread to subcortical structures (e.g., the hypothalamus). Thus, the pathways by which these cortical autonomic reponses were mediated were poorly understood, and the emphasis in research on central autonomic control shifted to subcortical controlling systems.

In the early 1900's, the hypothalamus was identified as a major visceromotor region (Karplus and Kreidl, 1910). From this early work, the central visceromotor system became conceived as consisting essentially of the hypothalamus and its neural connections with the preganglionic motor neurons (see Nauta, 1972). The hypothalamus was considered to be the "head ganglion" of the autonomic nervous system (Fulton, 1946) and was also thought to be the effector mechanism of visceral changes related to emotional expression (MacLean, 1949). In 1937 that James Papez proposed that the hypothalamus, the anterior thalamic nuclei, the gyrus cinguli, the hippocampus and their connections constituted an anatomical circuit which could elaborate the functions of central emotion, the so called "Papez circuit". MacLean (1952) broadened the concepts of the Papez circuit to include additional structures and termed the resulting complex the "limbic system". MacLean (1949) felt that certain elements of the limbic system besides the hypothalamus dealt not only with emotion but with visceral functions as well, and he viewed the limbic system as the organism's "visceral brain". In recent years this concept of the limbic system as the "visceral brain" has been somewhat neglected,

with greater emphasis being placed on the role of the limbic system in memory and motivation (Swanson, 1983).

Cortical Control of Autonomic Function: Medial Frontal/Anterior Cingulate Stimulation Studies

Electrical stimulation of the medial frontal-anterior cingulate (MFC) cortex has elicited complex somatomotor, autonomic (cardiovascular, respiratory, gastric motility and pupillary responses) and behavioral effects. Only the cardiovascular and respiratory responses will be discussed in the present account. The reader is referred to Kaada (1960) for further discussion of the other somatomotor, autonomic and behavioral responses elicited from this cortical region.

Cardiovascular Responses

It is well-established that the cardiovascular system can be influenced from the motor, premotor and other cortical areas outside those discussed in the present account (see Kaada, 1960). Spencer (1894) was the first to report arterial pressure alterations on excitation of the orbital surface of the frontal lobe. Smith (1944, 1945) evoked similar responses from the rostral portions of the cingulate and hippocampal gyri, and Kaada et al. (1949) reported similar responses from the anterior insular and temporal polar cortex in monkeys. These findings have been confirmed and further analyzed

in various species of animals. Rises as well as falls in arterial pressure have been recorded in the cat, dog, monkey and most recently rat on stimulating the anterior cingulate cortex (Smith, 1945; Kremer, 1947; Kaada et al., 1949; Speakman and Babkin, 1949; Kaada, 1951; Anand and Dua, 1956; Kaada, 1960; Lofving, 1961; Burns et al., 1983; Burns and Wyss, 1985). Similar effects have been obtained in man from the anterior cingulate cortex (Pool and Ransohoff, 1949).

The character of the response seems to depend on two factors. The first is the site of stimulation in the cortex. Pressor and depressor points have been located only a few millimeters apart. However, usually one type of response predominates from all points within a given area under the same experimental conditions. In the same animal the orbital surface and olfactory tubercle may yield opposite effects (Sachs et al., 1949), and the same may be true when comparing the posterior orbital surface and the temporal pole (Wall and Davis, 1951). Lofving (1961) reported that a depressor response was elicited from the dorsal portions of the anterior cingulate region, while a pressor response was elicited from a more ventral area of the anterior cingulate cortex. Burns et al. (1983) and Burns and Wyss (1985) reported that depressor responses could be elicited from the pre- and infralimbic regions of the rat MFC, while the caudal one-third of the anterior cingulate cortex elicit pressor responses (Burns and Wyss, 1985). The second factor influencing the response to stimulation is the level and type of anesthesia. Deepening the

anesthetic sometimes seems to favor depressor responses (Kaada, 1951); furthermore, under curare (Sachs et al., 1949) light ether (Bailey et al., 1943; Anand and Dua, 1956), pentabarbitol (Bailey and Sweet, 1940) or thiopental (Livingston et al., 1948; Chapman et al., 1950) anesthesia, pressor responses predominate on stimulation of the orbital surface whereas depressor responses are usually seen under diallyl barbituric acid (Dial) anesthesia (Delgado and Livingston, 1948; Sachs et al., 1949).

The arterial pressure effects are not secondary to the associated respiratory changes (Smith, 1945; Sachs et al., 1949; Chapman et al., 1950; Kaada, 1951), and there is no constant relationship between the direction of the respiratory and arterial pressure responses (Smith, 1945; Sachs et al., 1949; Kaada, 1951). Bilateral vagotomy abolishes or greatly reduces the depressor responses from the anterior cingulate cortex (Smith, 1945; Speakman and Babkin, 1949; Kaada, 1951). On the other hand, the pressor responses persist after vagotomy (Speakman and Babkin, 1949; Babkin and Speakman, 1950; Kaada, 1951). Since some fall in arterial pressure still may be obtained after bilateral vagotomy (Sachs et al., 1949; Kaada, 1951; Hoffman and Rasmussen, 1953), a dilation of the peripheral blood vessels through some extravagal route must also be assumed to occur. According to Sachs et al. (1949) arterial pressure changes (and respiratory arrest) persist after bilateral cervical vagotomy, splanchnicectomy and adrenalectomy, and after destruction of the hypothalamic paraventricular nuclei.

physostigmine prolongs the cardiac inhibition from the anterior cingulate and pyriform cortex (Smith, 1945).

Little is known regarding the descending pathways mediating the arterial pressure effects to the cardiovascular centers of the lower brain stem. A drop in arterial pressure has been obtained from a zone extending from the genual portion of the anterior cingulate cortex and through the septal, preoptic, hypothalamic and mesencephalic areas (Kabat et al., 1935). This "path" appears to coincide closely with that yielding inhibition of cortically and reflexly induced movements and respiration (see below). According to Wall and Davis (1951), the anterior cingulate cortex may possibly influence arterial pressure by a mechanism dependent on the anterior temporal lobe. Section of the fornix (Kaada, 1951) and pyramidal tract (Wall and Davis, 1951) leave the arterial pressure responses induced from the medial and basal cortical areas unaltered. Recent studies have revealed a direct descending projection from the rat MFC to the NTS in the dorsomedial medulla, and this pathway may be involved in mediating the autonomic effects seen after electrical stimulation of the MFC (van der Kooy et al., 1982, 1984; Terreberry and Neafsey, 1983).

Respiratory Responses

One of the most striking effects of the stimulation of the anterior cingulate cortex on the medial surface and the orbitoinsular cortex is the profound inhibition of respiratory movements. In 1945

Smith first reported the respiratory inhibitory effect exerted by the anterior cingulate cortex in the monkey. Tower (1936), working with lightly anesthetized cats, had previously included this region in her frontal inhibitory field which also comprised the entire gyrus proreus. The respiratory response from the anterior cingulate has been studied in the cat (Hodes and Magoun, 1942; Speakman and Babkin, 1949; Dunsmore and Lennox, 1950; Kaada, 1951; Anand and Dua, 1956), dog (Kremer, 1947; Clark, 1949; Speakman and Babkin, 1949; Kaada, 1951), monkey (Ward, 1948; Kaada et al., 1949; Kaada, 1951; Showers and Crosby, 1958) and man (Pool and Ransohoff, 1949; Liberson, 1951; Kaada and Jasper, 1952).

In the monkey the inhibitory area on the medial surface appears to correspond closely to the agranular anterior cingulate region. The responsive field extends through the subcallosal region towards the ventromedial edge of the frontal lobe where it seems to be continuous with the respiratory inhibitory area of the posterior orbital surface of the frontal lobe (Kaada et al., 1949; Kaada, 1951). There is an area with optimal effects in the region surrounding the genu of the corpus callosum (Kaada, 1951).

The inhibition obtained from these cortical regions concerns the active phase of the respiratory cycle, i.e. inspiration, with the chest assuming an expiratory position during the period of apnea. Variations in the stimulus parameters do not alter the character of the response, and no frequency-conditioned reversal of the respiratory

effects has been produced from these cortical areas in monkeys (Kaada, 1951).

In the cat and dog, as in monkeys, the optimal inhibitory zone on the medial surface is found just in front of and below the genu of the corpus callosum (Hodes and Magoun, 1942; Speakman and Babkin, 1949; Kaada, 1951). Weaker effects only are evoked from the rest of the anterior cingulate and subcallosal (infralimbic) cortex as depicted by Rose and Woolsey (1948). The effect has also been obtained in unanesthetized dogs and cats by stimulation through implanted electrodes (Clark et al., 1949; Kaada, 1951; Anand and Dua, 1956). The usual type of inhibitory response in cats and dogs to stimulation of these cortical areas is similar to that seen in monkeys; i.e. arrest in expiration.

Cytoarchitecture of Medial Frontal Cortex

The medial frontal cortex (MFC) of the rat is defined as that area of the neocortex on the medial aspect of the hemisphere rostral to the retrosplenial cortex and extending to the frontal pole. The following description of the cytoarchitecture of this cortical region is based on the architectonic maps of Krettek and Price (1977a), Zilles et al. (1980) and Vogt and Peters (1981) for the rat; M. Rose (1927) and Wree et al. (1983) for the mouse; and Brodmann (1909) and Rose and Woolsey (1948) for the rabbit (see Table 1, Figure 1), and on the examination of Nissl stained material (Figure 2).

Table 1 is an attempt to summarize and correlate the various studies on MFC cytoarchitecture. In recent studies (Krettek and Price, 1977a; Zilles et al., 1980; Vogt and Peters, 1981; Wree et al., 1983), there has been basic agreement as to the subdivisions of the MFC, although the names and extent of each show some variation (Table 1, Figures 1B-E). The cytoarchitectonic pattern we have delineated for the present study (Figure 1A) is in close agreement with that of Krettek and Price (1977a) and consists of four distinct areas termed the agranular medial (AgM), anterior cingulate (AC), prelimbic (PL) and the infralimbic (IL) regions. The earlier cytoarchitectonic studies of the MFC done by Brodmann (1909), M. Rose (1927) and Rose and Woolsey (1948) are also consistent with this scheme (Figures 1F-H, Table 1). M. Rose (1927) described six subdivisions within the MFC (IRcα, IRcβ, IRbα, IRbβ, IRaα, IRaβ). Four of these areas (IRcα, IRcβ , IRbβ, IRaβ) coincide with the dorsal and ventral divisions of the anterior cingulate cortex (ACd, ACv) described by Krettek and Price (see Figures 1B,F). Rose's areas IRbα and IRaα coincide with the PL and IL regions of MFC described by Krettek and Price (1977a). Brodmann's (1909) scheme included an area 23 (Figure 1G) which corresponds to the caudal portions of the ACd and ACv. Rose and Woolsey (1948) saw only four MFC sudivisions (Figure 1H), with their area La corresponding to rostral ACd, ACv and PL.

The ventrally located allocortical taenia tecta (tt, Figures 2A-C) has a conspicuous, densely packed layer II that easily

distinguishes it from the more dorsal IL cortex. Haberly and Price (1978) term this region the ventral taenia tecta (vtt), as opposed to the dorsal taenia tecta (dtt) which is situated ventral to the genu of the corpus callosum. The vtt is thought to be of olfactory origin, while the dtt is thought to be a direct rostral continuation of the hippocampal formation (Haberly and Price, 1978; Wyss and Sripanidkulchai, 1983). Haberly and Price (1978) also described a small, restricted area immediately dorsal to the vtt that has extensive reciprocal connections with the entorhinal cortex. They termed this region the dorsal peduncular cortex (DPC, Figures 2A,B). The DPC has a compact layer II and less compact layer III.

The infralimbic area, area 25 (IL, Figures 2A-C) lies immediately dorsal to the DPC/vtt and is characterized by a relatively indistinct laminar pattern (layers II and III are indistinguishable) and a very uneven border between layer I and layer II. The prelimbic area, area 32 (PL, Figures 2A-C) is dorsal to the IL and is characterized by a well defined laminar pattern. Layer II is prominent and even, while layer III shows pale, lightly stained neurons that are less densely packed than those in the adjacent lamina. Layer V contains large dark staining cells and layer VI is composed of horizontally elongated cells tightly packed into two thin layers.

The anterior cingulate area (AC) is subdivided into dorsal and ventral subdivisions. The dorsal subdivision (ACd, Figures 2A-D)

corresponds to the dorsal subdivision (ACd) of Krettek and Price (1977a) and area 24b of Vogt and Peters (1981). This area shows a thinner layer I as opposed to layer I of the IL or PL cortex, layer II is more densely packed than layer II of the PL cortex and the neurons are heavily stained while layer III is sparse. A broad, less densely packed layer V is also characteristic of this cortical subdivision. The ventral subdivision (ACv, Figure 1B; 24a, Figure 1D) of the AC region lies just dorsal to the corpus callosum and is similar to ACd but ACd has broader layers V and VI than does the ACv region.

On the dorsomedial edge of the hemisphere is a region termed the medial precentral area (Krettek and Price, 1977a) or the agranular medial area (AgM, Donoghue and Wise, 1982). This region is characterized by a dense layer II and a relatively pale, less densely packed layer III. Leonard (1969) referred to this region as the "shoulder cortex," and it has been thought to correspond to the frontal eye fields (Hall and Lindholm, 1974; Sinnamon and Galer, 1984).

To summarize the cytoarchitecture of the rodent MFC, there are four main neocortical subdivisions: the agranular medial (AgM), anterior cingulate (AC), prelimbic (PL) and infralimbic (IL) areas. The allocortical taenia tecta (tt) bounds the MFC ventrally.

Anatomical Studies of MFC Connections

Little was known of the afferent projections to the medial

frontal cortex (MFC) of the rat until the work of Leonard (1969). In that study, Leonard demonstrated, with the use of Fink-Heimer degeneration techniques, that the mediodorsal (MD) thalamic nucleus projected to an area of the medial aspect of the hemisphere roughly corresponding to Brodmann's areas 24 and 32 and to the insular cortex forming the dorsal bank of the rhinal fissure. Since that study, a variety of techniques have been used to demonstrate the major afferents from the thalamus, basal forebrain, and brainstem (see Kolb, 1984 for review of these studies).

The MFC has been shown to receive afferent input from the basal forebrain (Lamour et al., 1984), the hippocampus (Swanson and Cowan, 1977; Swanson, 1981) and the insular cortex (Saper, 1982a; Markowitsch and Guldin, 1983). Thalamic imputs to the MFC include projections from the midline and mediodorsal nuclei (Domesick, 1969, 1972; Leonard, 1969; Beckstead, 1976; Krettek and Price, 1977a; Herkenham, 1979). The basolateral amygdala also has direct projections to the MFC (Krettek and Price, 1977b; Price, 1981). Brainstem afferents to the MFC include projections from the A9 and A10 dopaminergic cells in the substantia nigra and the ventral tegmental area (Lindvall et al., 1974; Fallon and Moore, 1978a) and the parabrachial nuclei in the pons (Fulwiler and Saper, 1984).

Our knowledge of the efferent connections of the rat MFC is largely limited to two silver degeneration studies (Domesick, 1969; Leonard, 1969), an autoradiographic tracing study (Beckstead, 1979)

and a few studies of specific projections (Kita and Oomura, 1982; van der Kooy et al., 1982, 1984; Wyss and Sripanidkulchai, 1984). Many of the projections from the MFC reciprocate the afferent projections to the MFC; for example, the insular cortex, the basolateral amygdala, mediodorsal thalamic nucleus and the ventral tegmental area all have reciprocal connections with the MFC. In addition, several areas that do not project to the MFC do receive projections from the MFC. These include the central gray (Wyss and Sripanidkulchai, 1984), the superior colliculus (Hardy and Leichnetz, 1981; Wyss and Sripanidkulchai, 1984), the pontine gray (Wyss and Sripanidkulchai, 1984) and the NTS (van der Kooy et al., 1982, 1984; Terreberry and Neafsey, 1984). However, most of these studies examined the afferent and efferent connections of the anterior cingulate and prelimbic areas of the MFC; few studies examined the connections of the infralimbic cortex.

Central Autonomic Centers

Within the brain several areas are concerned with modulating automomic functions; these include the insular cortex, the hypothalamus, the amygdala, the parabrachial nuclei, the nucleus of the solitary tract, the dorsal motor nucleus of the vagus and the nucleus ambiguus. The neuroanatomical connections and functional considerations of each of these areas will be briefly addressed.

The insular cortex, located along the banks of the rhinal sulcus

on the lateral aspect of the rodent brain, has been implicated in the integration and regulation of gustatory and autonomic activities (Saper, 1982a; Shipley, 1982; Shipley and Sanders, 1982; Shipley and Geinisman, 1984). Several recent studies have demonstrated connections between the insular cortex and the medial portion of the mediodorsal thalamic nucleus (Gerfen and Clavier, 1979; Mraovitch et al., 1982a; Saper, 1982a; Guldin and Markowitsch, 1983; Sarter and Markowitsch, 1983) and the medial aspect of the ventrobasal thalamic nucleus (Mraovitch et al., 1982a; Saper, 1982a; Shipley and Geinisman, 1984). The insular cortex also has connections with the lateral hypothalamus (Kita and Oomura, 1981, 1982; Mraovitch et al., 1982; Saper, 1982a), the basolateral amygdala (Krettek and Price, 1977b; Gerfen and Clavier, 1979, Saper, 1982a; Sarter and Markowitsch, 1983) and the central nucleus of the amygdala (Ottersen, 1981, 1982; Saper, 1982a). The parabrachial nucleus in the pons has been shown to have extensive reciprocal connections with the insular cortex (Saper and Loewy, 1980; Saper, 1982a,b; Shipley and Sanders, 1982; Fulwiler and Saper, 1984; Yasui et al., 1985). The insular cortex also has been shown to project directly to the NTS in the dorsomedial medulla (Mraovitch et al., 1982a; Saper, 1982a; Shipley, 1982; van der Kooy et al., 1982, 1984).

The insular cortex has been referred to as a "visceral sensory" cortex due to the fact it is the site where gustatory taste afferent information terminates (Benjamin and Pfaffmann, 1955; Benjamin and

Akerts, 1959; Norgren and Wolf, 1975; Yamamoto et al., 1980; Shipley and Geinisman, 1984; Yamamoto, 1984). Shipley and Geinisman (1984) have suggested that pathways subserving olfactory, gustatory and visceral sensory modalities converge in the insular cortex in mice, suggesting the importance of the cortical integration of this sensory information in food selection and autonomic reactions related to the chemical senses. In addition to subserving taste and gustatory information, the insular cortex has also been shown to be concerned with cardiovascular regulation. Electrical stimulation of the insula elicits a pressor response accompanied by an increase in heart rate (Mraovitch et al., 1982a).

The paraventricular nucleus of the hypothalamus (PVN) has been shown to have reciprocal connections with the nucleus of the solitary tract (Conrad and Pfaff, 1976; Saper et al., 1976; Ricardo and Koh, 1978; Calaresu and Ciriello, 1980). Direct projections from the PVN to the intermediolateral cell column in the thoracic spinal cord have also been demonstrated (Saper et al., 1976). Stimulation of the PVN results in increases in arterial pressure and heart rate in bilaterally vagotomized cats (Ciriello and Calaresu, 1980). The lateral hypothalamus also has connections with numerous areas of the central nervous system, including the infralimbic cortex (Kita and Oomura, 1981, 1982), parabrachial nuclei (Kita and Oomura, 1982), the NTS and intermediolateral cell column of the thoracic spinal cord (Saper et al., 1976). The hypothalamus also receives direct inputs

from the NTS (Ricardo and Koh, 1978). The hypothalamus is known to have an important role in control of the cardiovascular system (Pitts et al., 1941; Schafer, 1960; Smith et al., 1960; Hilton, 1966; Folkow and Neil, 1971). There appears to be an anterior-posterior organization within the hypothalamus with the anterior region being involved in cardiodeceleration, vasodepressor responses, and baroreceptor augmentation, and the posterior regions mediating cardioacceleration, vasopressor responses, baroreceptor attenuation, defense reactions, and sympathetic vasodilation in skeletal muscle (Galosy et al., 1981).

The amygdala, located in the base of the temporal lobe, consists of several subnuclei, two of which are relevant to the present discussion, the central (CeA) and basolateral (BLa) amygdaloid nuclei. The Bla has connections with the insular cortex (Krettek and Price, 1977b; Macchi et al., 1978; Price, 1981; Otterson, 1982; Sarter and Markowitsch, 1983) and the pre- and infralimbic cortices of the frontal pole cortex (Krettek and Price, 1977b; Price, 1981; Ottersen, 1982). BLa also has heavy connections with the mediodorsal and interanteromedial thalamic nuclei (Krettek and Price, 1977a; Ottersen and Ben-Ari, 1979). The paraventricular and parataenial thalamic nuclei also project heavily to the CeA and BLa (Ottersen and Ben-Ari, 1979). The CeA has been shown to have reciprocal connections with the parabrachial nuclei (Hopkins and Holstege, 1978; Saper and Loewy, 1980; Fulwiler and Saper, 1984). The CeA also has descending

projections to the region of the NTS and dorsal motor nucleus of the vagus in the dorsomedial medulla (Krettek and Price, 1978; Schwaber et al., 1980, 1982; Higgins and Schwaber, 1983). The amygdaloid complex appears to exert a powerful influence on cardiovascular and other autonomic functions (Hilton and Zbrozyna, 1963; Heinemann et al., 1973; Mogenson and Calaresu, 1973). Reis and Oliphant (1964) elicited a vagally mediated bradycardia from the BLa, although tachycardia could sometimes be produced at the same sites. Pressor responses could also be produced and were generally preceded by bradycardia. Kaada (1972) suggests that the lateral amygdala mediates decreases in blood pressure whereas the corticomedial amygdala mediates increases in pressure. Mogenson and Calaresu (1973) showed that stimulation of the CeA elicited arterial hypotension in the anesthetized animal. However, in the awake animal, CeA stimulation elicits a pressor response (Galeno and Brody, 1983).

The parabrachial nucleus (PBN) in the dorsal pons is known to receive direct projections from the NTS (Loewy and Burton, 1978; Norgren, 1978; Ricardo and Koh, 1978), and the PBN also projects back to the NTS (Saper and Loewy, 1980). The PBN also has connections with the midline and ventromedial basal thalamic nuclei (Norgren and Leonard, 1973; Norgren, 1976; Saper and Loewy, 1980; Fulwiler and Saper, 1984). The PBN appears to be a relay for afferent gustatory information, relaying this information from the NTS to the taste nucleus of the thalamus (Norgren and Leonard, 1973; Norgren, 1976,

1978; Shipley and Sanders, 1982). Electrical stimulation of the PBN results in a pressor response, while the changes in heart rate observed after PBN stimulation appear to be species specific. In rabbits PBN stimulation elicits bradycardia (Hamilton et al., 1981), while in cats, PBN stimulation elicits tachycardia (Mraovitch et al., 1982b).

The NTS is considered to be one of the medullary autonomic nuclei, receiving visceral afferent fibers from the V, VII, IX and Xth cranial nerves (Torvik, 1956; Contreras et al., 1982). Within the NTS there is an anatomical and functional segregation of afferent terminations. The rostral portion of the NTS receives special visceral afferent fibers predominantly from the VII and IXth cranial nerves and is involved in mediating taste sensations (Torvik, 1956; Norgren, 1978). The caudal and intermediate portions of the NTS receive general visceral afferent fibers from the VII, IX and Xth cranial nerves. The terminations of the VII and IXth cranial nerves are confined basically to the lateral subnucleus of the NTS, while vagal afferents terminate extensively and almost exclusively in the medial subnucleus of the NTS (Torvik, 1956; Contreras et al., 1982; Kalia and Sullivan, 1982). It is the intermediate portions of the NTS that are important for the control of cardiovascular functions, as it is this region that serves to integrate a number of cardiovascular reflexes, including the baroreflexes (Muira and Reis, 1972; Ross et al., 1981).

Numerous studies have investigated the sites of termination of various visceral afferents, including baro- and chemoreceptors, pulmonary, cardiac and gastrointestinal afferents in the dorsomedial medulla. The commissural nucleus (cNTS) has been shown to receive chemoreceptor, baroreceptor and gastrointestinal afferent inputs (Kalia and Mesulam, 1980b; Kalia and Welles, 1980; Davies and Kalia, 1981; Kalia and Kropilak, 1982). The medial nucleus (mNTS) receives vagal afferent projections from the gastrointestinal tract, as well as cardiovascular and baroreceptor inputs (Kalia and Mesulam, 1980b; Kalia and Welles, 1980; Davies and Kalia, 1981, Kalia and Kropilak, 1982). The interstitial nucleus (iNTS) receives the major afferents from the larynx (Kalia and Mesulam, 1980b). The dorsolateral nucleus (dlNTS) receives predominantly baroreceptor and chemoreceptor afferents from the carotid sinus nerve (Davies and Kalia, 1981) and aortic depressor nerve (Kalia and Welles, 1980) and the dlNTS also receives terminations from irritant receptor afferents and lung stretch receptors (Kalia et al., 1984). The dorsal nucleus (dNTS) is known to receive selective afferent input from the carotid sinus nerve, the aortic nerve, the vagus nerve and from the heart (Kalia and Mesulam, 1980b; Kalia and Welles, 1980; Davies and Kalia, 1981; Kalia and Kropilak, 1982). The ventral (vNTS) and ventrolateral (vlNTS) nuclei have been associated with the terminations of vagal afferents from pulmonary stretch receptors and irritant receptors (Kalia, 1981a, b); they are as well the site where neurons involved in the

respiratory rhythmicity have been localized (Baumgarten and Nakayama, 1964; von Euler et al., 1973; Cohen, 1979). At the level of the area postrema, the vlNTS receives heavy projections from the carotid sinus nerve (Davies and Kalia, 1981).

The NTS has extensive connections with the dorsal motor nucleus of the vagus (DMN X) and the nucleus ambiguus (NA), the sites of first order vagal preganglionic motor neurons (Norgren, 1978; Geis and Wurster, 1980a; Kalia and Mesulam, 1980a,b; Rogers et al., 1980; Kalia and Sullivan, 1982). Additionally, Loewy (1981) reported a small projection from the NTS to the intermediolateral cell column in the thoracic spinal cord in the cat. Thus, the NTS seems capable of influencing activity in both the parasympathetic and sympathetic nervous systems.

Another area of the medulla that has been associated with a wide range of visceral and endocrine functions including cardiovascular control (Loeschcke et al., 1970; Guertzenstein and Silver, 1974; Feldberg, 1976), respiration (Mitchell et al., 1963; Loeschcke et al., 1970; Schafke and See, 1970) and vasopressin release (Bisset et al., 1975; Fukuda et al., 1980) is the ventrolateral medulla (VLM). Electrical and chemical stimulation of the VLM have been shown to elicit arterial hypertension and tachycardia (Guertzenstein and Silver, 1974; Ciriello and Calaresu, 1977; Dampney et al., 1982). It has been suggested that effects on the sympathetic nervous system are mediated by direct pathways from the VLM to spinal sympathetic

centers, including the intermediolateral cell column in the thoracic spinal cord (Chung et al., 1975; Oldfield and McLachlan, 1980; Loewy and McKellar, 1981; Loewy et al., 1981). Thus, this region has the capability of influencing activity in the sympathetic nervous system.

Technical Considerations

Since several different methodological techniques will be employed in the present studies, each will be discussed briefly in the following sections.

Horseradish Peroxidase Histochemistry

The use of horseradish peroxidase (HRP) histochemistry in tracing neural connections in the central nervous system was first introduced by LaVail and LaVail (1972). Since then, the use of HRP histochemistry has become one of the most frequently employed techniques for tracing neural connections. When using HRP histochemistry, two issues must be addressed. The first is which type of HRP is to be used, as there are various forms available, each with its own properties. The second issue to be considered is which histochemical protocol will be followed for visualizing the HRP enzyme.

In the present studies, HRP conjugated with wheat germ agglutinin (WGA) will be used. This form of HRP was first introduced by Gonatas et al. (1979) and has been shown to be much more sensitive

than free HRP. Wheat germ agglutinin is a non-toxic lectin that enhances the uptake of HRP into neurons via endocytosis (Gonatas et al., 1979; Mesulam, 1982). A second advantage to using WGA-HRP as opposed to other forms of HRP is that WGA-HRP has also been shown to be a very good anterograde tracer, (Mesulam and Mufson, 1980; Trojanowski et al., 1981).

When deciding on which histochemical protocol to follow for visualization of the enzyme, one must consider the sensitivity of the method and the amount of artifact that may be present after the procedure. At the present time, the procedure by Mesulam (1978), which utilizes tetramethylbenzidene (TMB) as the chromagen, appears to be the most sensitive method for visualizing HRP. In later experiments we chose to use a modification of Mesulam's TMB protocol (1978) for the visualization of the WGA-HRP (Gibson et al., 1984). This method is as sensitive as the original TMB method but minimizes the artifact often associated with the enzymatic reaction that is utilized in the visualization process by using a filtration pump system that filters out small particulate matter that may lead to the formation of small crystalline rods, which may cause difficulty in interpreting the results.

One problem that is often encountered with the TMB procedure is estimating the size of the injection site. Due to the high sensitivity of the TMB procedure, the injection sites appear quite large after processing with TMB. Mesulam (1982) discusses the various

experimental factors that may influence the apparent size of the injection site (i.e. the volume, concentration and pressure of the injection), as well as factors such as survival time, fixation and histochemical parameters. The choice of chromagen used in the histochemical visualization of the HRP seems to greatly affect the size of the injection site. In tissue processed with diaminobenzidene (DAB), the injection site contains a central dense core surrounded by a fainter halo. Some have suggested that uptake and transport occurs only from the center (Bunt et al., 1975; Jones, 1975; Wong-Riley, 1974), while others have shown that the halo also contributes to the area of effective uptake (Dursteler et al., 1977). The tetramethylbenzidene (TMB) method does not allow a clear distinction between a center and a halo; however, two regions can be discerned. In the immediate vicinity of the injection, the reaction-product is very dense and individual neurons cannot be identified. This zone is surrounded by a region where the reaction-product is still dense but individual neurons can be identified. Mesulam (1982) designates the first zone as the injection site. A second criterion we have employed for determining the site of effective uptake of WGA-HRP considers the retrograde labeling seen in the contralateral cerebral cortex. Since the areas of frontal cortex injected in these studies have been shown to have connections to homotypical regions of the contralateral cortex (Markowitsh and Guldin, 1983), the zone of effective uptake was determined by examining the contralateral hemisphere and defining

those areas of homotypic cortex that had a moderate number of retrogradely labeled neurons.

The question of whether or not HRP is taken up only by axon terminals and not by intact or injured fibers of passage still remains unanswered. Brodal et al. (1983) reported that WGA-HRP was taken up and retrogradely transported by damaged but not intact fibers of passage while no anterograde transport was seen either in damaged or intact fibers of passage. Steindler (1982) reported that WGA was not taken up and transported by intact fibers but when the fibers were injured, uptake and transport occurred. These data would seem to indicate that WGA-HRP is in fact taken up and retrogradely transported by both axon terminals and injured fibers of passage. In the present study, care was taken in introducing the pipette in order to minimize fiber damage. The placement of the pipette always avoided the underlying cortical white matter and the use of pressure injections also minimized the possibility of excessive damage to the tissue since Herkenham and Nauta (1977) reported that the use of iontophoresis may induce damage to axons, increasing the possibility of uptake of tracer by fibers of passage.

In addition, Mesulam (1982) discusses several factors that must be considered in anterograde HRP histochemistry. First, since many regions that receive anterograde transport may also contain retrogradely labeled neurons, it is sometimes difficult to determine if the extracellular reaction-product is within dendritic branches of

labeled cell bodies or if there is also labeling of axons. This problem was especially evident in the thalamus where several areas exhibited such heavy labeling that it required careful inspection to discern anterograde labeling from retrograde labeling. Secondly, anterograde labeling lacks a definitive morphology, making it difficult to differentiate "terminal labeling" from labeled fibers of passage. In the present studies, the term "anterograde label" refers to presumed pre-terminal and terminal axonal labeling. This label appears very dense due to the arborization or branching of terminal axons at their point of termination. Labeled fibers of passage appear less dense and often can be seen as several labeled dots in a row, much like "beads on a string." Finally, it must be stressed that anterograde "axonal terminal labeling" can only be verified as "terminal labeling" if the appropriate electron microscopic analysis of the tissue is done.

Intracortical Microstimulation

Several technical issues concerning the intracortical microstimulation technique should be addressed. One potential problem in electrical stimulation experiments is the spread of electrical current from the tip of the electrode to regions distant from the point of stimulation. The results of the present experiments suggest that this problem does not compromise our results. The most convincing evidence for this statement is that stimulation of adjacent

regions of the MFC resulted in different responses. For example, points located in the dorsal anterior cingulate cortex were mostly non-responsive to low intensity stimulation (< 50 uamps) while points within the adjacent pre- and infralimbic cortices resulted in changes in cardiovascular (HR, BP) and respiratory activity at relatively low thresholds (< 50 uamps); often non-responsive points were located only 0.5 mm away from responsive points. Further, relatively low currents (10-50 uamps) were effective in eliciting responses, thus diminishing the effective current spread. Ranck (1975) has estimated that the radius of effective current spread from a 50 uamp stimulus is 500 um and that from a 10 uamp stimulus is 150 um.

A second potential problem is that the damage caused by an electrode track might interact with an electrical stimulus delivered at a later time point (Wyss and Goldstein, 1976). To determine if tissue damage caused by the electrode track altered the results, some points were stimulated during the descent and then restimulated again upon withdrawal after the entire track had been investigated. The responses seen were only slightly attenuated when stimulation was applied the second time. Additionally, in cases in which a second or third penetration was made 0.5-1.0 mm rostral or caudal to the site of a previous penetration, the responses to stimulation on these "later" tracks appeared to be of equal amplitude to the responses evoked by by the initial penetration.

Specific Aims

This dissertation was undertaken to determine if the infralimbic region of the rat medial frontal cortex could be classified as part of the "visceral brain" based on anatomical and physiological criteria, perhaps serving as a "visceral motor region." To investigate this hypothesis, four sets of experiments were designed to determine:

1. the origins of the afferent projections to the infralimbic and prelimbic cortices.

2. the areas of the central nervous system which receive direct projections from the infralimbic and prelimbic cortices.

3. the sites within the rat medial frontal cortex which elicit changes in heart rate, blood pressure and respiration upon electrical stimulation.

4. the effects of pharmacological agents and lesions of the vagi and pyramidal tracts on the physiological responses elicited from this cortical area.

These studies should provide us with some insight into the functional significance and relevance of this cortical region, hopefully shedding some light onto its role in overall cerebral cortical structure and function.

Table 1.

Comparison of medial frontal cortex (MFC) cytoarchitecture.

The results of seven studies on MFC cytoarchitecture are presented in this table. Under each author heading are the subdivisions of MFC that were described in that report. See text for abbreviations.

Krettek + Price '77a (rat)	Zilles et al. '80 (rat) Wree et al. '83 (mouse)	Vogt + Peters '81 (rat)	M. Rose '27 (mouse)	Brodmann '09 (rabbit)	Rose + Woolsey '48 (rabbit)
PrCm	PrCm	4	4 , 6	4 , 6	Prag
ACd	C1	24b	IRcα ,IRcβ	24, 23	La
ACv	C2	24a	IRBβ ,IRAβ		
PL	C4	32	IRBα	32	
IL	C3	25	IRAα	25	IL
TT	HP	TT	TT		TT

Figure 1.

A-D: Surface diagrams of the medial aspects of the rat brain which demonstrate the topography of the cortical areas discussed in the present study. A: The topographic pattern used in the present study. B: Cortical map from Krettek and Price (1977a). C: Cortical map from Zilles et al. (1980). D: Cortical map from Vogt and Peters (1981). See text for abbreviations.

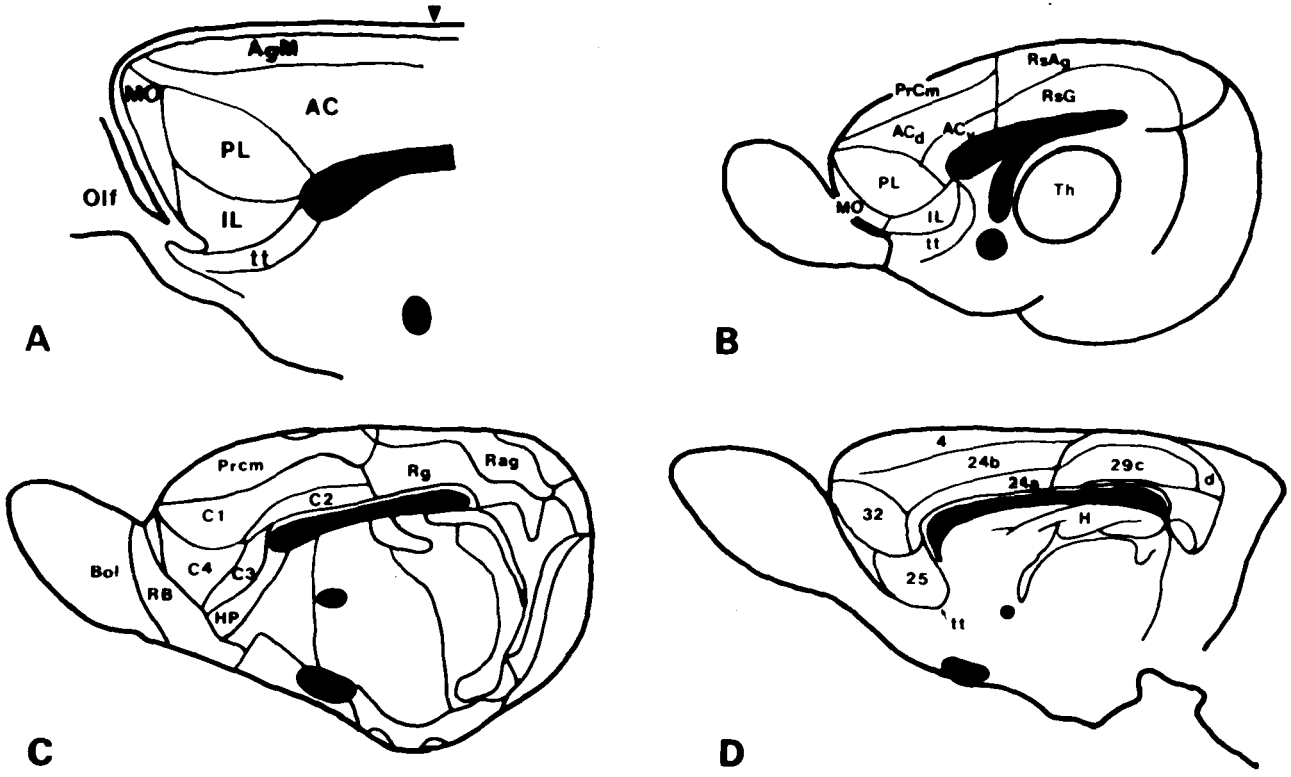
AgM
MO
AC
PL
Olf
IL
tt
A
RsAg
PrCm
RsG
ACd
ACv
PL
Th
MO
IL
tt
B
Prcm
Rg
Rag
C1
C2
Bol
C4
C3
RB
HP
C
4
24b
29c
d
24a
32
H
25
tt
D

Figure 1 cont.

E-G: Surface diagrams of the medial aspects of the mouse (E,F) and rabbit (G,H) brain which demonstrate the topography of the cortical areas discussed in the present study. E-F: Cortical maps from Wree et al. (1983) and M. Rose (1927), respectively, illustrating the cortical areas on the medial surface of the mouse brain. G-H: Cortical maps from Brodmann (1909) and Rose and Woolsey (1948), respectively, showing the cortical areas on the medial aspect of the rabbit brain. See text for abbreviations.

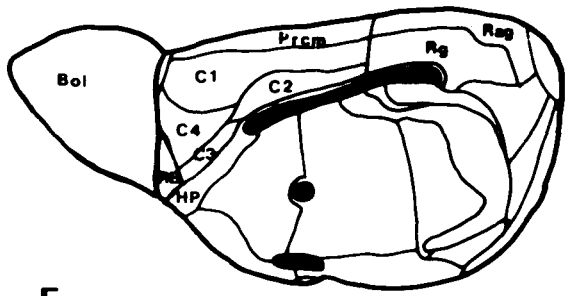
Bol
C1
Prcm
Rg
Rag
C2
C4
C3
HP

E

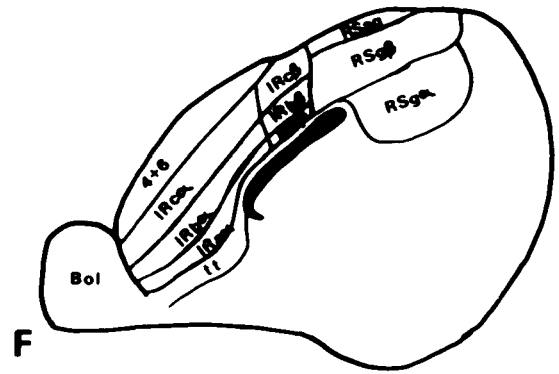
Bol
4+6
IRca
IRg
tt

F

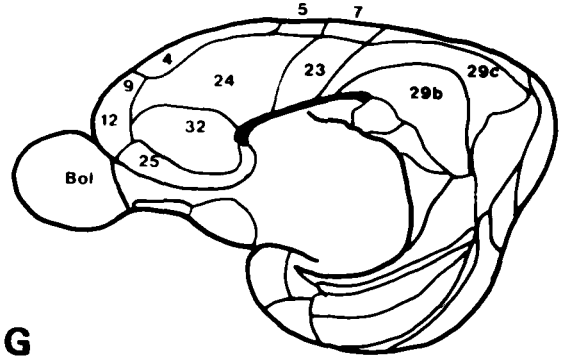
5
7
4
9
24
23
29b
29c
12
32
25
Bol

G

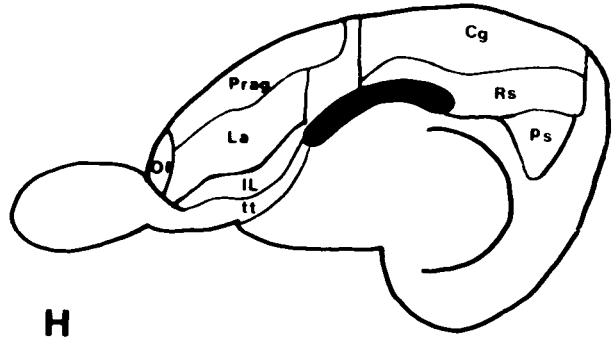
Cg
Prag
Rs
La
Ps
IL
tt

H

Figure 2.

A-D: Rostral to caudal series of photomicrographs (2X) at 500 um intervals through the rat medial frontal cortex (MFC). The arrows indicate the boundaries of each cytoarchitectonic subdivision. The sections were 50 um thick and stained with a modified silver stain (Merker, 1983).

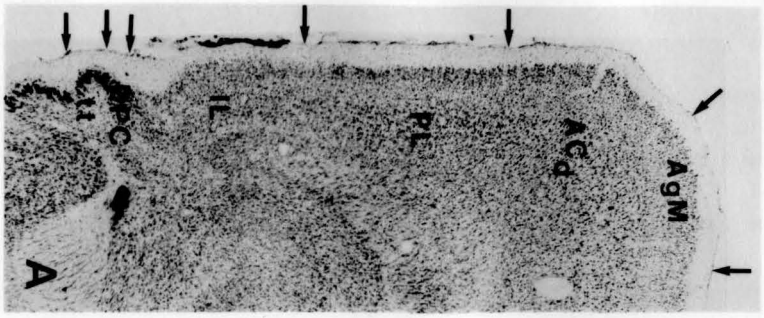
A
tt
DPC
IL
PL
ACd
AgM

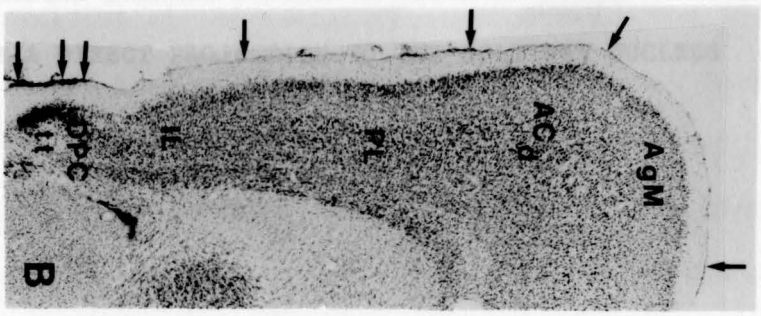
B
tt
DPC
IL
PL
ACd
AgM

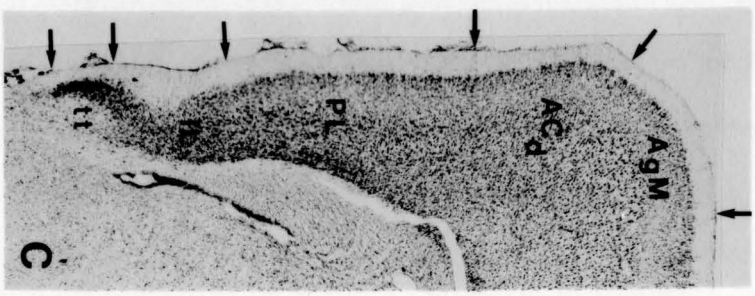
C
tt
IL
PL
ACd
AgM

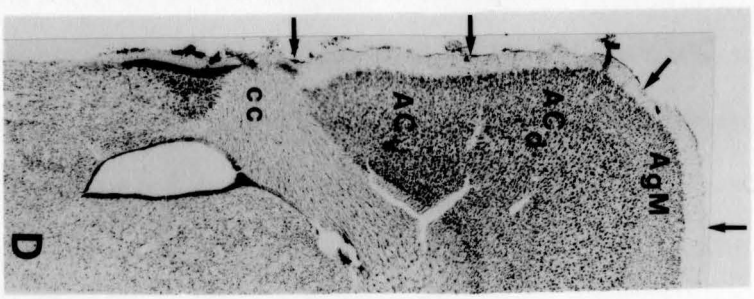
D
cc
ACV
ACd
AgM

CHAPTER III

RAT MEDIAL FRONTAL CORTEX: A VISCERAL MOTOR REGION WITH A DIRECT PROJECTION TO THE SOLITARY NUCLEUS

ABSTRACT

Pressure injections of the neuroanatomical tracer wheat germ agglutinin conjugated with horseradish peroxidase (WGA-HRP) were made into either the dorsal medulla or the medial frontal cortex of the rat. Following brainstem injections, retrogradely labeled neurons were found in the infralimbic (IL), prelimbic (PL) and anterior cingulate (AC) regions of the medial frontal cortex. The IL labeling consisted of a dense band of neurons and was bilateral. Cells in the PL and AC regions were less densely packed. After cortical injections, anterograde labeling was seen in the nucleus of the solitary tract (NTS) of the dorsomedial medulla. Label was seen throughout the rostral-caudal extent of the NTS and was bilateral, although heavier contralaterally. The projection from the IL cortex to the NTS suggests that this cortical area may function as a "visceral" cortical region that may play a role in regulating autonomic functions.

INTRODUCTION

Physiological studies by Kaada (1951, 1960) and Lofving (1961) described changes in heart rate and blood pressure following electrical stimulation of the anterior cingulate cortex in cats and monkeys. Similar responses were achieved by stimulating the insular

cortex and adjacent portions of the temporal pole and the orbital cortex on the ventral surface of the brain. Recently, Mraovitch et al. (1982a) reported that electrical stimulation of the laterally located insular cortex in rats could elicit increases in heart rate and blood pressure. Additionally, Burns et al. (1983) and Terreberry and Neafsey (1984) demonstrated that electrical stimulation of the rat anterior cingulate cortex, on the medial aspect of the cerebral hemisphere, resulted in decreases in heart rate and blood pressure. Thus, in rats as in other species, it appears that two regions of the cerebral cortex are involved in cardiovascular functioning: one located laterally and one on the medial aspect of the hemisphere.

The pathways by which the cortex elicits its control of cardiovascular functions are not well defined at this time. However, recently it has been shown that, in the rat, the laterally located insular cortex projects directly to the NTS (Mraovitch et al., 1982a; Saper, 1982; Shipley, 1982; van der Kooy et al., 1982); a sparse projection from the anterior cingulate region to the NTS was described by only one laboratory (van der Kooy et al., 1982). Therefore, we chose to investigate this cortical projection from the anterior cingulate region to the NTS in more detail, specifically looking at the size and distribution of the projection. To answer these questions, we employed the retrograde and anterograde transport of wheat germ agglutinin conjugated horseradish peroxidase (WGA-HRP). Following injections of WGA-HRP into the dorsomedial medulla in the

vicinity of the NTS, the presence and location of retrogradely labeled cortical neurons was determined. Then WGA-HRP was injected into these cortical areas to determine if they project directly to the NTS complex. A portion of these data have appeared elsewhere (Terreberry and Neafsey, 1983).

MATERIALS AND METHODS

A total of 24 adult Long Evans male rats (300-500 grams) was used in this study. Animals were anesthetized with Ketamine HCl (100 mg/kg, IP; supplemental doses of one-quarter the initial dose were given when necessary to maintain a constant level of anesthesia) and then placed into a stereotaxic frame. A heating pad controlled by a rectal temperature probe was used to maintain the animal's body temperature between 36-38 degrees celcius. Following surgical exposure of the skull and the neck musculature, the cisterna magna was opened in order to allow access to the dorsomedial medulla. A portion of the occiput was removed in order to expose more fully the underlying brainstem. The obex was identified and was used as the reference point for all injections.

A 1.0 ul Hamilton syringe fitted with a glass pipette (tip diameter 50 um) was filled with a 1% WGA-HRP (Sigma) solution in 0.9% saline. The syringe was mounted on a Kopf micromanipulator which was used to position the pipette just lateral (0.1-0.75 mm) to the

midline, to a depth of 0.25-0.75 mm from the brainstem surface at points 0.0-2.5 mm rostral to obex; this location of the injection site always included the NTS. Pressure injections of 0.01-0.03 ul of WGA-HRP were performed over a 15-20 minute period, after which time the pipette was withdrawn and the wound sutured closed.

After a 48 hour survival time, the animals were reanesthetized with sodium pentabarbitol (40 mg/kg, IP) and transcardially perfused with 0.9% saline, 1.25% glutaraldehyde - 1% paraformaldehyde and finally with a 10% buffered sucrose solution according to the procedure of Rosene and Mesulam (1978). The brains were removed, placed in a cold 30% sucrose phosphate buffer solution and allowed to sink (2-3 days). Frozen sections 50 um thick were cut coronally on a sliding microtome, and two alternating series of sections collected. Both sets of sections were reacted with tetramethylbenzidene (TMB) using a modification of Mesulam's (1978) procedure (Gibson et al., 1984). The TMB reactions were stopped, and the sections were rinsed and mounted from cold sodium acetate buffer (pH 3.3) onto subbed slides. The sections were oven dried overnight (temperature between 50-60 degrees celcius). One set was rapidly dehydrated in a graded series of ethanol, cleared in xylene and coverslipped using Depex. The second set of sections was counterstained in 1% pyronin Y, rapidly dehydrated and coverslipped using Depex. Some loss of label occurs in the ethanol, but this loss was usually minimal and did not greatly affect the results. The counterstained series were used to determine

cytoarchitectonic boundaries.

Each section was examined under brightfield, darkfield and polarized light microscopy for the presence and localization of retrograde label. A series of line drawings were made at 400 um intervals through the brain using a Bausch and Lomb projecting scope. The retrogradely labeled neurons were then plotted onto these line drawings utilizing a camera lucida drawing tube attached to an Olympus BH-1 microscope.

Four of the rats received injections of WGA-HRP into the medial frontal cortex. The same surgical procedures that were used for the brainstem injections were followed for the cortical injections. Instead of fully exposing the brainstem, the left cortex was exposed by removing a small piece of the calvaria overlying the MFC. Following a pressure injection of 1% WGA-HRP into the MFC (0.2-0.6 mm lateral to the midline, 3.0-4.0 mm rostral to bregma, 3.0-4.0 mm deep from the cortical surface, 0.01-0.03 ul total), the wound was sutured closed and a two day survival period was observed. The same perfusion and histological protocols were followed for the cortical injections as were described for the brainstem injections.

Each brainstem section was examined under brightfield, darkfield and polarized light microscopy for the presence and localization of anterograde label. A series of line drawings were made at 200 um intervals through the brainstem using a Bausch and Lomb projecting scope. The anterograde label was then plotted onto these line

drawings utilizing a camera lucida drawing tube attached to an Olympus BH-1 microscope.

RESULTS

Retrograde Labeling in the MFC

In 17 experiments, the injection site encompassed a good portion of the dorsal medulla. Figure 1C shows a typical injection site which involved the NTS bilaterally. Structures involved included the nucleus of the solitary tract (NTS), dorsal motor nucleus of the vagus (DMN X), the dorsal column nuclei (NC, NG), the hypoglossal nuclei (XII) and portions of the surrounding reticular formation. The trigeminal nuclei were spared, and the pyramidal tracts were unaffected by the injection site. The pattern and location of cortical neurons projecting to the NTS will be illustrated chiefly by reference to experiment HRP RT 8 (Figures 1,2).

After an injection of WGA-HRP into the dorsal medulla (Figure 1C), retrogradely labeled neurons were seen bilaterally within the medial frontal cortex (Figures 1A,B). Figure 1A shows the location of these cells within the medial frontal cortex. The cells were localized predominantly within the infralimbic (IL) region, as well as in the ventral portions of the prelimbic (PL) region. A few scattered neurons were also seen labeled in the anterior cingulate cortex (AC). The insular cortex, located on the lateral aspect of the hemisphere

along the rhinal sulcus, also contained numerous labeled neurons (Figure 2A). Retrogradely labeled neurons were seen in the primary somatosensory cortex (not illustrated), probably indicating that the dorsal column nuclei were involved in the injection. The second somatosensory area also contained labeled cells after the dorsal medullary injection (not illustrated).

Figures 2B,C illustrate the retrogradely labeled cells seen in the central nucleus of the amygdala and in the paraventricular nucleus of the hypothalamus. Since the retrograde labeling observed in these subcortical areas was essentially the same as observed by Saper et al. (1976), Hopkins and Holstege, (1978), and Schwaber et al. (1982), it will not be described in further detail in the present report.

Anterograde Labeling in the NTS

After an injection of WGA-HRP into the MFC (Figure 3A), anterogradely labeled axons were seen bilaterally in the NTS. The labeling of the NTS was found throughout the rostral-caudal extent of the NTS, with a slightly heavier projection to more caudal levels. Figures 3D,E illustrates the anterograde label in the caudal NTS, just below the level of the obex. With unilateral injections into the MFC the label appeared to be heavier contralateral to the injection site. No other nuclei within the medulla showed the presence of anterograde label after an MFC injection of WGA-HRP. Thus, it appears that the neurons labeled in the PL and IL cortices after a brainstem injection

do in fact project directly to the NTS complex.

DISCUSSION

The finding of the present study that the infralimbic region (IL) of the medial frontal cortex (MFC) has a substantial direct descending projection to the NTS complex lends support to the hypothesis that the IL cortex is a visceral or autonomic cortical area. Van der Kooy et al. (1982) had previously reported a much sparser projection from the IL cortex to the NTS, but their study emphasized the projections from the insular cortex to the NTS.

Physiological studies have shown that electrical stimulation of the anterior cingulate cortex can elicit changes in various autonomic parameters, such as blood pressure, heart rate and respiration (Smith, 1945; Ward, 1948; Kaada, 1951, 1960; Lofving, 1961). Similar responses have been observed in rodents. Burns et al. (1983) reported a decrease in blood pressure upon electrical stimulation of the rat MFC, specifically the infraradiata a and b (PL and IL) cortical areas. Terreberry and Neafsey (1984) report that stimulation of the IL regions in awake and anesthetized rats results in a rapid decrease in heart rate that is often accompanied by a drop in arterial blood pressure. Stimulation of this region also results in decreased gastric motility (Neafsey and Hurley, 1984).

The insular cortex, located along the banks of the rhinal

sulcus, has a direct descending projection to the (NTS) in the dorsomedial medulla (Mraovitch et al., 1982a; Saper, 1982; Shipley, 1982; van der Kooy et al., 1982). Electrical stimulation of the insular cortex produces a wide spectrum of autonomic adjustments, ranging from pressor, heart rate and cardiac output changes to respiratory, piloerection, pupillary, salivary and pyloric responses in several species including cats, dogs and monkeys (Smith, 1938; Kaada, 1951; von Euler and Folkow, 1958; Wall and Davis, 1951; Hall et al., 1977). Mraovitch et al. (1982a) reported similar pressor and heart rate responses upon electrical stimulation of the rodent insular cortex.

It therefore appears that two cortical areas may be considered cortical autonomic regions, the insula and the infralimbic cortex. The insular cortex has been referred to as the "visceral sensory" cortex owing to the fact that the sense of taste is represented there (Benjamin and Akert, 1959; Norgren and Leonard, 1973; Yamamoto et al., 1980; Shipley and Geinisman, 1984). This visceral sensory cortex is located just lateral to the primary (SI) and secondary (SII) somatosensory areas. The infralimbic region (IL) of the MFC lies medial to the primary somatic motor cortex (AgL) and the frontal eye fields (FEF; Hall and Lindholm, 1974; Donoghue and Wise, 1982; Neafsey and Sievert, 1982; Leichnetz et al., 1983). This topographical relationship suggests that the IL visceral cortex may function primarily as a "visceral motor" cortical area. Cytoarchitectonically,

the IL cortex resembles the primary motor cortex in that they both are agranular, lacking a distinct layer IV. Based on cytoarchitecture, it would appear that the IL cortex is part of an agranular cortical motor system. With this in mind, an interesting topography of the rat frontal cortex becomes evident if one looks at a coronal view of the rodent frontal pole (Figure 4). From medial to lateral the following cortical areas are found: visceral motor, frontal eye fields, somatic motor, somatic sensory, visceral sensory and olfactory sensory (piriform cortex). The subsequent studies of this dissertation will attempt to further explore this notion of the infralimbic cortex as a "visceral" region.

Figure 1.

A: Nissl stained coronal section through the medial frontal cortex, illustrating the location of retrogradely labeled neurons after an injection of WGA-HRP into the dorsomedial medulla. Arrowheads on the cortical surface indicate cytoarchitectonic borders. Labeled cells are denoted by the circles and the area enclosed by the box is shown at higher magnification in B. Note that the labeled cells are localized within IL and PL cortex. Scale bar = 250 um. B: High power (10X) view of the area enclosed by the box in A. Arrows indicate the location of retrogradely labeled neurons. C: Unstained coronal section through the lower medulla illustrating a typical brainstem injection site (0.04 ul of 1% WGA-HRP). The arrow indicates the path of the pipette. Note the spread to the contralateral NTS in the region dorsal to the central canal. Scale bar = 250 um.

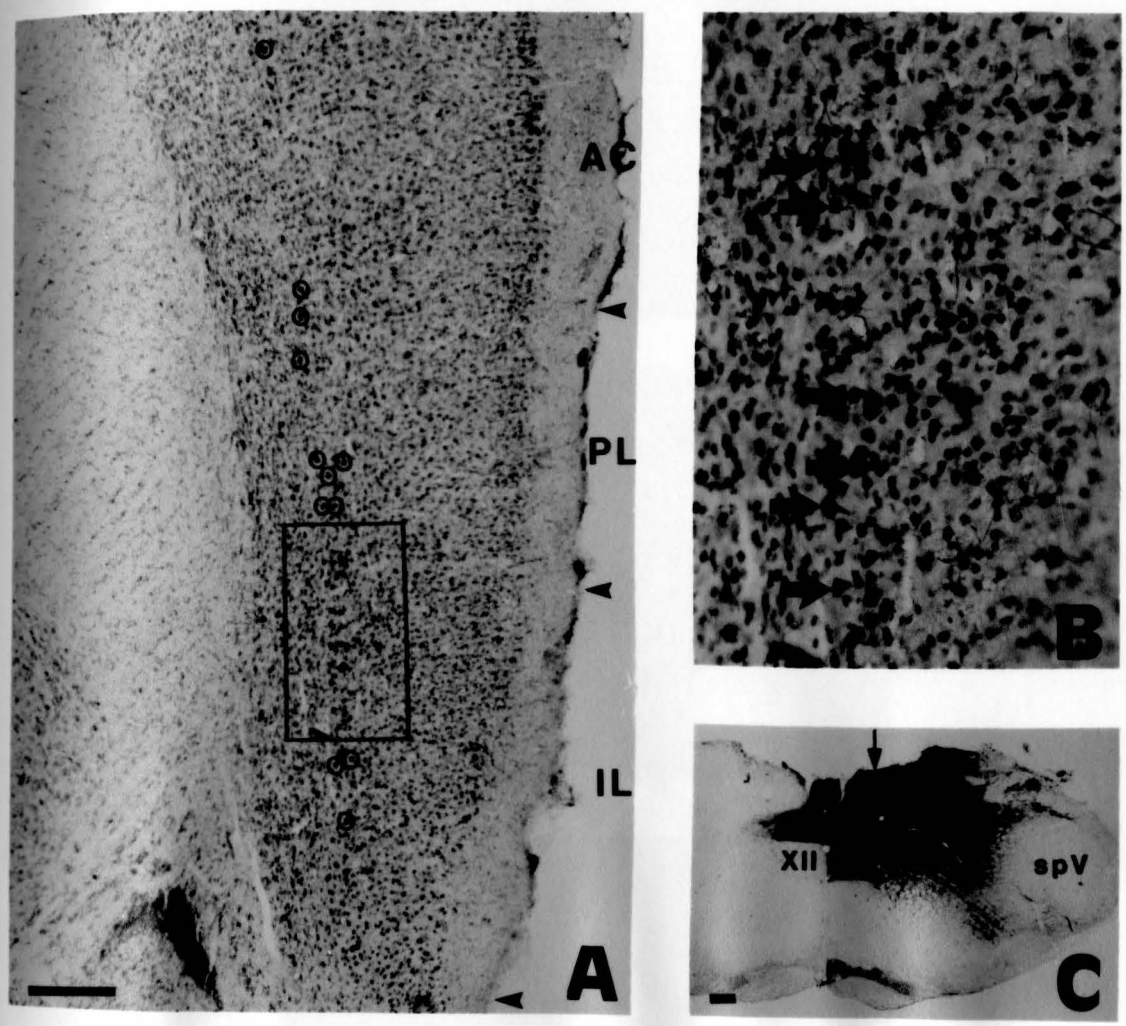
AC
PL
IL
A
B
XII
spV
C

Figure 2.

Photomicrographs of retrogradely labeled neurons seen after a dorsomedial medullary injection (Figure 1C). A: Nissl stained coronal section through the left insular cortex. The cortical surface is to the lower left. Labeled cells are seen in the deep layers of the insular cortex. B: Nissl stained coronal section through the amygdala. Labeled neurons are seen heavily within the medial aspect of the central nucleus (Ce). C: Nissl stained coronal section through the rostral hypothalamus illustrating retrograde labeling in the paraventricular nucleus. Scale bar = 100 um.

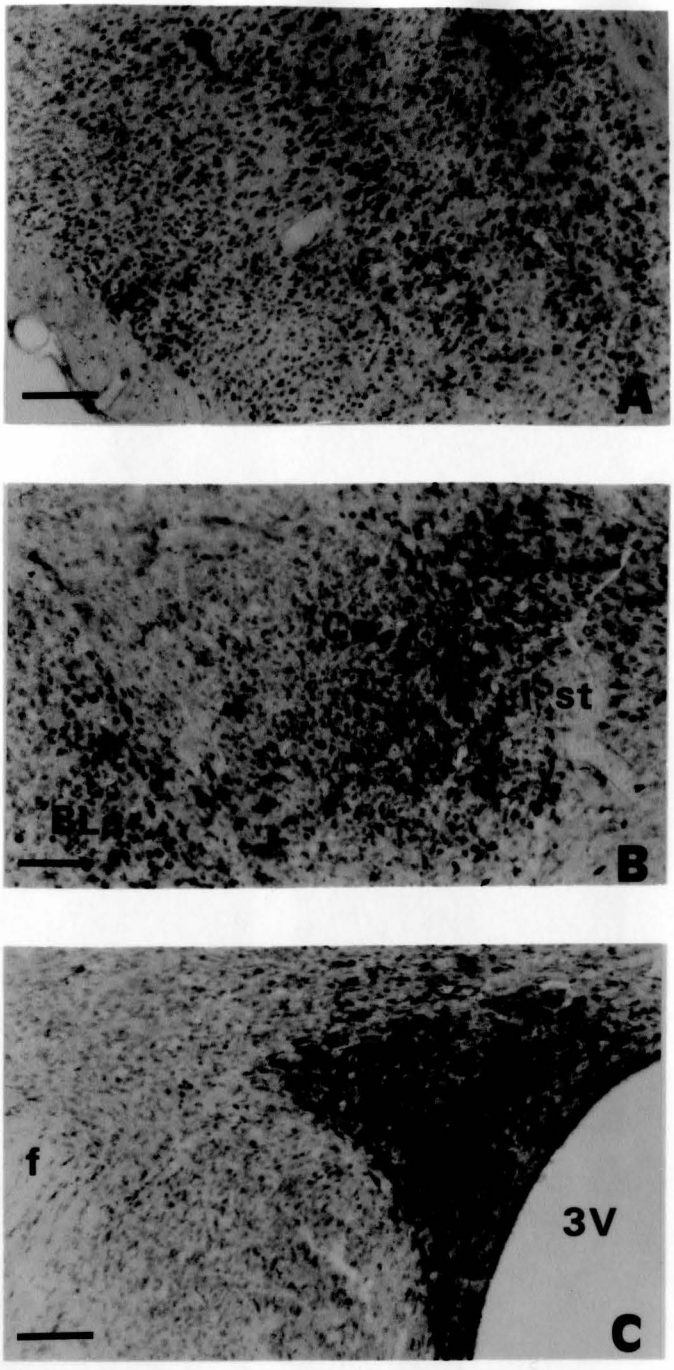
A
st
BLA
B
f
3V
C

Figure 3.

Photomicrographs illustrating the anterograde labeling in the NTS after an injection of WGA-HRP into the MFC. A: Nissl stained coronal section through the MFC indicating the injection site. Areas involved included the IL and PL cortices. B+D: Coronal sections through rostral and caudal levels of the NTS, respectively. C+E: High power darkfield photomicrographs of the areas enclosed by the boxes in B+D, respectively. White arrows indicate anterograde label localized within the NTS. Scale bars in B+D = 500 um, scale bars in C+E = 100 um.

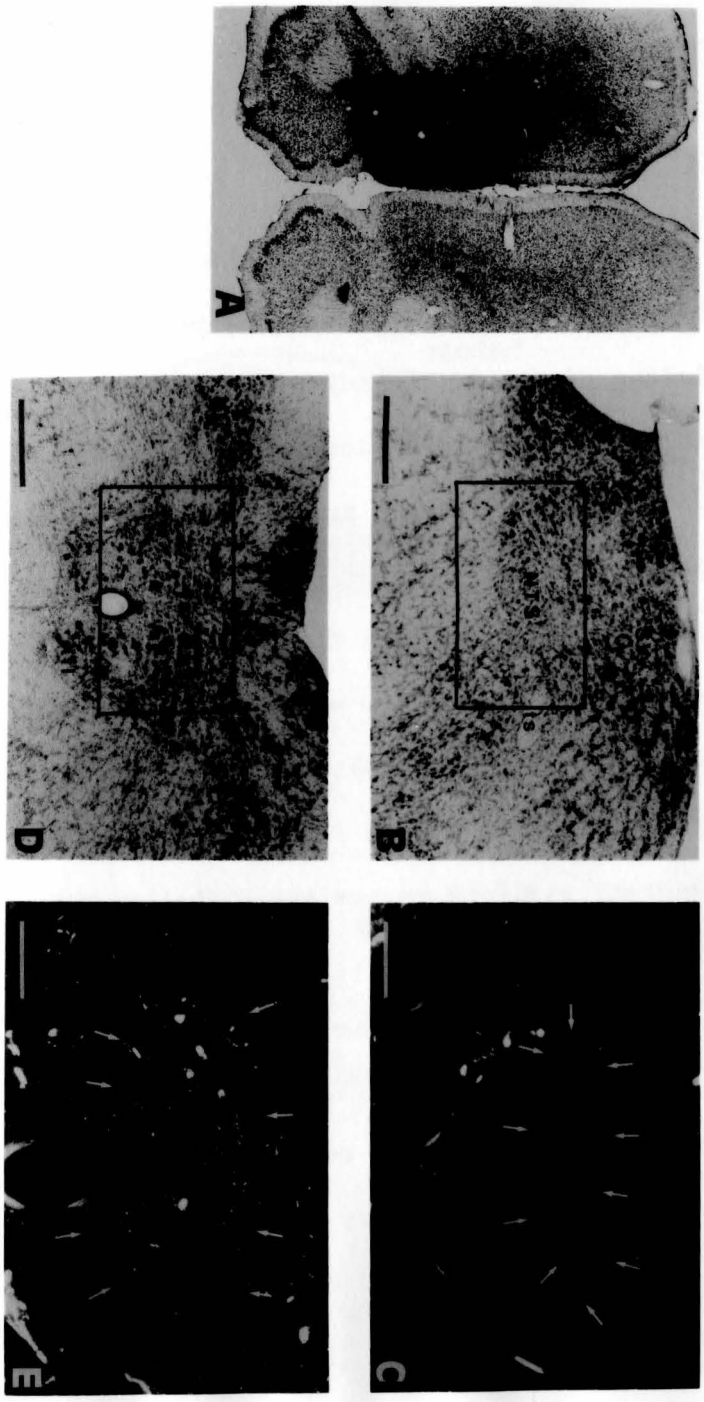
A
B
D
C
E

Figure 4.

Schematic diagram of the topographic organization of the rat medial frontal cortex (MFC). Arrow heads indicate the borders between the functional subdivisions of the MFC; which are visceral motor, frontal eye fields, somatic motor, somatic sensory, visceral sensory and olfactory sensory. The visceral motor area is made up of the pre- and infralimbic cortices, while the anterior cingulate and agranular medial areas constitute the frontal eye fields. The AgL region corresponds to somatic motor or primary motor cortex. The somatic sensory cortex is comprised of the primary and secondary somatosensory cortices. The insular cortex comprises the visceral sensory region, and the olfactory sensory piriform cortex and olfactory tubercle occupy the ventral surface of the brain. Abbreviations: AC, anterior cingulate cortex; Acb, nucleus accumbens; AgM, agranular medial cortex; AgL, agranular lateral cortex; Cl, claustrum; CP, caudate-putamen; DPC, dorsal peduncular cortex; Gr (SI), primary somatosensory cortex; Gr (SII), secondary somatosensory cortex; IL, infralimbic cortex; Ins, insular cortex; Pir, piriform cortex; PL, prelimbic cortex; tt, taenia tecta.

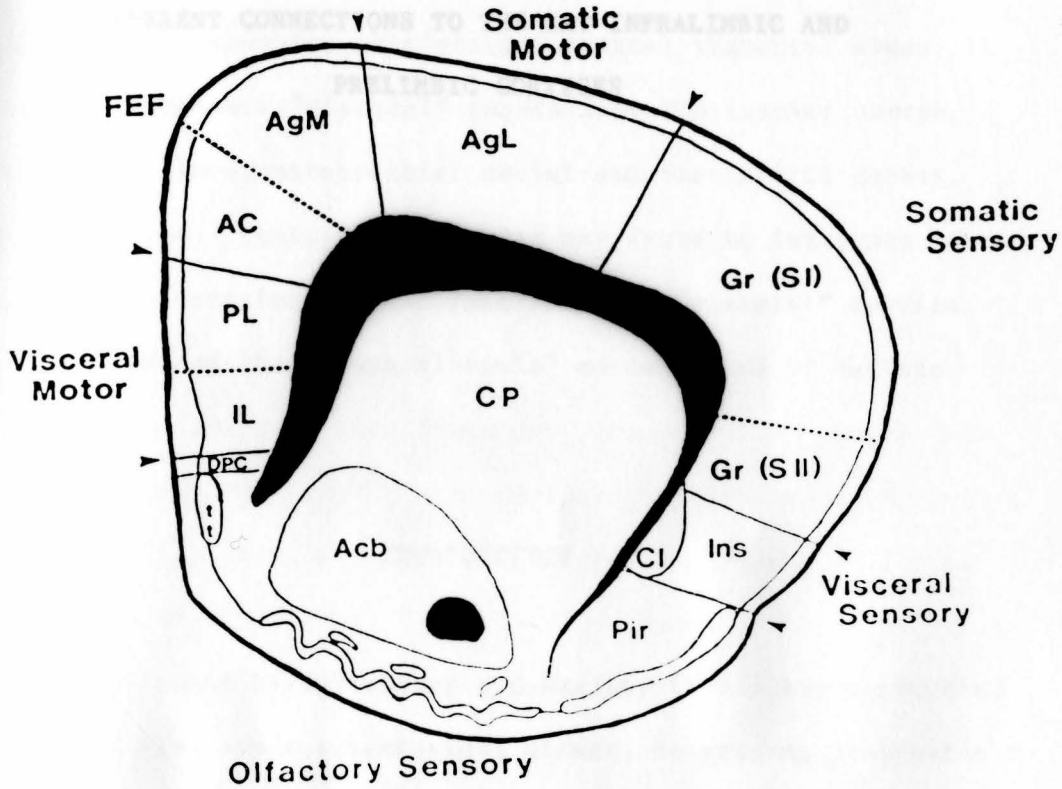
Somatic
Motor
FEF
AgM
AgL
AC
Somatic
Sensory
Gr (SI)
PL
Visceral
Motor
CP
IL
DPC
Gr (S II)
Acb
Cl
Ins
Visceral
Sensory
Pir
Olfactory Sensory

CHAPTER IV

AFFERENT CONNECTIONS TO THE RAT INFRALIMBIC AND PRELIMBIC CORTICES

ABSTRACT

Utilizing the retrograde transport properties of wheat germ agglutinin conjugated horseradish peroxidase (WGA-HRP), the afferent projections to the pre- and infralimbic cortices were determined. The infralimbic (IL) cortex located on the medial surface of the cerebral hemisphere appears to receive heavy inputs from "limbic" structures, including the hippocampus, amygdala and ventral tegmental area. IL also receives numerous "visceral" inputs from the insular cortex, lateral hypothalamus, parabrachial nuclei and the lateral dorsal tegmental nucleus. Thus, the IL cortex may serve to integrate limbic and visceral information and may function as a "visceral" cortical area, being part of the "visceral brain" as described by MacLean (1949).

INTRODUCTION

A recent study by Terreberry and Neafsey (1983) has shown that the IL cortex also has a substantial, direct, descending projection to the nucleus of the solitary tract, similar to the one described from the insular cortex. The IL cortex is the most ventral subdivision of the medial frontal cortex (MFC), a region that is part of the mediodorsal-projection cortex of the rat (Leonard, 1969; Domesick, 1972; Beckstead, 1976) and that is thought to be homologous to the

primate prefrontal cortex. At present, there is disagreement over the question of whether or not the IL cortex receives afferent projections from the mediodorsal nucleus and should be included in the rat's prefrontal cortex (Krettek and Price, 1977a; Sarter and Markowitsch, 1983). The present study investigated the afferent connections to the IL region of the rat MFC utilizing the retrograde transport of wheat germ agglutinin conjugated horseradish peroxidase (WGA-HRP). The primary goal of this study was to define the functional characteristics of this part of the medial frontal cortex, based on afferent inputs to this region.

MATERIALS AND METHODS

A total of 13 adult Long Evans male rats (300-500 grams) was used in this study. Thirty animals received injections of wheat germ agglutinin conjugated to horseradish peroxidase (WGA-HRP) into the medial frontal cortex (MFC).

Animals were anesthetized with Ketamine HCl (100 mg/kg, IP; supplemental doses of one-quarter the initial dose were given when necessary to maintain a constant level of anesthesia) and then placed into a stereotaxic frame. A heating pad controlled by a rectal temperature probe was used to maintain the animal's body temperature between 36-38 degrees celcius. Following surgical exposure of the skull and the neck musculature, the cisterna magna was opened in order

to allow the cerebrospinal fluid to drain and thus, prevent cortical swelling. A small, 2x2 mm piece of calvaria overlying the left MFC was then removed using a low-speed drill. The dura was removed from the exposed cortex, and the cortex bathed in warmed mineral oil.

A 1.0 ul Hamilton syringe fitted with a glass pipette (tip diameter 50 um) was filled with a 1% WGA-HRP (Sigma) solution in 0.9% saline. The syringe was mounted on a Kopf micromanipulator which was used to position the pipette just lateral (0.2-0.6 mm) to the midline, to a depth of 3.0-4.0 mm from the cortical surface at points 3.0-4.0 mm rostral to bregma. Pressure injections of 0.01-0.03 ul of WGA-HRP were performed over a 15-20 minute period, after which time the pipette was withdrawn and the wound sutured closed.

After a 48 hour survival time, the animals were reanesthetized with sodium pentabarbitol (40 mg/kg, IP) and transcardially perfused with 0.9% saline, 1% glutaraldehyde - 4% paraformaldehyde and finally with a 10% buffered sucrose solution according to the procedure of Rosene and Mesulam (1978). The brains were removed, placed in a cold 30% sucrose phosphate buffer solution and allowed to sink (2-3 days). Frozen sections 50 um thick were cut coronally on a sliding microtome, and two alternating series of sections collected. Both sets of sections were reacted with tetramethylbenzidene (TMB) using either Mesulam's (1978) procedure or a recent modification of Mesulam's procedure (Gibson et al., 1984) that reduces the artifact that can occur with TMB histochemistry. The TMB reactions were stopped, and

the sections were rinsed and mounted from cold sodium acetate buffer (pH 3.3) onto subbed slides. The sections were oven dried overnight (temperature between 50-60 degrees celcius). One set was rapidly dehydrated in a graded series of ethanol, cleared in xylene and coverslipped using Depex. The second set of sections was counterstained in 1% pyronin Y, rapidly dehydrated and coverslipped using Depex. The counterstained series were used to determine the cytoarchitectonic and nuclear boundaries.

Each section was examined under brightfield, darkfield and polarized light microscopy for the presence and localization of retrogradely labeled neurons. These data were plotted on a series of line drawings of each brain (400 um intervals) that were drawn utilizing a camera lucida drawing tube attached to an Olympus BH-1 microscope. For illustration purposes these data were then replotted onto a series of "standard" coronal sections traced from the Paxinos and Watson (1982) stereotaxic atlas.

RESULTS

In 10 WGA-HRP experiments the injection site involved the infralimbic (IL) cortex. Three of these were very large injections and also included portions of the anterior cingulate (AC), prelimbic (PL), and IL cortices (Figures 1A-C). In four, cases the injection sites were located primarily in the AC and PL cortices, with only a

small involvement of the dorsal IL region (Figures 1D-G). Three other cases involved the PL and IL cortices, with little or no involvement of the AC cortex (Figures 1H-J, 2B). Three other injections were centered in the PL cortex only, with only a slight involvement of the IL and AC cortices (Figures 1K-M, 2A). By comparing the set of structures labeled by injections involving IL to those labeled after involvement of adjacent areas, the connections characteristic of the infralimbic cortex were determined. Minor differences in labeling patterns appeared to be due to the exact placement of the injections. The afferent projections to the prelimbic and infralimbic cortices will be illustrated chiefly by references to two experiments, HRP RT 40 (Figures 2A, 3-5) which involved only the PL region and HRP RT 46 (Figures 2B, 6-8) which involved the PL and IL regions. These two cases illustrate results typical of two or three cases of each type of injection into the MFC.

HRP RT 40 (PL)

In the cerebral cortex retrogradely labeled neurons were seen ipsilaterally in layers II and V in the infralimbic (IL), prelimbic (PL) and dorsal anterior cingulate (ACd) areas (Figures 3A,B), as well as in the deeper layers of the ventral anterior cingulate (ACv) area (Figure 3C). Cells in the ipsilateral ventral agranular insular cortex and underlying claustrum also were labeled after a prelimbic injection (Figures 3B,C). In addition, a few labeled neurons were

also seen in the supragranular layers of the ipsilateral visual cortex, area 18 (Figures 3F,G). Contralateral to the injection site, labeled neurons were seen in the homotypic PL cortex (Figures 3A,B). Labeled neurons were also seen bilaterally in the deeper layers of the insular cortex (Figure 3B). A substantial number of retrogradely labeled pyramidal cells were also seen in the ventral subiculum and adjacent portions of the ipsilateral hippocampal formation (Figures 3G-I, 5B).

Only a few retrogradely neurons were seen in ventral forebrain structures after a PL injection, and these were found ipsilaterally in the ventral pallidum (VP, not illustrated) and the horizontal nucleus of the diagonal band (HDB, not illustrated). However, the ipsilateral basolateral nucleus of the amygdala (BLa) contained numerous heavily labeled neurons in its central portion (Figures 3E,F, 5A).

Within the dorsal thalamus, several nuclei contained retrogradely labeled cells after this PL injection. These included the anteromedial (AM, Figures 3D, 4B), anteroventral (AV, Figure 3D) and parataenial (Pt, Figures 3D-F, 4A) nuclei, as well as the nucleus reuniens (Re) and the rhomboid (Rh) nucleus located just dorsal to nucleus reuniens (Figures 3E,F, 4B). As expected, the lateral segment of the mediodorsal (MD) nucleus contained labeled cells (Figures 3E,F, 4D). Within the intralaminar nuclei, a small number of retrogradely labeled neurons were seen in the centromedial (Cem), paracentral (PC) and centrolateral (CL) nuclei (Figures 3E,F, 4C). The zona incerta

(ZI) showed only a few labeled neurons, at its caudal extent (Figure 2F). In the hypothalamus, a few labeled neurons were seen in the ipsilateral lateral hypothalamus (LH, Figure 3D).

Retrogradely labeled neurons were also seen in numerous brainstem nuclei following a PL injection. In the midbrain, the ventral tegmental area (VTA) contained a few labeled cells (Figures 3G-I), as did the caudal linear nucleus of the raphe (CLi, Figure 3J) and the dorsal raphe (DR, Figures 3K,L). Pontine structures with labeled neurons included the nucleus cuneiformis (Cun, Figure 3L), lateral dorsal tegmental nucleus (LDTg, Figures 3K, 5C) and the locus coeruleus (LC, Figures 3M, 5D). No labeled cells were seen in any brainstem structure caudal to these levels following a PL injection.

HRP RT 46 (PL/IL)

The pattern of cortical labeling seen after an injection of the PL/IL region was similar to that just described, with two notable differences. First of all, the labeling seen in the insular cortex and underlying claustrum was much denser than that seen in the previous experiment, and the label extended much farther caudally (Figures 6B-H). The second difference was that numerous labeled neurons were seen in the entorhinal cortex following a PL/IL injection (Figures 6F-H), whereas no label was seen in the entorhinal cortex after a PL injection (Figures 3F-H). The CA1 and CA2 portions of the ipsilateral hippocampal formation contained many retrogradely labeled

pyramidal cells, as did the ipsilateral ventral subiculum (Figures 6G,H, 8C).

As before, retrogradely labeled neurons were seen in the ipsilateral VP (Figure 6D) and HDB (Figure 6C), but the number of labeled cells in both of these areas was greater than that seen after a PL injection. Additionally, labeled cells were seen in the ventral division of the vertical nucleus of the diagonal band (VDBV, Figure 6C) and in the lateral preoptic area (LPO, Figures 6C,D).

Within the amygdala the BLa contained densely packed, heavily labeled neurons throughout its rostral-caudal extent (Figures 6E,F, 8A). The basomedial (BM) and lateral (La) subnuclei of the ipsilateral amygdala also contained a few scattered labeled neurons (Figures 6E,G).

Within the thalamus, the ipsilateral AM, Pt, MD, Rh, Re and intralaminar (Cem, CL) nuclei all contained retrogradely labeled cells (Figures 6D-F, 7A-C), similar to the results of the PL injection. In addition, the ventromedial (VM), submedius (SM) and paraventricular (PV) nuclei also were labeled after a PL/IL injection (Figures 6D-F, 8A,D), and the lateral dorsal (LD) and ventrolateral (VL) nuclei also contained a few scattered labeled cells (Figure 6E). The ZI contained slightly more labeled cells after a PL/IL injection than were seen following a PL injection (Figures 6E-G). The ipsilateral LH contained retrogradely labeled neurons throughout its rostral-caudal extent (Figures 6E-G). At the level of the diencephalic-mesencephalic

junction, numerous retrogradely labeled neurons were seen in the area medial to the parafascicular nucleus (Figures 6F, 8B); this region appears to be the rostral extension of the periaqueductal gray (PAG). Also at this level, numerous labeled cells were seen in the ipsilateral prerubral field (PR, Figure 6G).

Within the brainstem following the PL/IL injection, various nuclei contained retrogradely labeled neurons. These included the VTA (Figures 6G-I, 8D), CLi (Figure 6J) and the DR (Figures 6K,L) in the midbrain; the labeling of the VTA and DR was heavier than the labeling seen after a PL injection. Also labeled were cells in the PAG (Figures 6I-K), median raphe (MnR, Figures 6K,L) and the raphe pontis (RPn, Figures 6M, 8E,F). The retrorubral field (RRF) contained numerous labeled cells (Figure 6J), as did the oralis division of the pontine reticular nucleus (PnO, Figures 6K,L) where the labeling was bilateral. Labeled cells were also seen bilaterally within the pontine LDTg and LC nuclei after this injection (Figure 6M). The parabrachial nuclei (PBN) also contained a few retrogradely neurons after a PL/IL injection; and this label was bilateral, within both the ventral (medial) and dorsal (lateral) subdivisions of the PBN (Figures 6L,M).

Summarizing the data from the two experiments presented, Table 1 provides a comparison of the relative amounts of retrograde labeling seen in various areas after each type of injection. With a few exceptions this table illustrates the agreement concerning the

afferents to IL between the WGA-HRP results after a PL/IL injection and the results of a PL only injection.

DISCUSSION

Afferents to IL

The results of the present study indicate that the IL region receives inputs from numerous areas of the neuraxis and that many of the structures which project to IL may be considered to be either limbic or visceral structures. The data suggest that the IL region may serve to integrate limbic and visceral inputs and the results of stimulation studies indicate that this region may act as a "visceral cortical" representation, in much the same way as the insular cortex serves as a "visceral sensory" area.

Limbic Inputs to IL

Limbic afferents to IL demonstrated by the present study include the projections from the basal forebrain (VDBV), the hippocampus, the mediodorsal, reuniens, anteromedial and parataenial thalamic nuclei, the amygdala and the ventral tegmental area. All these structures have been classified as parts of the limbic system by various authors (MacLean, 1952; Heimer and Wilson, 1975; Herkenham, 1978; Kelley and Stinus, 1984; Loughlin and Fallon, 1984). Figure 9A illustrates these limbic afferents to IL.

Within the basal forebrain, only injections of the prelimbic region resulted in labeling of the horizontal division of the diagonal band (HDB) while labeled neurons were observed in both the vertical and the horizontal limbs of the diagonal band after IL injections. These data agree with that of Lamour et al. (1984) in the rat and Irle and Markowitsch (1984) in the cat which showed that IL received projections from both the HDB and VDBV but that the projection from the VDBV was heavier. Similarly, Saper (1984) reported that the IL/PL region of MFC receive projections from the dorsolateral margin of the HDB, a region corresponding to what we term the VDBV (see Figure 5C; pg. 326, Figure 9 of Saper, 1984). However, Irle and Markowitsch (1984) also reported a distinct projection from the substantia innominata to the IL region in the cat, but our data did not show this projection to be very significant in the rat, in agreement with Lamour et al. (1982, 1984).

The labeling of the hippocampal formation after IL injections, specifically within the ventral portions of CA1 and CA2 and the ventral subiculum, confirms earlier findings. Studies utilizing both retrograde transport of fluorescent dyes and the anterograde transport of tritiated amino acids have shown that the IL cortex receives direct afferents from the ventral portions of the hippocampal formation (Swanson and Cowan, 1977; Swanson, 1981). In contrast, the labeling of the entorhinal cortex after an injection of the PL/IL region is likely due to spread of the injection site into the taenia tecta (tt),

located just ventral to the IL cortex. Heavy reciprocal projections between the ventral taenia tecta (vtt) and the entorhinal cortex have been previously reported (Haberly and Price, 1978; Wyss and Sripandikulchai, 1983), but these studies did not find entorhinal projections to IL.

Concerning the limbic nuclei of the dorsal thalamus, our data confirm previous reports which have demonstrated thalamocortical projections to the IL cortex from the nucleus reuniens (Powell and Cowan, 1954; Jones and Leavitt, 1974; Krettek and Price, 1977a; Herkenham, 1978) and parataenial (Pt) nucleus (Powell and Cowan, 1954; Jones and Leavitt, 1974; Kelley and Stinus, 1984). Several studies have also described projections from the anteromedial (AM) nucleus to IL cortex (Domesick, 1969; Beckstead, 1976; Guldin et al., 1981). However, there is presently some disagreement over whether or not the mediodorsal (MD) nucleus projects to IL. Several studies have denied such a projection (Beckstead, 1976; Krettek and Price, 1977a; Saper, 1982a) while several recent studies have reported the existence of a direct MD-IL projection (Guldin et al., 1981; Sarter and Markowitsch, 1983, 1984). Our data seem to support the latter groups. After injections involving the IL cortex, we observed retrogradely labeled neurons in both the lateral and medial portions of MD. The label in the lateral segment confirms numerous earlier reports that lateral MD projects to PL regions of the medial prefrontal cortex (Leonard, 1969; Domesick, 1972; Beckstead, 1976; Krettek and Price, 1977a). The label

in the medial segment of MD confirms earlier reports by Sarter and Markowitsch (1983, 1984) in rats and by Guldin et al. (1981) in the mouse that MD projects to IL. Thus, it appears that the label seen in the medial segment of MD does represent a real population of cells that project to the IL cortex, but this projection is much sparser than the projections from lateral MD to PL and from medial MD to the insular cortex. This MD-IL projection may in fact be reciprocal, because in our material we have observed what appears to be anterograde terminal label in medial MD after IL injections and, in addition, in a recent study by Young et al. (1984) retrogradely labeled neurons were seen in IL cortex after injections of fluorescent dyes into MD (see their Figure 5).

Of the limbic thalamic nuclei that project to IL, the reuniens nucleus is noteworthy because it appears to receive afferent input from the parabrachial nucleus (PBN). It has been reported that the PBN projects directly to Re and the gustatory nucleus of the thalamus (Norgren and Leonard, 1973; Norgren, 1976; Herkenham, 1978). Of particular interest is the fact that the region of the PBN that projects to Re seems to receive general visceral afferent information from the NTS (Herkenham, 1978; Ricardo and Koh, 1978). Thus, there exists a multisynaptic pathway by which general visceral afferent information may reach the IL cortex; the pathway consists of the projection from the NTS to PBN, the projection from PBN to Re and finally the thalamocortical projection from Re to IL.

Labeling seen in the basolateral nucleus of the amygdala (BLa) after PL/IL injections was consistent with previous reports which have described direct projections from the posterior portions of the BLa to PL and IL regions in the MFC (Krettek and Price, 1977b; Price, 1981; Sarter and Markowitsch, 1983, 1984). A similar projection was found to exist in cats, originating from the basal magnocellular nucleus of the feline amygdala (Llamas et al., 1977; Macchi et al., 1978).

Of the numerous brainstem regions exhibiting retrogradely labeled cells after IL injections, the ventral tegmental area (VTA) may be considered a limbic structure. The VTA is considered to correspond to the A10 dopaminergic cell group (Dahlstrom and Fuxe, 1964; Lindvall et al., 1974) and is the source of the mesolimbic dopaminergic projection to the medial frontal cortex (Lindvall et al., 1974; Simon et al., 1979; Loughlin and Fallon, 1984). A second dopaminergic cell group, A9, corresponding to the substantia nigra (SN) also contributes dopaminergic input to the MFC (Loughlin and Fallon, 1984), but our data were inconclusive as to whether or not the SN projects directly to the IL region of MFC.

Visceral Inputs to IL

Visceral afferents to IL include the projections from the insular cortex, the paraventricular nucleus of the thalamus, the lateral hypothalamus, the parabrachial nucleus and the lateral dorsal tegmental nucleus. All of the structures listed above do have direct

connections with the NTS (Ricardo and Koh, 1978; Saper, 1982a), and this is the basis for classifying them as visceral. Figure 9B illustrates these visceral afferents to IL.

The IL region receives a substantial bilateral input from the insular cortex. These findings are in agreement with the findings in the rat (Saper, 1982a; Markowitsch and Guldin, 1983) and in the hamster (Reep and Winans, 1982a,b) that the insular cortex has substantial reciprocal connections with the IL region of the MFC. Our data showing that homotypical cortical areas of IL and PL are interconnected by callosal projections confirm the similar findings of Markowitsch and Guldin (1983).

Our data indicate that the paraventricular (PV) nucleus of the thalamus projects to IL. To our knowledge this is the first study to report a direct PV-IL connection. This projection is relatively small but it is interesting because PV is known to receive direct ascending inputs from the NTS (Ricardo and Koh, 1978). Thus, visceral afferent information may reach IL via several routes. The first being directly from the NTS to PV and then to IL. A second slightly more circuitous route for visceral afferent information to take is from the NTS to the PBN, from there visceral information may reach the reuniens nucleus of the thalamus or the insular cortex, both areas that project to IL. A third route involves projections from the NTS to the PV thalamic nucleus which in turn has projections to BLa which projects to IL.

The lateral preoptic area (LPO) of the forebrain also exhibited

retrogradely labeled cells after IL injections. Kita and Oomura (1981) demonstrated a similar finding after HRP injections into the rat prefrontal cortex. Also consistent with Kita and Oomura (1981) was the finding of retrogradely labeled cells in the lateral hypothalamus after IL/PL injections.

Of the numerous brainstem regions exhibiting retrogradely labeled cells after IL injections, the lateral dorsal tegmental nucleus (LDTg) and the parabrachial nucleus (PBN) are most notable. The LDTg located in the dorsal pons appears to send a direct projection to the IL cortex. This finding confirms an earlier report that demonstrated retrograde labeling of neurons in the LDTg after WGA-HRP injections of the IL cortex (see Saper 1982b, Figure 2, #R27). Groenewegen and van Dijk (1984) reported that the dorsal tegmental region (including both the dorsal tegmental nucleus of Gudden and the dorsolateral tegmental nucleus) projects to the "medial frontal cortex," but these authors did not elaborate as to which subdivision(s) of the MFC receives these projections.

The PBN in the dorsolateral pons appears to send only a minor projection to the IL cortex. This finding was surprising due to the fact that the PBN is known to project heavily to the "visceral sensory" insular cortex in rats (Saper and Loewy, 1980; Saper, 1982b; Fulwiler and Saper, 1984). Utilizing autoradiographic anterograde tracing techniques, contradicting results on PBN-IL projections have been reported (Saper and Loewy, 1980; Saper, 1982b). However,

recently a third study, utilizing retrograde transport of HRP has demonstrated a small projection from the medial PBN to the ventralmost portion of the IL cortex, immediately adjacent to the taenia tecta (Fulwiler and Saper, 1984). This finding is consistent with our data that if the ventralmost portion of the IL region is involved in the injection, a few retrogradely labeled cells are seen in the PBN. If the ventral IL is not involved in the injection, then no labeled cells are seen in the PBN.

Other Inputs to IL

There are several areas that project to IL that do not fit into either the limbic or visceral category. These include the anterior cingulate cortex, the claustrum, the ventromedial and submedius thalamic nuclei, the area medial to the parafascicular nucleus, the locus coeruleus and the various raphe nuclei that project to IL.

Reep (1983) reported that in the hamster, area 24, the anterior cingulate cortex (AC) also projects to the IL region. We did see labeled cells in AC after our injections but due to spread of tracer along the pipette track, which traversed the AC cortex, it was difficult to interpret the label seen in the AC region. Therefore, from the present study it is not clear whether the AC region of the rat cortex projects to IL or not.

Two additional cortical areas exhibited retrogradely labeled cells after injections of the MFC, but this labeling seems to be due

to spread of the injection site to adjacent cortical areas outside of IL. Area 18 of the visual cortex showed a few labeled cells which can be attributed to involvement of the AC region of the MFC. The medial precentral cortex, corresponding to the agranular medial cortex defined by Donoghue and Parham (1983) and possibly representing the rodent homolog of the frontal eye fields (Leonard, 1969; Hall and Lindholm, 1974; Neafsey and Sievert, 1982) receives direct projections from visual cortex (Miller and Vogt, 1984; Reep et al., 1984).

In our data, we found retrogradely labeled neurons in the dorsal claustrum, and this label seems to be due to involvement of the dorsally located AC region and not due to IL involvement. With respect to this labeling seen in the claustrum, several recent studies are noteworthy. In an HRP study of afferent connections to the medial precentral (Pcm) region of the MFC in the rat, numerous retrogradely labeled neurons were seen in the ipsilateral claustrum after Pcm injections (Reep et al., 1984). A similar study showed that the claustrum projected to both anterior and posterior cingulate cortices, areas 24 and 29, respectively (Finch et al., 1984). In the cat a similar claustral-cingulate projection, with substantial projections to the cingulate, retrosplenial, entorhinal and subicular cortices, arising from the dorsal claustrum has been reported (Markowitsch et al., 1984).

Several studies have described widespread projections from the ventromedial (VM) nucleus, including projections to IL (Herkenham,

1979; Kolb, 1984). The submedius (SM) nucleus has also been shown to project to IL (Powell and Cowan, 1954; Jones and Leavitt, 1974; Krettek and Price, 1977a). The SM has been associated with pain, receiving direct afferent inputs from the spinal cord (Craig and Burton, 1981).

The locus coeruleus (LC) corresponds to the A6 region of the brainstem containing norepinephrine synthesizing neurons (Dahlstrom and Fuxe, 1964), and it has been shown that LC projects to almost the entire neocortex, including the medial frontal cortex (Jones and Moore, 1977). Thus, the IL region receives a direct noradrenergic input from LC. The IL cortex also receives direct serotonergic inputs from the raphe nuclei, particularly the dorsal raphe (DR). The DR, containing serotonergic cell bodies, projects to widespread regions of the central nervous system, including the IL cortex (Conrad et al., 1974).

A summary of the major afferent inputs to the IL cortex is shown in Figure 9. On medial views of a sagittal section of the rat brain the afferents to IL are schematically represented. Figure 9A illustrates the limbic afferents to IL while Figure 9B illustrates the visceral afferents to IL. Not all the IL afferents are shown; excluded from the figure are the inputs from the insular cortex, VM and SM thalamic nuclei, the retrorubral field, the area medial to the parafascicular nucleus, the locus coeruleus and the raphe nuclei. Limbic inputs to IL include the ventral division of the vertical limb

of the nucleus of the diagonal band (VDBV) and the basolateral amygdala (BLa). The ventral CA1 field of the hippocampal formation (CA1), along with the ventral subiculum also project heavily to IL. Limbic thalamic inputs to IL arise from the parataenial (Pt), anteromedial (AM), reuniens (Re), rhomboid (Rh) and to a small degree the mediodorsal nucleus (MD). Brainstem afferents include the ventral tegmental area (VTA). Visceral inputs to IL include insular cortex (not illustrated), the lateral preoptic area (LPO) and the lateral hypothalamus (LH). Visceral thalamic inputs arise from the paraventricluar (PV) nucleus. Brainstem afferents include the lateral dorsal tegmental (LDTg) nucleus and a slight projection from the parabrachial (PBN) nucleus.

Functional Considerations

From the present account, it is evident that the IL cortex receives inputs from numerous areas of the central nervous system, many of which may be considered limbic or visceral structures. The "visceral sensory" insular cortex also receives numerous inputs which are limbic or visceral, and many of the inputs to the IL and insular cortices are similar. Table 2 attempts to represent this fact by listing those areas that project to both the IL and insular cortices (IL + INS), the IL cortex only (IL) and the insular cortex only (INS). By comparing the inputs to the IL and insular cortices, two items become evident. First, the two cortical areas receive a large number

of inputs from similar areas, implying that they both may have similar functions. Whether or not the same neurons project to both cortical areas is not known. Secondly, the majority of the inputs to IL can be classified as limbic while the insular cortex receives more visceral inputs than the IL cortex does.

The term "limbic system" was originally defined by MacLean (1952) to include phylogenetically ancient cortical structures and the subcortical nuclei that share direct connections with them. This concept was based on a combination of functional and anatomical evidence that indicated that contiguous parts of the brain are involved in the elaboration of emotional expression and that parts of this "system" may constitute what MacLean (1949) termed the "visceral brain". Since then, the contents of the "limbic system" have been steadily expanding so that many areas of the brain are now being considered to be within the "limbic system". Brodal (1981) points out that there is no consensus as to what the limits of the limbic system are, and that the term "limbic system" appears to be on its way to including all brain regions and functions.

The present study does not offer a basis for redefining the "limbic system," but does tend to reestablish and emphasize the importance of the visceral component of limbic functions. The IL cortex appears to receive heavy limbic inputs from the hippocampus, amygdala and ventral tegmental area. In the previous chapter (see Chapter III), we have shown that IL projects directly to a visceral or

autonomic structure, the nucleus of the solitary tract (NTS). Thus, the IL cortex provides a direct pathway from limbic structures to visceral or autonomic structures. Thus, the older concept of the limbic system as the "visceral brain" should not be forgotten, and the data we have presented in the present study indicate that the IL cortex may serve as a "visceral cortical region" for the limbic system.

Figure 1.

Medial frontal cortex injection sites. A set of line drawings illustrating the injection sites of thirteen WGA-HRP experiments. A-C: WGA-HRP injections that involved the AC, PL and IL regions of the MFC (RT 18, RT 51, RT 56). D-G: WGA-HRP injections that involved the AC and PL regions of the MFC (RT 19, RT 20, RT 21, RT 25). H-J: WGA-HRP injections that involved the PL and IL regions of the MFC (RT 24, RT 29, RT 46). K-M: WGA-HRP injections that involved only the PL region of the MFC (RT 39, RT 40, RT 43).

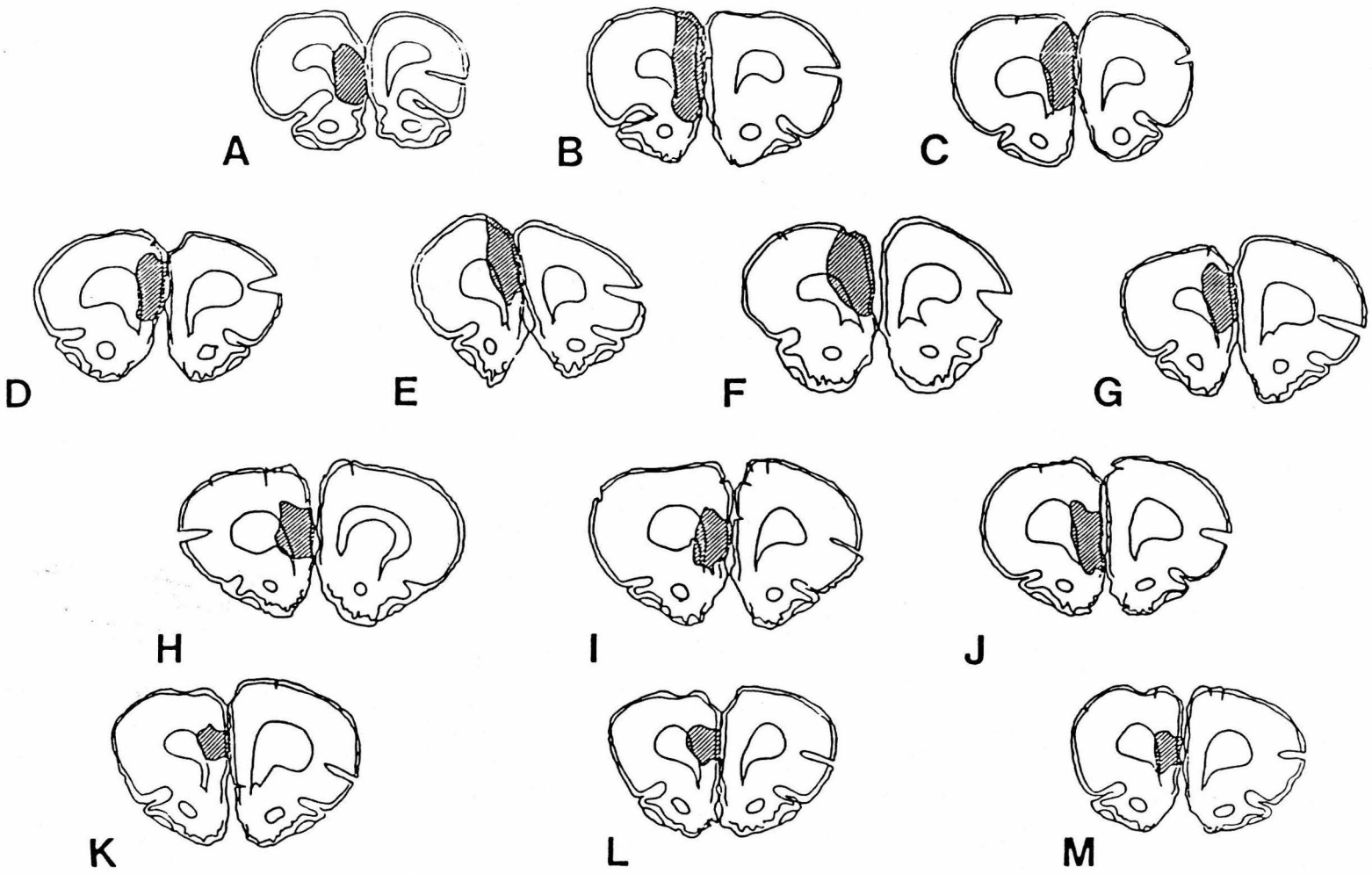
A
B
C
D
E
F
G
H
I
J
K
L
M

Figure 2.

Brightfield photomicrographs (2X) of Nissl stained coronal sections through the medial frontal cortex to illustrate the extent of the WGA-HRP injection sites described in this report. A: Experiment RT 40, involving the PL cortex. B: Experiment RT 46, involving the PL and IL cortices.

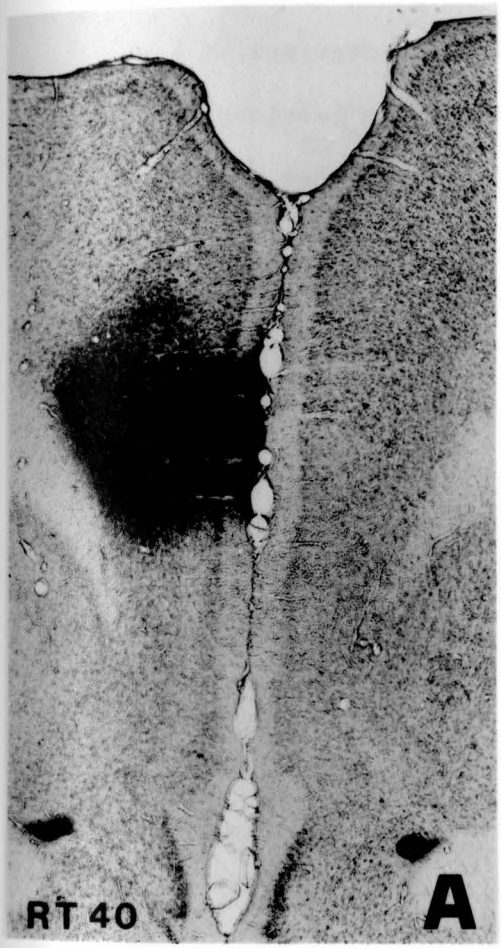
RT 40
A

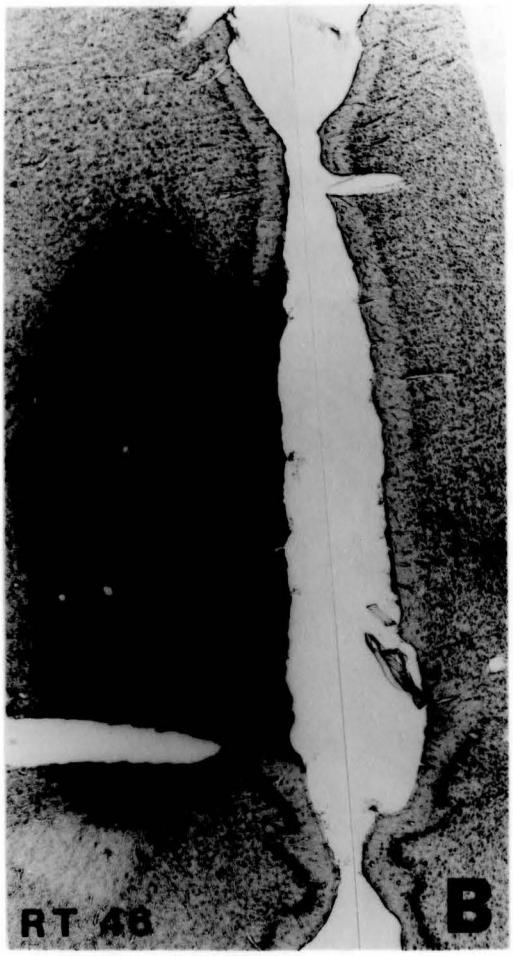
RT 46
B

Figure 3.

A-F: Rostral-caudal series of coronal outline drawings at 1 mm intervals illustrating the pattern of retrograde labeling seen after a WGA-HRP injection of PL cortex (Figure 2A). Each dot represents a single retrogradely labeled neuron.

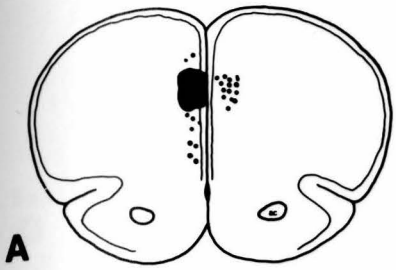

A

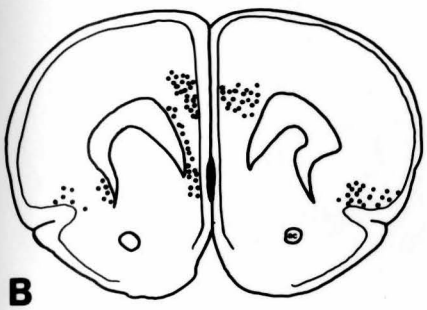

B

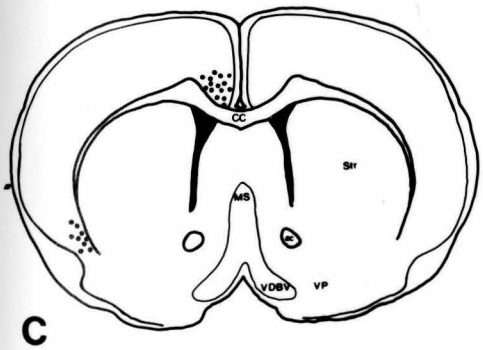
CC
Str
MS
VDBV
VP

C

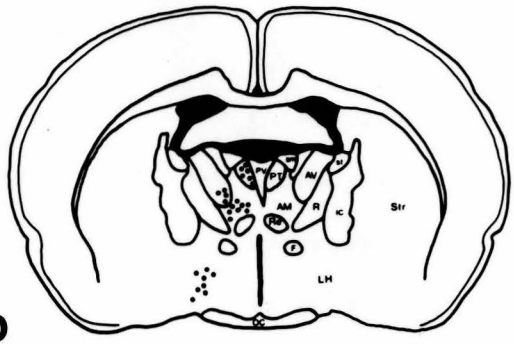
AV
AM
R
ic
Str
LH
cc

D

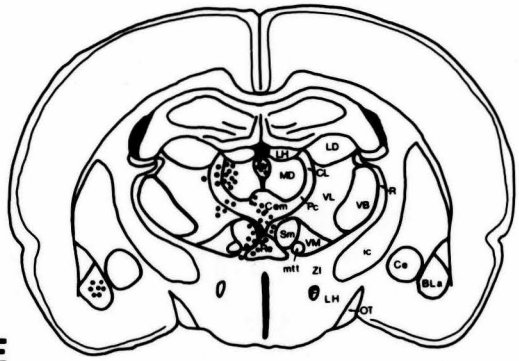
LH
LD
MD
CL
VL
Pc
VB
R
Sm
VM
mtt
ZI
ic
Ce
BLa
LH
ot

E

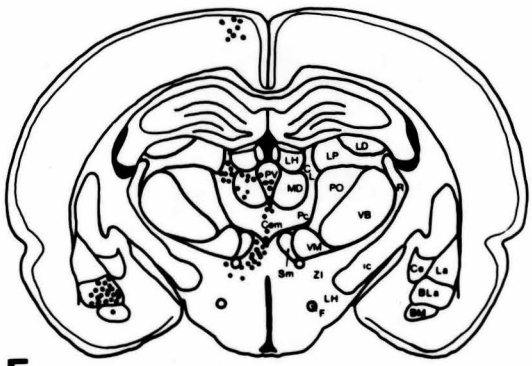
LH
LD
LP
MD
PO
Pc
VB
VM
Sm
ZI
ic
Ce
La
BLa
LH

F

Figure 3 cont.

G-N: Rostral-caudal series of coronal outline drawings at 1 mm intervals illustrating the pattern of retrograde labeling seen after a WGA-HRP injection of PL cortex (Figure 2A). Each dot represents a single retrogradely labeled neuron.

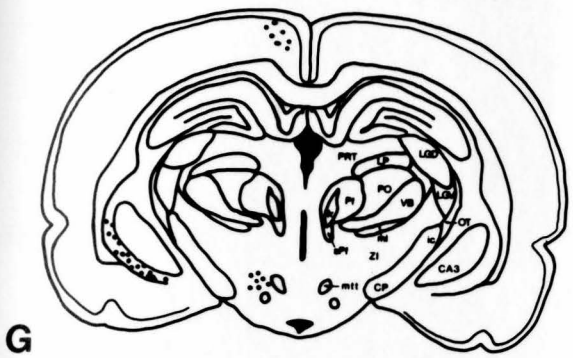
PRT
LP
LGD
Po
VB
LGM
Pn
Rt
ZI
CA3
mtt
CP

G

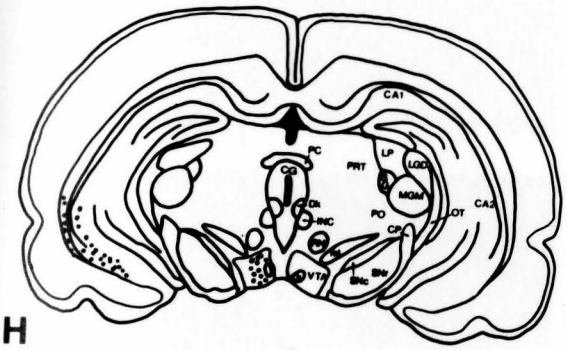
CA1
PC
PRT
LP
LGD
MGM
Po
CP
CA3
VTA
SNc

H

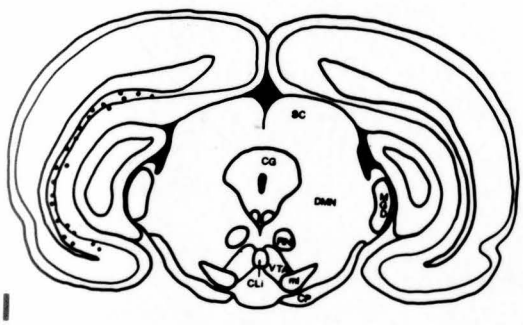
SC
CG
DMN
CLi

I

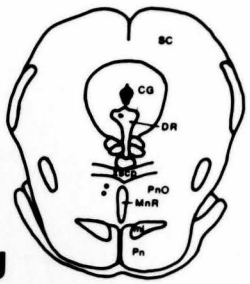
SC
CG
DR
PnO
MnR
Pn

J

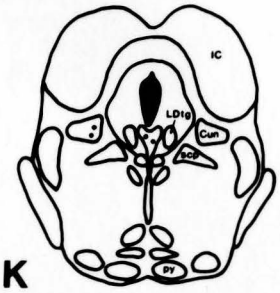
IC
LDtg
Cun
scp
PY

K

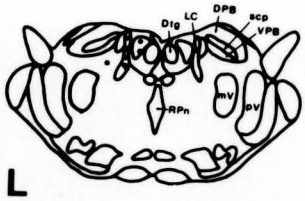
DPB
LC
Dtg
scp
VPB
RPn
mV
PV

L

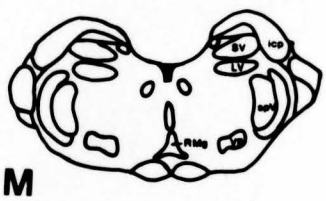
SV
LV
RMg

M

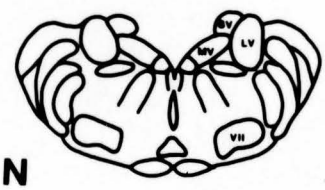
SV
LV
mV
VII

N

Figure 4.

Darkfield photomicrographs of the retrograde labeling observed in the thalamus after a PL injection (Figure 2A). The corresponding line drawing is indicated in parenthesis. A: Retrogradely labeled neurons in the parataenial (Pt) nucleus (Figure 3D). B: Retrogradely labeled cells in the rhomboid (Rh) and anteromedial (AM) nuclei. Labeled neurons are also seen in the nucleus reuniens located immediately dorsal to the rhomboid nucleus (Figure 3E). C: Retrograde labeling of neurons in the centrolateral (CL) and paracentral (PC) intralaminar nuclei (Figure 3E). D: Retrogradely labeled neurons in the lateral segment of the mediodorsal (MD) nucleus. A few labeled cells can also be seen in the medial segment of MD in the lower right of the figure (Figure 3F). Scale bars = 100 um.

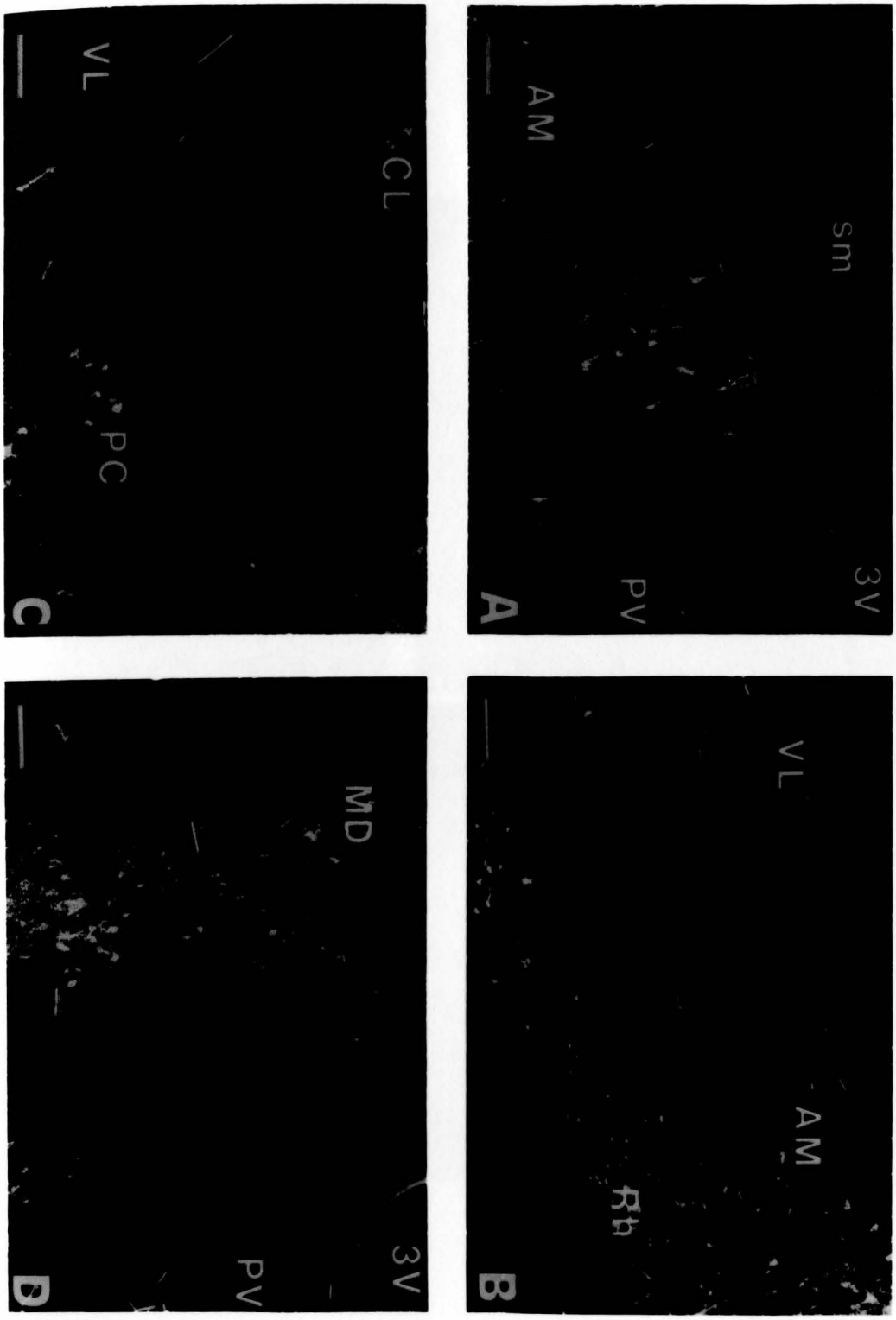
A
sm
3V
AM
PV
B
VL
AM
Rh
PV
C
CL
VL
PC
D
MD
3V
PV

Figure 5.

Darkfield photomicrographs of retrogradely labeled neurons after a PL injection (Figure 2A). The corresponding line drawing is indicated in parenthesis. A: Labeling seen in the basolateral (BLa) nucleus of the amygdala (Figure 3F).. B: Retrogradely labeled cells in the ventral CA1 region of the hippocampus. Arrows indicate labeled neurons. Medial is to the right. (Figure 3H). C: Retrogradely labeled neurons in the lateral dorsal tegmental nucleus (LDTg) in the dorsal pons (Figure 3L). D: Retrograde labeling of neurons in the locus coeruleus (LC, Figure 3L). Scale bars = 100 um.

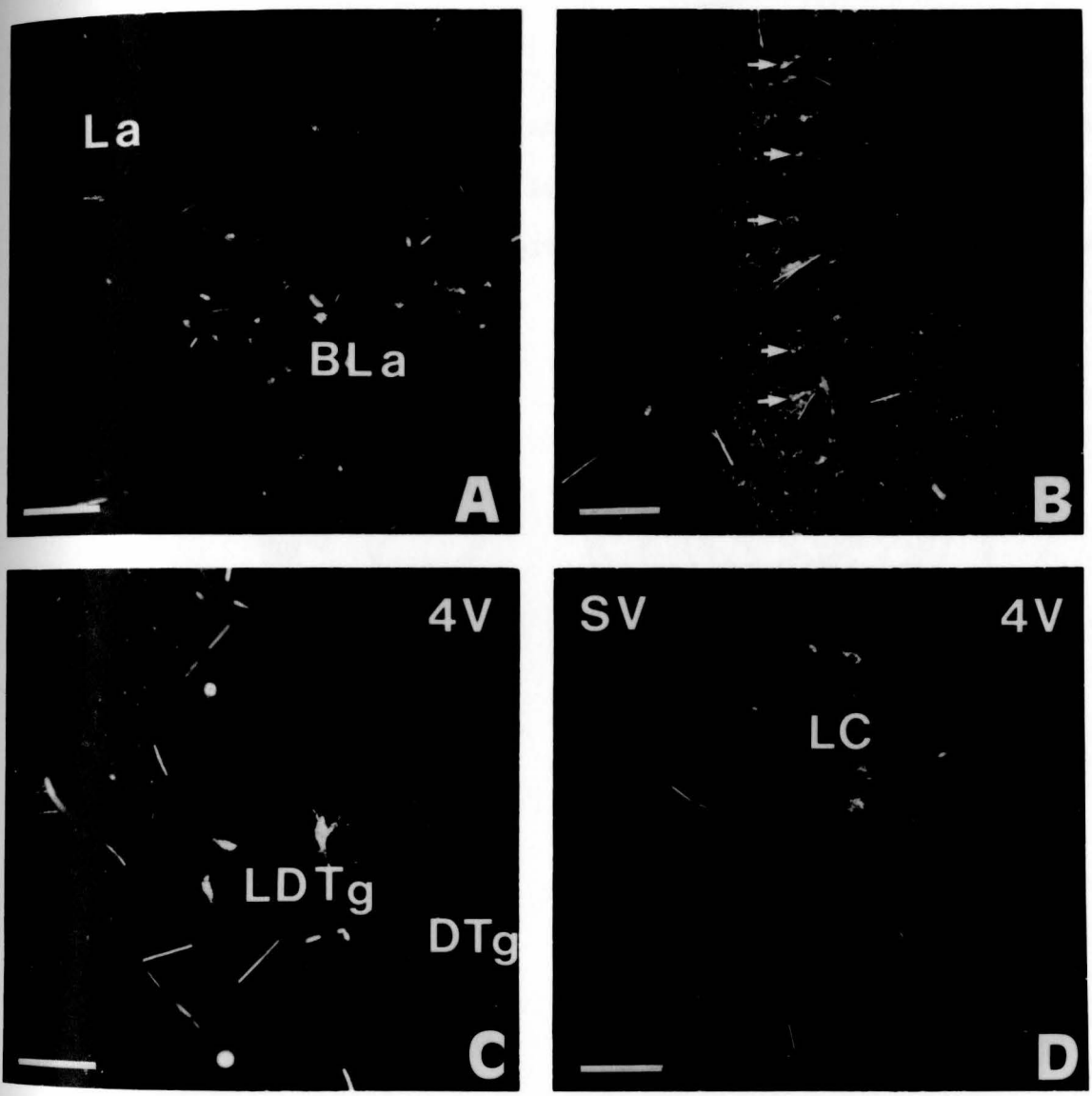
La
BLa
A
B
4V
LDTg
DTg
C
SV
4V
LC
D

Figure 6.

A-F: Rostral-caudal series of coronal outline drawings at 1 mm intervals illustrating the pattern of retrograde labeling seen after a WGA-HRP injection of PL/IL cortex (Figure 2B). Each dot represents a single retrogradely labeled neuron.

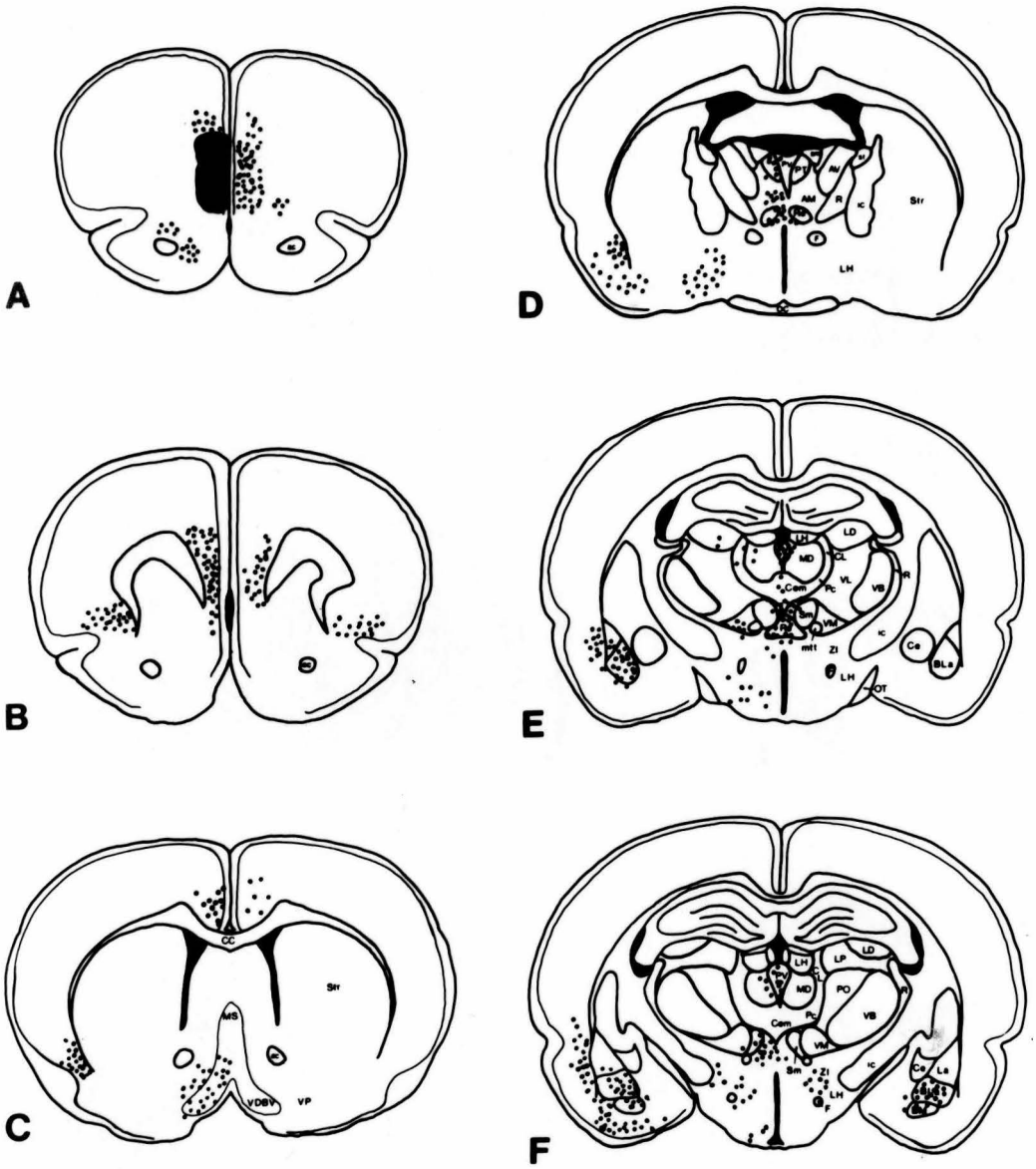
A
B
C
D
E
F
CC
Str
MS
VDB
VP
AM
AV
R
IC
LH
LD
LP
MD
PO
VL
VB
Pc
Cem
VM
Zi
mt
Ce
BLa
La
OT

Figure 6 cont.

G-N: Rostral-caudal sreies of coronal outline drawings at 1 mm intervals illustrating the pattern of retrograde labeling seen after a WGA-HRP injection of PL/IL cortex (Figure 2B). Each dot represents a single retrogradely labeled neuron.

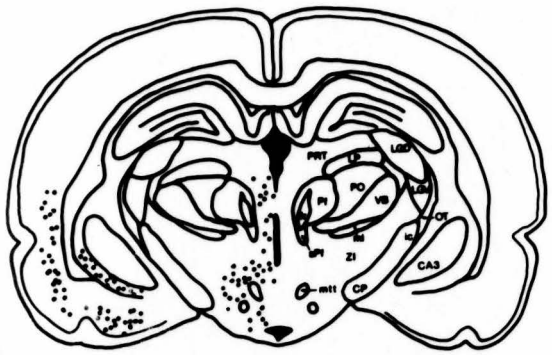
PRT
LP
LGd
PO
VB
Pt
ZI
CA3
CP
mt

G

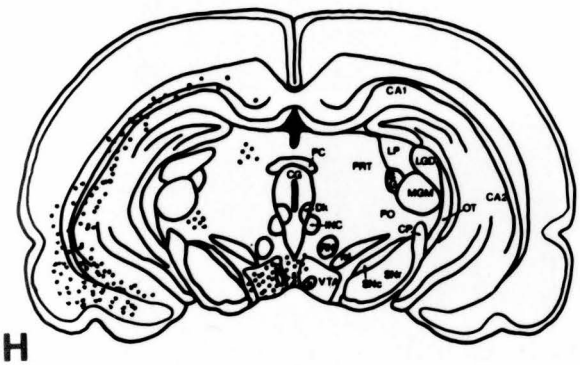
CA1
PC
LP
LGd
PRT
CG
MGm
PO
CA2
CP
SNC
SNr
VTA

H

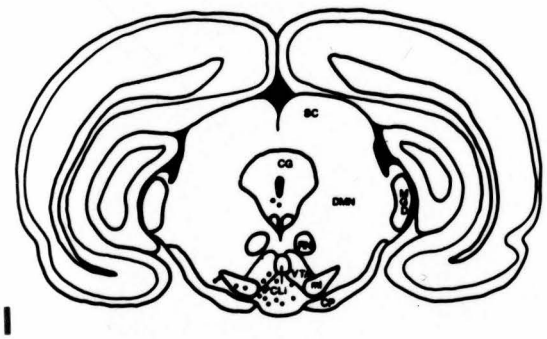
SC
CG
DMN
VTA
RN

I

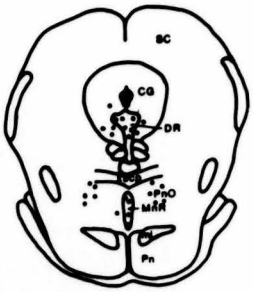
SC
CG
DR
PnO
MRN
Pn

J

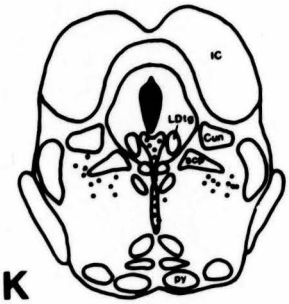
IC
LDtg
Cun
scp
PY

K

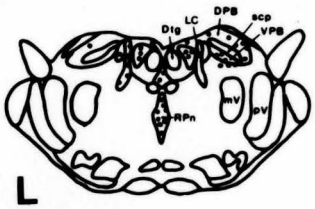
DPB
LC
Dtg
scp
VPB
RPn
MV
SV

L


SV
LV
RMg

M

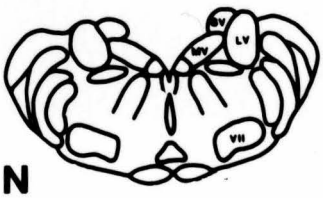
SV
LV
MN
VN

N

Figure 7.

Darkfield photomicrographs of the retrograde labeling in the thalamus seen after a PL/IL injection (Figure 2B). Corresponding line drawing is indicated in parenthesis. A: Retrogradely labeled neurons in the parataenial (Pt) and paraventricular (PV) nuclei. The retrograde labeling in Pt is difficult to see because of the heavy anterograde labeling in Pt (Figure 6D). B: Retrograde labeling of neurons in the rhomboid (Rh), reuniens (Re) and medial aspect of the ventromedial (VM) nuclei (Figure 6E). C+D: Pattern of retrograde labeling in the mediodorsal (MD) nucleus. C: Rostral MD showing label along the MD-PV junction (this level not shown in the line drawings). D: Caudal MD, labeled neurons can be seen in the medial segment of MD, as well as in the paraventricular (PV) nucleus located medial to MD (Figure 6F). Scale bars = 100 um.

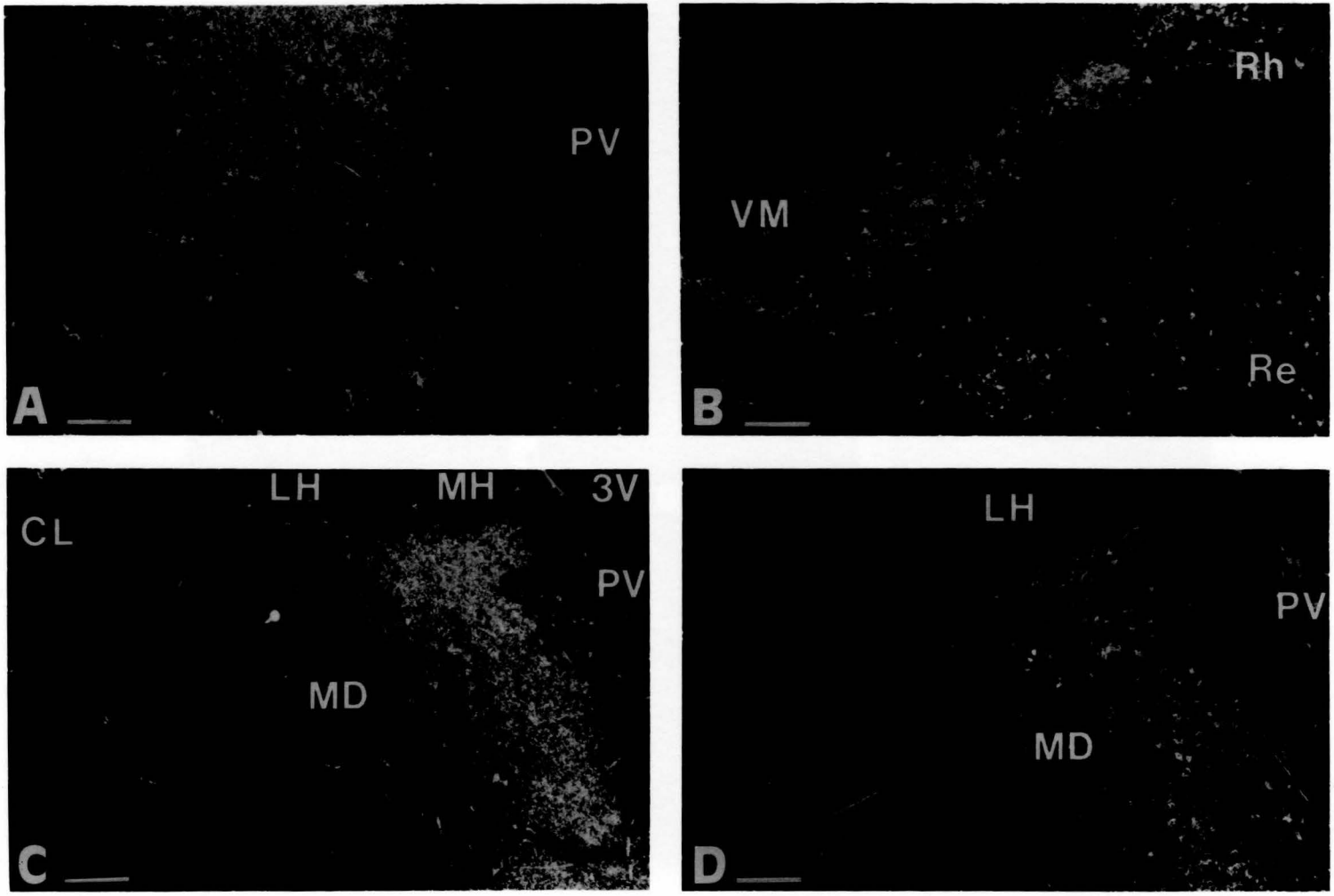
PV
A
Rh
VM
Re
B
LH
MH
3V
CL
PV
MD
C
LH
PV
MD
D

Figure 8.

Darkfield photomicrographs of retrogradely labeled neurons after a PL/IL injection (Figure 2B). Corresponding line drawing is indicated in parenthesis. A: Retrogradely labeled neurons within the amygdala. Labeled cells are localized within the basolateral (BLa) nucleus, with a few scattered neurons labeled in the lateral (La) nucleus (Figure 6F). B: Arrows indicate retrogradely neurons in the area medial to the parafascicular (Pf) nucleus. This area may correspond to the rostral extension of the periaqueductal gray (Figure 6G). C: Labeling in the ventral hippocampus, CA1 and the ventral subiculum (Figure 6H). D: Retrogradely labeled neurons in the ventral tegmental area (VTA) of the ventral mesencephalon (Figure 6H). E: Retrogradely labeled neurons in the lateral dorsal tegmental (LDTg) nucleus. Notice the absence of labeling within the dorsal tegmental nucleus of Gudden (DTg, Figure 6L). F: Labeling of cells in the locus coeruleus (LC, Figure 6L). Scale bars = 100 um.

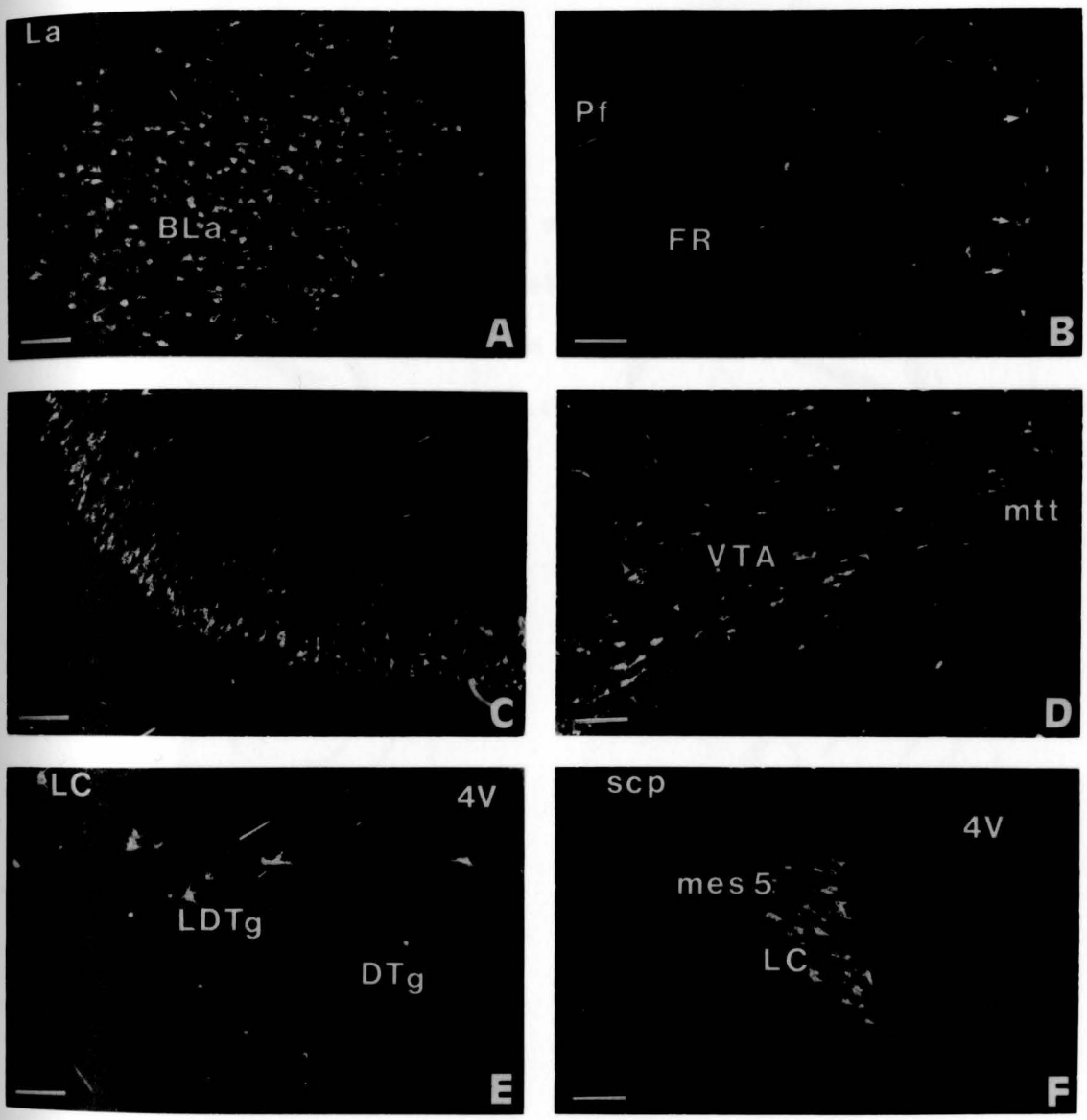
La
BLa
A
Pf
FR
B
C
VTA
mtt
D
LC
4V
LDTg
DTg
E
scp
4V
mes 5
LC
F

Figure 9.

Afferents to IL cortex

Schematic drawings of a medial view of the rat brain illustrating the major inputs to the IL cortex. Afferents not shown include the insular cortex, VM and SM thalamic nuclei, retrorubral field, locus coeruleus and raphe inputs from PnO, MnR and RPn. A: Limbic inputs to IL. B: Visceral inputs to IL. See text for abbreviations.

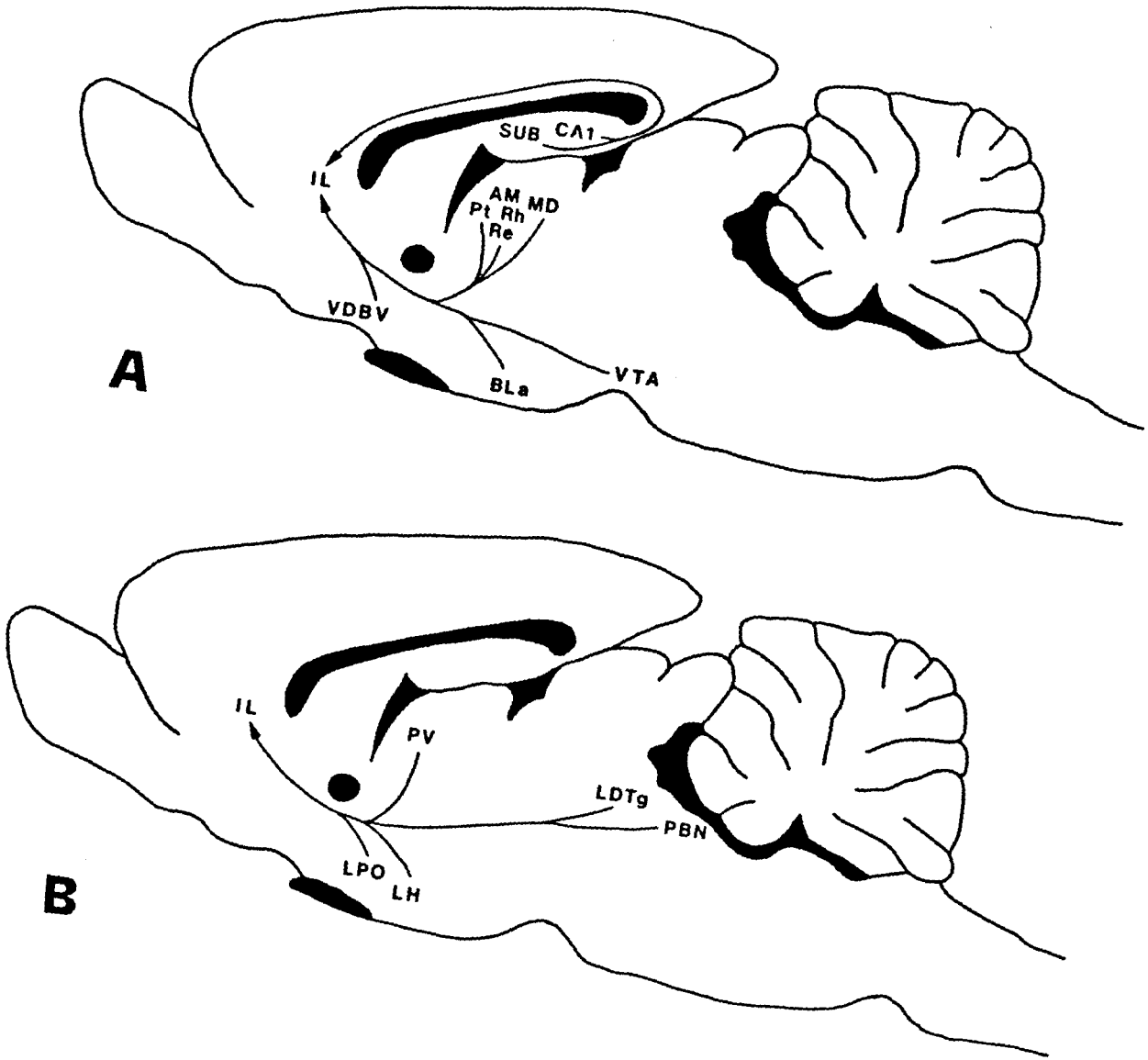
A
SUB
CA1
IL
AM
Pt
Rh
MD
Re
VDBV
BLa
VTA
B
IL
PV
LDTg
PBN
LPO
LH

Table 1.

The relative amount of retrograde labeling seen in various areas after two different MFC injections is shown in this table. The two injections correspond to HRP RT 40 and HRP RT 46, respectively. See text for abbreviations.

Table 1. Comparison of the relative amount of retrograde labeling seen after various MFC injections.

	PL (HRP)	PL/IL (HRP)
insular cortex	+	+++
hippocampus	+++	+++
lat. preoptic	+	++
lat. hypothalamus	+	++
VDBV	-	++
HDB	+	++
MD	++	++
PV	+	++
Pt	+	+
Rh	++	++
Re	++	+++
SM	-	+
AM	++	++
BLa	++	+++
VTA	+	+++
Pf/PAG	-	++
LDTg	+	+
LC	+	++
PBN	-	+
Raphe	+/-	+

\- = no labeling
\+ = light labeling
++ = moderate labeling
+++ = heavy labeling

Table 2.

Comparison of the afferent inputs to both the infralimbic and insular cortices (IL + INS), the IL cortex only (IL) and the insular cortex only (INS). See text for abbreviations.

Table 2. Comparison of afferent projections to infralimbic and insular cortices.

IL + INS	IL	INS
BLa	SUB/CA1	VBm
MD	PV	PBN
Pc/Cem	Re	
Pt	Rh	
LH	VDBV	
VTA	LPO	
LDTg	AM	
LC		
DR		

CHAPTER V

EFFERENT PROJECTIONS FROM THE RAT INFRALIMBIC AND PRELIMBIC CORTICES

ABSTRACT

Pressure injections of the anterograde tracer wheat germ agglutinin conjugated horseradish peroxidase (WGA-HRP) were made into the medial frontal cortex (MFC) of the rat. Presumed anterograde terminal labeling was seen in numerous brain areas. The infralimbic (IL) region of the MFC sends projections to central limbic structures (hippocampus, central gray, basolateral amygdala), central motor structures (ventral striatum, pontine nuclei, inferior olive) and central visceral structures (insular cortex, lateral hypothalamus, lateral dorsal tegmental nucleus, NTS). The label in the NTS was localized within cardiovascular and respiratory subnuclei of the NTS. These data suggest that the IL cortex may function as a "visceral motor" cortex, involved in CNS control of several visceral or autonomic functions. The IL cortex may serve as part of the "visceral brain," linking limbic and autonomic activity.

INTRODUCTION

The recent finding of a direct descending projection from the infralimbic region (IL) of the medial frontal cortex (MFC) to the nucleus of the solitary tract (NTS) in the rat (van der Kooy et al., 1982, 1984; Terreberry and Neafsey, 1983) prompted the present study which reexamined the efferent projections from this cortical region

using anterograde transport of WGA-HRP. Previous studies have described the projections from this cortical region (Domesick, 1969; Leonard, 1969; Beckstead, 1979; van der Kooy et al., 1984; Wyss and Sripanidkulchai, 1984), but none of these studies focused specifically on projections from IL. The present study has confirmed many of the findings of earlier studies and also provides a detailed description of the pattern of terminations within the various subnuclei of the NTS of fibers which arise from the IL cortex.

MATERIALS AND METHODS

A total of 30 adult Long Evans male rats (300-500 grams) was used in this study. Animals were anesthetized with Ketamine HCl (100 mg/kg, IP; supplemental doses of one-quarter the initial dose were given when necessary to maintain a constant level of anesthesia) and then placed into a stereotaxic frame. A heating pad controlled by a rectal temperature probe was used to maintain the animal's body temperature between 36-38 degrees celcius. Following surgical exposure of the skull and the neck musculature, the cisterna magna was opened in order to allow the cerebrospinal fluid to drain and thus prevent cortical swelling. A small, 2x2 mm piece of calvaria overlying the left MFC was then removed using a low-speed drill. The dura was removed from the exposed cortex, and the cortex bathed in warmed mineral oil.

A 1.0 ul Hamilton syringe fitted with a glass pipette (tip diameter 50 um) was filled with a 1% WGA-HRP (Sigma) solution in 0.9% saline. The syringe was mounted on a Kopf micromanipulator which was used to position the pipette just lateral (0.2-0.6 mm) to the midline, to a depth of 3.0-4.0 mm from the cortical surface at points 3.0-4.0 mm rostral to bregma. Pressure injections of 0.01-0.03 ul of WGA-HRP were performed over a 15-20 minute period, after which time the pipette was withdrawn and the wound sutured closed.

After a 48 hour survival time, the animals were reanesthetized with sodium pentabarbitol (40 mg/kg, IP) and transcardially perfused with 0.9% saline, 1% glutaraldehyde - 4% paraformaldehyde and finally with a 10% buffered sucrose solution according to the procedure of Rosene and Mesulam (1978). The brains were removed, placed in a cold 30% sucrose phosphate buffer solution and allowed to sink (2-3 days). Frozen sections 50 um thick were cut coronally on a sliding microtome, and two alternating series of sections collected. Both sets of sections were reacted with tetramethylbenzidene (TMB) using either Mesulam's (1978) procedure or a recent modification of Mesulam's procedure (Gibson et al., 1984) that reduces the artifact that can occur with TMB histochemistry. The TMB reactions were stopped, and the sections were rinsed and mounted from cold sodium acetate buffer (pH 3.3) onto subbed slides. The sections were oven dried overnight (temperature between 50-60 degrees celcius). One set was rapidly dehydrated in a graded series of ethanol, cleared in xylene and

coverslipped using Depex. The second set of sections was counterstained in 1% pyronin Y, rapidly dehydrated and coverslipped using Depex. The counterstained series were used to determine cytoarchitectonic and nuclear boundaries. The criteria and nomenclature of Kalia and Sullivan (1982) was followed in determining the boundaries of the subnuclei of the NTS (Figures 7-10).

Each section was examined under brightfield, darkfield and polarized light microscopy for the presence and localization of what appears to be anterograde axonal and terminal labeling (see Mesulam, 1982). A series of line drawings were made at 400 um intervals through the brain using a Bausch and Lomb projecting scope. The anterograde label was then plotted onto these line drawings utilizing a camera lucida drawing tube attached to an Olympus BH-1 microscope. For illustration purposes and to facilitate comparison between experiments, these data were then replotted onto a series of "standard" coronal sections traced from the Paxinos and Watson (1982) stereotaxic atlas of the rat brain. The cytoarchitectonic subdivision of the MFC described by Krettek and Price (1977a) was employed (see Chapter II).

RESULTS

In 13 experiments, the injection site involved the infralimbic (IL) cortex. Three of these were very large injections and also

included portions of the anterior cingulate (AC), prelimbic (PL) and IL cortices (see Figures 1A-C, Chapter IV). In four cases the injection sites were located primarily in the AC and PL cortices, with only a small involvement of the IL region (see Figures 1D-G, Chapter IV). Three other cases involved the PL and IL cortices, with little or no involvement of the AC cortex (see Figures 1H-J, Chapter IV; Figure 1B). Finally, three injections were centered in the PL cortex only, with only a slight involvement of the IL and AC cortices (see Figures 1K-M, Chapter IV; Figure 1A). By comparing the set of structures labeled by injections involving IL to those labeled after involvement of adjacent cortical areas, the efferent connections characteristic of the infralimbic cortex were determined. Minor differences in labeling patterns appeared to be due to the exact placement of the injections. The efferent projections from the infralimbic cortex will be illustrated chiefly by reference to two experiments, HRP RT 40 (Figures 1A, 2,3) which injected the PL cortex with a minor involvement of the AC cortex and HRP RT 46 (Figures 1B, 4-6) which injected both the PL and IL regions. Additionally, data from a third experiment, HRP RT 18, which also injected both the PL and IL cortices and resulted in exceptionally heavy anterograde labeling in the NTS, will be presented to further illustrate the pattern and extent of the cortico-solitary projections which arise from the infralimbic cortical region (Figures 7-11). Each of these three cases illustrate results typical of several other similar

injections into the MFC.

RT 40 (PL)

Anterograde axonal labeling was seen ipsilaterally within the layers V and VI of the prelimbic and infralimbic regions (Figures 2A,B), as well as in layers V and VI of the ventral anterior cingulate cortex (Figures 2C,D) and the retrosplenial granular cortex (Figure 2G). Sparse anterograde label was also seen ipsilaterally within area 18 of visual cortex (Figures 2G,H). Bilaterally, anterograde label was seen in both the insular cortex and the underlying claustrum and more ventral endopiriform nucleus (Figures 2B-D). Contralateral to the injection site, anterograde axonal label was seen in the deeper layers of the homotypic PL cortex and the dorsal portion of the IL cortex (Figure 2A). Moderate amounts of anterogradely transported label were seen in the ventral portions of the ipsilateral hippocampal formation (CA1) and the ventral subiculum after a PL injection (Figures 2G-I, 3D).

Anterograde labeling of subcortical forebrain structures was limited to the caudate-putamen. In addition to labeled fibers in the pencil bundles coursing toward the internal capsule, sparse anterograde label was seen primarily dorsally and medially within the neostriatum (Figures 2B-E). The pattern of labeling was similar bilaterally, although more dense on the ipsilateral side.

Within the amygdaloid complex, anterograde axonal labeling was

consistently seen in the basolateral (BLa) nucleus (Figures 2E,F, 3C). This label was contained predominantly to the medial aspect of the nucleus and was seen bilaterally, although it appeared that the labeling was slightly denser in the contralateral side. The lateral (La) nucleus and the central (Ce) nucleus showed a few scattered labeled axons, but this labeling pattern was inconsistent from animal to animal.

Numerous nuclei within the dorsal thalamus contained anterograde axonal labeling following a PL injection. At rostral thalamic levels, label was seen in the parataenial (Pt) nucleus, the dorsomedial portion of the anteromedial (AM) nucleus, the nucleus reuniens (Re) and in the reticular (R) nucleus (Figures 2D, 3A). The rhomboid (Rh) nucleus, occupying the region just dorsal and between the reuniens nuclei, also contained anterograde label. At mid-thalamic levels, anterograde label was seen in the lateral habenular nucleus, the lateral and intermediate segments of the mediodorsal (MD) nucleus and sparsely within the centrolateral (CL), paracentral (Pc) and centromedial (Cem) intralaminar nuclei (Figures 2E, 3B). The submedius (Sm) nucleus and the Re and Rh nuclei also showed slight labeling at this mid-thalamic level (Figure 2E), and the medial aspect of the zona incerta (ZI) also contained anterogradely transported label. At caudal thalamic levels, the lateral segment of MD, CL, Pc, Cem and the medial ZI all contained anterograde label (Figure 2F). The overall pattern of labeling was similar bilaterally, with a much

heavier distribution on the ipsilateral side. Within the hypothalamus, moderate anterograde label was seen in the rostral levels of the lateral hypothalamus (LH, Figure 2D).

In the midbrain, anterograde label was seen bilaterally in the region medial to the parafascicular (Pf) nucleus (Figure 2G); the ipsilateral label appeared denser. This area appears to be the rostral continuation of the central gray (CG). The dorsal and lateral portions of the CG also exhibited anterograde labeling after a PL injection (Figures 2H-K). This projection was bilateral with the ipsilateral component being more extensive. The ipsilateral pretectum (PRT), as well as the deeper layers of the ipsilateral superior colliculus (SC), also showed anterograde labeling (Figures 2H-J). Also labeled in the midbrain was the ipsilateral ventral tegmental area (VTA), with sparse label restricted to the rostral half of this area (Figure 2H).

In the pons, anterograde label was seen in the lateral dorsal tegmental (LDTg) nucleus (Figures 2K,L), dorsal raphe (DR, Figures 2J,K) and in the ventromedial subnucleus of the pontine (Pn) nuclei (Figure 2J). Both the LDTg label and Pn label were bilateral but heavier ipsilaterally.

Within the medulla, the only structures that exhibited the presence of label were the nucleus prepositus hypoglossi (Figure 2N) and the inferior olivary complex (IO). The IO label was seen bilaterally in the ventral lateral outgrowth subdivision of the

principle olivary nucleus (Figure 2R).

RT 46 (PL/IL)

The pattern of cortical labeling seen after a PL/IL injection was similar to that just described for a PL injection, but there were some significant differences. There was little, if any, label within the anterior cingulate cortex (Figures 4B,C), and there was no anterograde label seen in the visual cortex as was seen for the PL injection (compare Figures 2G,H to Figures 4G,H). The entorhinal cortex displayed sparse anterograde label (Figure 4G), while the claustrum and endopiriform nucleus were labeled bilaterally (Figures 4B-F). The piriform cortex was also lightly labeled ipsilaterally after a PL/IL injection (Figure 4A).

Anterogradely labeled fibers of passage were seen within the ipsilateral cingulum bundle, located immediately dorsal to the cortical white matter and ventral to the neurons of the anterior cingulate and retrosplenial cortices (Figures 4D-H). Within the hippocampal formation, label was seen in the CA1, CA2 and slightly in the CA3 subdivisions of the ipsilateral hippocampal formation (Figure 4H). The ventral subiculum had only a sparse amount of labeling.

In the subcortical forebrain, anterograde axonal transport was seen within the dorsal, medial aspect of the caudate-putamen (Figures 4B-D), and heavily labeled fibers were seen coursing through the striatum enroute to the internal capsule. The pattern was similar

bilaterally but denser on the ipsilateral side. In addition to the striatal labeling, the nucleus accumbens, occupying the region just medial to the anterior commissure (ac) showed considerable bilateral labeling (Figures 4A-C); the olfactory tubercle, along the ventral surface of the brain, also contained light anterograde axonal labeling (Figure 4C). The labeling of the olfactory tubercle avoided the islands of Calleja and the ventral pallidum. The cellular bridges between the ventral nucleus accumbens and the olfactory tubercle also exhibited light anterograde labeling (Figure 6A). Sparse anterograde label was also seen in the medial septum (MS) and in the ipsilateral ventral division of the vertical limb of the diagonal band (VDBV, Figure 4C).

Within the amygdala, the medial aspect of the BLa contained anterogradely labeled terminals (Figures 4E,F). This labeling pattern was bilateral, with a slightly denser projection to the contralateral side. The lateral (La) nucleus also exhibited sparse anterograde labeling (Figures 4E,F).

Within the thalamus, the Pt, medial AM, Re, rhomboid, CL, Pc, Cem and Sm nuclei all contained anterograde labeling (Figures 4D-F, 5A,C), similar to the results of the PL injection; the label within Pt, however, was much denser. Additionally, anterograde label was also seen in the paraventricular (PV) nucleus and the medial and intermediate segments of MD (Figures 4D-F, 5B,D). The lateral dorsal (LD) nucleus contained sparse anterograde label, as did the

ventromedial (VM) nucleus (Figures 4E,F). The just described pattern of labeling within the thalamus was similar on both sides, but the ipsilateral label was much more dense than the contralateral label. The ipsilateral lateral preoptic area and LH were also moderately labeled (Figures 4D-F).

Areas of the midbrain which showed anterograde label following a PL/IL injection included the region medial to the parafascicular (Pf) nucleus which was labeled bilaterally (Figure 4G). Sparse label was also seen in the ipsilateral PRT (Figure 4H), while the VTA was heavily labeled (Figures 4H,I). The central gray (CG) was heavily labeled ipsilaterally and lightly labeled contralaterally (Figures 4H-K, 6B). The substantia nigra pars reticulata (SNr) also contained a few labeled axons (Figures 4H, 6C) as did the caudal linear raphe (CLi) nucleus (Figure 4I).

Within the pons, bilateral label was seen in the medial subnucleus of the Pn (Figures 4J, 6E), and in the nucleus cuneiformis (Cun, Figure 4K). Heavy label was seen bilaterally in the LDTg (Figures 4K,L, 6D), with the denser labeling occurring ipsilaterally. Light labeling of the locus coeruleus (LC) and the dorsal parabrachial (DPB) nucleus was also observed (Figure 4L). Three pontine raphe nuclei exhibited anterograde label after this PL/IL injection, the DR (Figures 4J,K), the median raphe (MnR, Figures 4J,K) and the nucleus raphe pontis (RPn, Figure 4L).

Medullary structures containing anterograde label included the

nucleus raphe magnus (RMg, Figure 4M), the nucleus prepositus hypoglossi (Figure 4N), the inferior olive (IO) and the nucleus of the solitary tract (NTS). The label in the IO was localized in the lateral portion of the ventral lateral outgrowth subnucleus of the principle olive and in the more medially located Beta subnucleus of the medial accessory olive (Figures 4Q,R, 6F). The label within the NTS was seen bilaterally throughout most of the rostro-caudal extent of the nucleus; however, the densest label was seen contralaterally and caudally in the region of the commissural nucleus of the NTS (Figures 4O-S). The nucleus ambiguus region was carefully checked for the presence of anterograde label, but none was found there.

RT 18 (PL/IL)

To further illustrate the anterograde labeling within the NTS, the data from a third experiment with especially heavy labeling in the NTS will be presented. In experiment HRP RT 18 an injection of WGA-HRP was made into the left MFC (see insert in Figure 7). This injection involved a good portion of the IL and PL regions and also involved the more dorsal AC cortex slightly. Using a camera lucida drawing tube, high power (20X objective) drawings were made through four levels of the NTS and the anterograde labeling was then plotted onto these drawings (Figures 7-10). Nuclear boundaries were determined utilizing the criteria and nomenclature of Kalia and Sullivan (1982).

In rostral levels of the NTS (0.7 mm rostral to obex) moderate anterograde labeling was seen in the intermediate (INTS), ventral (vNTS) and in the lateral portion of the medial (mNTS) subnuclei of the NTS (Figures 7, 11A). Light anterograde labeling was observed in the ventrolateral (vlNTS) and the dorsomedial aspect of the medial (mNTS) NTS subnuclei. The dorsal (dPSR), lateral (lPSR) and ventral (vPSR) parasolitarius regions all contained light anterograde label at rostral NTS levels (Figure 7). There also was labeling within the dorsal motor nucleus of the vagus (DMN X).

Figure 8 illustrates the pattern of labeling seen in the NTS at the level of the obex. Moderate to heavy anterograde labeling was seen in the vNTS and the adjacent lateral aspect of the DMN X. At this level, light labeling of the INTS, mNTS, vlNTS, the dorsolateral (dlNTS) and the interstitial (iNTS) NTS subnuclei was seen (Figures 8, 11C). Additionally, the dPSR and lPSR again contained only a small amount of anterograde axonal labeling.

At a level caudal to obex (0.9 mm caudal to obex) moderate to heavy anterograde labeling was seen in the vNTS and the dorsal vlNTS as well as in the area immediately dorsal to the INTS, the dorsal parasolitarius region (Figures 9, 11E). Also at this level light labeling of the iNTS, mNTS and commissural (cNTS) nuclei was seen in addition to light anterograde labeling of the DMN X (Figure 9). At extreme caudal levels of the NTS (1.6 mm caudal to obex) heavy anterograde label was observed in the cNTS, and numerous labeled

fibers could be seen ascending in the decussating fibers of the pyramidal tracts (pyx, Figures 10, 11G).

DISCUSSION

Efferents from IL

The results of the present study indicate that the IL region of the rat MFC projects to a set of CNS structures, many of which can be considered as either central limbic structures, central motor structures that are either elements of the ventral striatal-pallidal system proposed by Heimer and Wilson (1975) or elements of the cerebellar projection system, or central visceral structures. Thus, while the IL region appears to integrate limbic and visceral inputs (see Chapter IV), the output from this area appears to be primarily that of a "visceral motor system." The projections to limbic brain areas will be discussed first, followed by a discussion of the projections to the ventral striatal-pallidal and cerebellar "motor" sytems, and, finally a discussion of the projections to visceral brain regions.

Limbic Outputs from IL

Several areas that may be considered limbic structures receive inputs from IL. These include the VDBV of the forebrain, the anteromedial (AM) and submedius (SM) thalamic nuclei, the hippocampus,

the basolateral amygdala and the central gray matter. These structures have been shown to be associated with the hippocampus or other components of the "limbic" system (MacLean, 1949; Swanson, 1983). Figure 12A illustrates these limbic efferents from IL.

The vertical limb of the ventral division of the diagonal band (VDBV) is one of the forebrain structures which receives projections from the IL cortex. The literature on cortical projections to the VDBV is limited, but an autoradiographic study by Beckstead (1979) did report a small projection from the PL cortex to the region in the forebrain that corresponds to what we term the VDBV. Labeling seen in this area after a PL/IL injection was heavier than that seen after a PL injection, suggesting that the IL cortex also projects to this area of the basal forebrain. The VDBV is believed to be the site of cholinergic cells (see Fibiger, 1982 for review) that project to the hippocampus and related areas of the cerebral cortex, including IL (Mesulam et al., 1983; Lamour et al., 1984; Chapter IV).

Several investigators have reported cortico-thalamic projections to AM and SM originating from the rodent PL and IL cortices (Herkenham, 1978, 1979; Beckstead, 1979; van der Kooy et al., 1984). It appears that the connections between IL and AM and SM are reciprocal, as the previous Chapter (IV) illustrated AM-IL and SM-IL projections (Chapter IV). The lateral habenular nucleus also exhibited anterograde labeling after our MFC injections, confirming previous findings that the AC and PL regions of the MFC project to the

medial portion of the lateral habenula (Beckstead, 1979; Greatrex and Phillipson, 1982). The amount of label in the lateral habenular nucleus did not appear to increase when IL was involved in the injection, suggesting that IL sends only a sparse projection at best to this nucleus.

Our data indicate that PL and IL project to ventral portions of the hippocampal formation and the ventral subiculum. Thus, the IL cortex and the hippocampal formation are reciprocally connected. The basolateral amygdala (BLa) receives projections from IL, as does the lateral (La) amygdaloid nucleus. These findings are consistent with those of van der Kooy et al. (1984) but are in disagreement with the findings of Ottersen (1981; 1982) who reported that IL projects only to the La and central (Ce) amygdaloid nuclei. The projections from IL to BLa provide a possible pathway for IL modulation of limbic and visceral functions. It has been shown that BLa projects to the hippocampus and ventral subiculum (Krettek and Price, 1977c) and also to the nucleus accumbens and olfactory tubercle of the ventral striatum (Krettek and Price, 1978a). BLa also has connections with the lateral hypothalamus and the bed nucleus of the stria terminalis (Krettek and Price, 1978a). The central amygdaloid nucleus receives projections from BLa (Krettek and Price, 1978b; Nitecka et al., 1981), and it in turn projects to the NTS (Schwaber et al., 1980; 1982).

The present study indicates that the IL cortex projects to the ventromedial region of the central gray matter (CG) while PL projects

more dorsolaterally in the CG. These findings are supported by those of Wyss and Sripanidkulchai (1984) who reported that IL projects to the ventral quadrant of the CG while the PL and AC cortical regions project to the dorsal/lateral quadrant of CG. The projection from IL to the CG may function in modulating nociceptive stimuli as stimulation of the ventral portion of the CG produces analgesia (Lewis and Gebhart, 1977), and a recent study (Hardy, 1985) has reported similar analgesic effects following stimulation of the MFC.

Another area of the mesencephalon that exhibited anterograde labeling after MFC injections was the superior colliculus. This labeling can be attributed to involvement of the AC and PL regions of the MFC, as it has been shown that the AC/PL cortex has direct projections to the deeper layers of the superior colliculus (Beckstead, 1979; Hardy and Leichnetz, 1981; Wyss and Sripanidkulchai, 1984).

Central Motor System Outputs from IL

Areas that receive direct projections from IL and may be considered elements of the central motor system include the ventral striatum (nucleus accumbens, olfactory tubercle), the mediodorsal, parataenial and reuniens thalamic nuclei, the ventral tegmental area and adjacent substantia nigra, the pontine nuclei and the inferior olive. Figure 12B illustrates these motor efferents from IL.

The ventral striatum is composed of both the nucleus accumbens

(Acc) and the olfactory tubercle (OT) (Heimer and Wilson, 1975; Heimer et al., 1982). Following a PL/IL injection, the present study found moderate-dense anterograde label in Acc and light label in OT, in agreement with a recent study by Jayaraman (1985) which reported a direct IL-Acc projection in the cat. A study by Newman and Winans (1980a) reported a sparse projection from IL to OT in the hamster, similar to our findings in the rat. The anterograde labeling seen in the caudate-putamen is most likely due to PL projections and does not appear to result from projections from IL cortex. A projection from PL cortex to the medial aspect of the striatum has been previously reported in the rat (Beckstead, 1979) and the cat (Royce, 1982).

The mediodorsal thalamic nucleus (MD) is considered with the ventral striatal-pallidal structures because it receives projections from the ventral pallidum (Goldschmidt and Heimer, 1980; Groenewegen and Nauta, 1982; Young et al., 1984). Our data indicate that MD receives a projection from the PL cortex, confirming earlier reports (Beckstead, 1979; Ribak and Fallon, 1980; Groenewegen and Nauta, 1982; van der Kooy et al., 1984). In addition, the IL cortex also appears to project bilaterally to the medial portion of MD. This confirms studies of van der Kooy et al. (1984) who reported anterograde labeling in both the lateral and medial portions of MD after WGA-HRP injections of PL/IL cortex and Young et al. (1984) who reported retrograde labeling of neurons in the infralimbic cortex after fluorescent dye injections of MD.

Based on their projections to the ventral striatum, the parataenial (Pt) and reuniens (Re) thalamic nuclei will also be considered with the ventral striatal-pallidal system (Newman and Winans, 1980a,b). Our finding of direct projections from IL cortex to these thalamic nuclei confirms an earlier report by van der Kooy et al. (1984), and are another example of reciprocal connections between IL and related thalamic nuclei (Chapter IV).

The ventral tegmental area (VTA) is included as part of the ventral striatal-pallidal system since it provides the dopaminergic innervation of the ventral striatum (Fallon and Moore, 1978a; Newman and Winans, 1980a,b), much like the substantia nigra which provides dopaminergic innervation to the caudate-putamen (Fallon and Moore, 1978b; Beckstead et al., 1979). The anterograde labeling seen in the VTA after a PL/IL injection confirms the findings of Beckstead (1979) who reported a prominent projection to the VTA from the PL cortex and the findings of Phillipson (1979) who demonstrated a projection from IL to the VTA. Another area of the mesencephalon that exhibited anterograde labeling after MFC injections was the medial portion of the substantia nigra pars reticulata (SN). There are conflicting reports on MFC projections to SN, with several earlier studies denying the presence of MFC-SN projections (Bunney and Aghajanian, 1976; Tulloch et al., 1978), while several recent studies have reported direct PL-SN projections (Beckstead, 1979; van der Kooy et al., 1984; Wyss and Sripanidkulchai, 1984). Our data indicate that IL also

projects to SN pars reticulata.

Heimer and his coworkers (Heimer and Wilson, 1975; Heimer et al., 1982) has proposed the concept of a ventral striatal-pallidal motor system that parallels the classical dorsal striatal system. Figure 13 schematically illustrates both the classical dorsal striatal system and the ventral striatal-pallidal system. It appears that the IL cortex may be a part of this ventral striatal-pallidal system by way of its connections to with the olfactory tubercle, nucleus accumbens and mediodorsal and parataenial thalamic nuclei. Functionally, Heimer et al. (1982) believe that the ventral striatal system exists in parallel with the dorsal striatal system for planning and initiation of movements, but they were noncommittal in assigning a specific function to the ventral striatum as a whole. Although the function of the ventral striatum remains unknown at this time, suggestions have been made that this is an area of limbic input influencing motor activity (Mogenson et al., 1980; Newman and Winans, 1980a; Heimer et al., 1982). If the IL cortex is part of this system, then the combination of visceral and limbic projections suggests that perhaps the ventral striatum functions, at least in part, as a "visceral" striatum that functions in parallel to the traditional dorsal "somatic" striatal system. This concept is slightly different from Heimer's concept that limbic striatal system's motivational outputs are expressed via the somatic striatal system. We suggest that the two systems function largely in parallel to each other rather

than sequentially.

Turning to the cerebellar aspect of the central motor system, the dorsomedial region of the medial Pn (Mihailoff et al., 1981) also showed the presence of anterograde label after PL/IL injections while only the ventromedial subdivision of Pn was labeled after PL injections. These findings are in general agreement with a recent report by Wyss and Sripanidkulchai (1984). Anterograde labeling was also seen in several IO subnuclei after MFC injections. Injections that involved only the PL cortex resulted in anterograde labeling of the ventral lateral outgrowth of the principle olive while injections that also involved the IL cortex resulted in labeling of the Beta subnucleus of medial accessory olive as well. These projections have not been previously described since most previous studies (Brown et al., 1977; Swenson and Castro, 1983) have focused on sensorimotor cortex projections which terminate primarily in the dorsal accessory olive. The regions of Pn and IO that receive IL projections send their efferents to the vermis and fastigial nucleus of the cerebellum, regions where electrical stimulation has been shown to elicit changes in cardiovascular functions (Muira and Reis, 1969; 1970; Achari and Downman, 1970; Al-Senawi and Downman, 1983). These observations suggest that there is a visceral cerebellar system, paralleling the extensively studied somatic cerebellar system.

Visceral Outputs from IL

Areas which receive direct inputs from IL and may be considered visceral structures include the insular cortex, lateral hypothalamus, paraventricular nucleus of the thalamus, parabrachial nucleus, lateral dorsal tegmental nucleus and the nucleus of the solitary tract (NTS). The basis for classifying these regions as visceral is that each one either receives direct projections from the NTS or projects directly to the NTS (Ricardo and Koh, 1978; Saper, 1982a). Figure 12C illustrates these visceral efferents from IL.

The IL region sends a substantial bilateral projection to the insular cortex, and this projection extends further caudally than the PL projection to the insular cortex (compare Figures 2E-G and Figures 4E-G). This finding is in agreement with findings in the rat (Beckstead, 1979; Saper, 1982a; Markowitsch and Guldin, 1983) and in the hamster (Reep and Winans, 1982a,b) that the insular cortex has substantial reciprocal connections with the IL region of the MFC. This interconnection and integration of the visceral sensory and visceral motor cortex is similar to the interconnection of the primary somatosensory and primary motor cortices (Donoghue and Wise, 1982; Donoghue and Parham, 1983). Our data showing homotypical cortical areas of IL and PL interconnected by callosal projections confirm the similar findings of Markowitsch and Guldin (1983).

Several additional cortical areas exhibited anterograde labeling after injections of the MFC, but this labeling appears to be due to spread of the injection site into adjacent cortical areas outside of

IL. Anterograde labeling of the retrosplenial cortex and area 18 of the visual cortex can be attributed to involvement of the AC region of the MFC which has direct efferent projections to the retrosplenial and visual cortices, including area 18 (Vogt and Miller, 1983; Miller and Vogt, 1984). The sparse anterograde labeling of the entorhinal cortex after an injection of the PL/IL region appears to be due to spread of the injection site into the taenia tecta (tt) located ventral to the IL cortex. Heavy reciprocal connections have been reported between the ventral tt and the entorhinal cortex (Haberly and Price, 1978; Wyss and Sripanidkulchai, 1983).

Concerning the anterograde labeling seen in visceral regions of the diencephalon, our data confirm previous reports that have demonstrated reciprocal connections between the IL cortex and the lateral hypothalamus (Kita and Oomura, 1981, 1982b; van der Kooy et al., 1984). This IL-LH pathway is a potential avenue by which IL can modulate visceral function due to descending projections to central autonomic structures from LH (Saper et al., 1976; Loewy et al., 1979). A study by Kita and Oomura (1981) also reported a substantial projection from IL to the lateral preoptic area, and our data concurs with this finding. Our results also indicate that the paraventricular (PV) nucleus of the thalamus receives a small projection from the IL cortex. Although van der Kooy et al. (1984) did not specifically report a similar projection to PV, in their Figure 6B anterograde label can be seen in the area just medial to the parataenial (Pt)

nucleus, an area likely to include PV. PV receives direct projections from the NTS (Ricardo and Koh, 1978) and projects to the IL cortex (see Chapter IV), making the descending projections from IL to PV an example of reciprocal thalamo-cortical connections.

Of the brainstem areas that exhibited anterograde labeling after MFC injections, three can be considered as visceral structures: the lateral dorsal tegmental nucleus (LDTg), the parabrachial nucleus (PBN) and the nucleus of the solitary tract (NTS). The LDTg appears to have reciprocal connections with IL. The finding of direct LDTg-IL projections (see Chapter IV) confirms earlier reports by Saper (1982b) and Groenewegen and van Dijk (1984). The finding of a direct descending projection to LDTg from IL has not been previously reported, but van der Kooy et al. (1984) reported that the MFC projects to the area surrounding the LDTg, but not to the LDTg itself. The LDTg has been described as the pontine micturition center, involved in the micturition reflex (Loewy et al., 1979) and descending projections from LDTg to the intermediolateral cell column (IML) in the sacral spinal cord have been reported (Loewy et al. 1979). Thus, the IL cortex may influence parasympathetic outflow via this pathway through the LDTg. It is possible that the input to IL from the subfornical organ (SFO), a region of the brain that is considered an important mediator of the central actions of angiotensin (Lind et al., 1985), may have access to the LDTg and the micturition pathway via the pathway from IL to LDTg. Thus, the IL cortex may be involved in a

central fluid volume control system via its connections with the SFO and LDTg.

The projection from the IL cortex to the PBN in the dorsolateral pons confirms similar findings in the cat (Yasui et al., 1985). However, in the rat, there have been conflicting reports as to whether or not the IL cortex projects to the PBN (Saper, 1982b; van der Kooy et al., 1984). In the study by Saper, the retrograde labeling seen in the IL cortex after injections of WGA-HRP into the PBN was thought to be due to involvement of the surrounding tissue by the injection, specifically involvement of the central gray matter. Our data concurr with Saper's in that the IL projects to the central gray, but our data also appear to indicate that IL projects to the PBN, in agreement with the results of a recent study by van der Kooy et al. (1984). This projection from IL to PBN is another pathway by which IL may control visceral functions such as heart rate, as stimulation of the PBN elicits bradycardia (Hamilton et al., 1981).

The present study indicates that the IL cortex sends direct projections to several subnuclei of the NTS; these include the ventral (vNTS), ventrolateral (vlNTS), intermediate (INTS), lateral portion of the medial (mNTS) and the commissural (cNTS) subnuclei. Other areas of the NTS showed anterograde labeling after MFC injections but the densest labeling was observed in the subnuclei just listed. These findings are in basic agreement with those of van der Kooy et al. (1984), who reported that MFC injections (including PL and IL)

resulted in anterograde labeling of the lateral NTS and the dorsal portion of the medial NTS. The anterograde labeling seen in the dorsal motor nucleus of the vagus (DMN X) in the present study was sparse, which may explain why it was not reported by van der Kooy et al. (1984). The vlNTS, vNTS and iNTS are the major NTS subnuclei associated with respiratory control (Baumgarten and Nakayama, 1964; von Euler et al., 1973; Cohen, 1979; Kalia, 1981a,b); the dlNTS, dNTS and cNTS are involved in baro- and chemoreflexes (Kalia and Mesulam, 1980b; Kalia and Welles, 1980; Davies and Kalia, 1981; Kalia and Kropilak, 1982); while the mNTS is associated with gastrointestinal functions (Kalia and Mesulam, 1980b; Kalia and Welles, 1980; Davies and Kalia, 1981; Kalia and Kropilak, 1982). The projections from IL to these subnuclei indicate that respiratory, gastrointestinal and cardiac functions may be modulated by the activity of the IL cortex.

Consistent with these observations, several recent stimulation studies have shown that changes in blood pressure, heart rate, respiratory patterns and gastric motility can be elicited by electrical stimulation of the IL cortex (Burns et al., 1983; Neafsey and Hurley, 1984; Terreberry and Neafsey, 1984; Burns and Wyss, 1985).

The IL cortex may also influence vagal outflow directly. The present study found that the IL cortex projects to the dorsal and lateral portions of the DMN X and to areas immediately adjacent to the DMN X. In addition, Shapiro and Miselis (1983) reported that dendrites of DMN X neurons extend into the adjacent NTS, thus raising

the possibility that IL efferents terminate directly upon DMN X motor neurons. However, if these are direct IL projections to the DMN X, the absence of direct IL projections to the nucleus ambiguus, a major site of parasympathetic preganglionic projections of the vagus to the heart (Geis and Wurster, 1980), is somewhat surprising. Further studies are required to resolve this issue.

Summary

The IL cortex projects to areas involved in motor control (ventral striatum, pons, inferior olive), as well as directly to central visceral areas (lateral hypothalamus, lateral dorsal tegmental nucleus, NTS). The prominent "motor" orientation of these projections is evidence in support of the proposed functional role of the IL cortex as a "visceral motor cortex". It should be noted that the IL cortex also receives projections from and projects to several limbic structures. This association of limbic and visceral functions reinforce the concept of the limbic system as the "visceral brain" (MacLean, 1949; see Chapter IV).

Figure 1.

Brightfield photomicrographs (2X) of Nissl stained coronal sections through the medial frontal cortex to illustrate the extent of the WGA-HRP injection sites described in this report. A: Experiment RT 40, involving the PL cortex. B: Experiment RT 46, involving the PL and IL cortices.

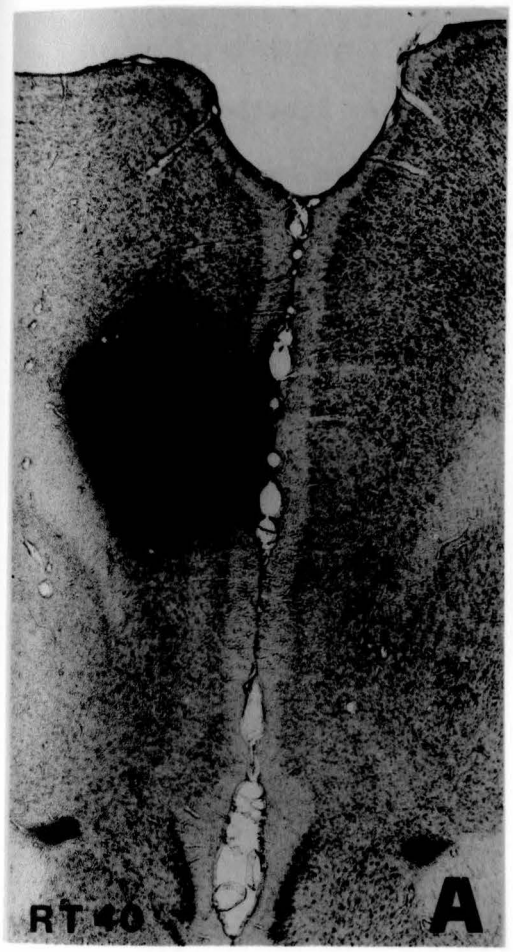
RT 40
A

Figure 2.

A-F: Rostral-caudal series of coronal outline drawings at 1 mm intervals illustrating the pattern of anterograde labeling seen after a WGA-HRP injection of PL cortex (Figure 1A). Dots represent terminal labeling while lines denote labeled fibers.

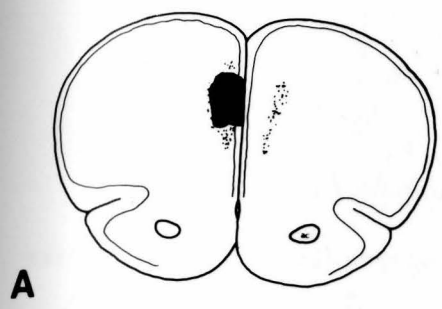

A

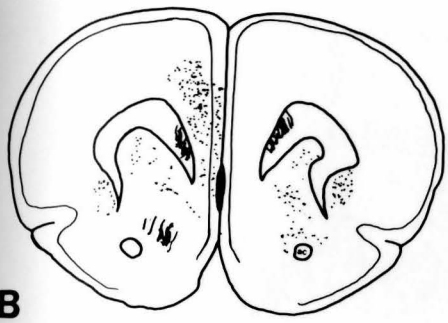

B

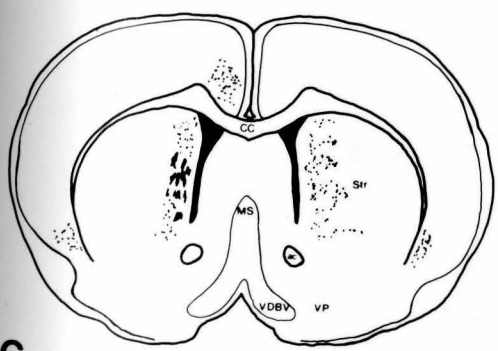
CC
Str
MS
VDB
VP

C

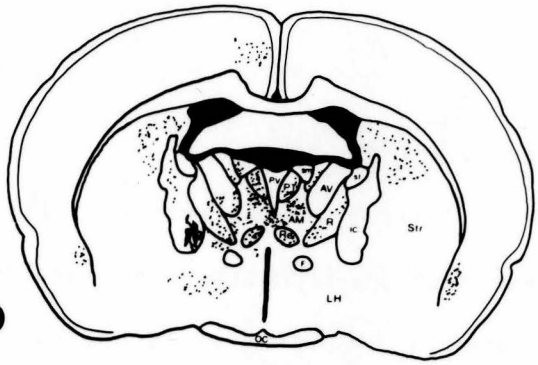
AV
AM
R
IC
Str
LH
CC

D

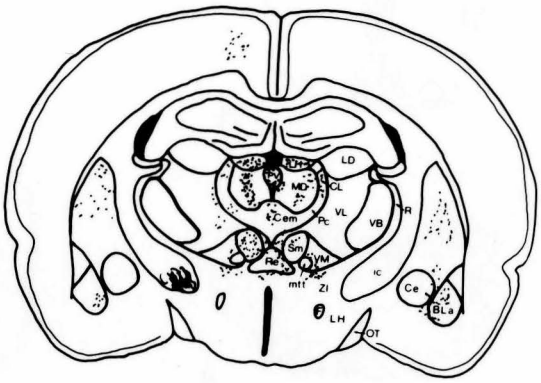
LD
MD
CL
Cem
Pc
VL
VB
R
Sm
VM
Rt
mtf
ZI
IC
Ce
BLa
LH
OT

E

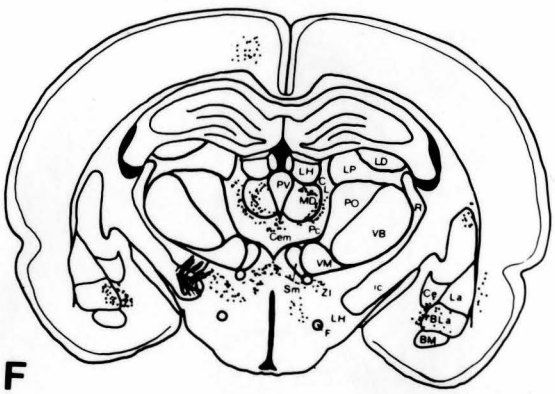
LH
LP
LD
PV
C
MD
PO
R
Cem
Pc
VB
VM
Sm
ZI
IC
Ce
La
BLa
BM
LH

F

Figure 2 cont.

G-N: Rostral-caudal series of coronal outline drawings at 1 mm intervals illustrating the pattern of anterograde labeling seen after a WGA-HRP injection of PL cortex (Figure 1A). Dots represent terminal labeling while lines denote labeled fibers.

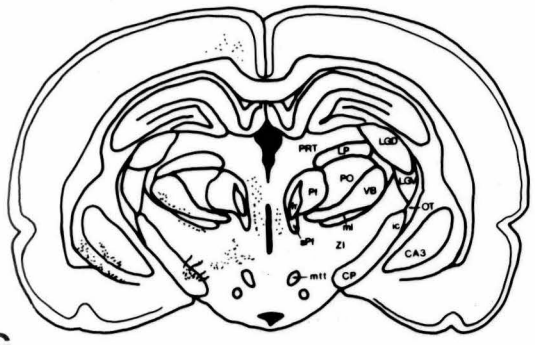
PRT
LP
LGD
PO
VB
LGM
Pt
OT
IC
sPf
ZI
CA3
mtt
CP

G

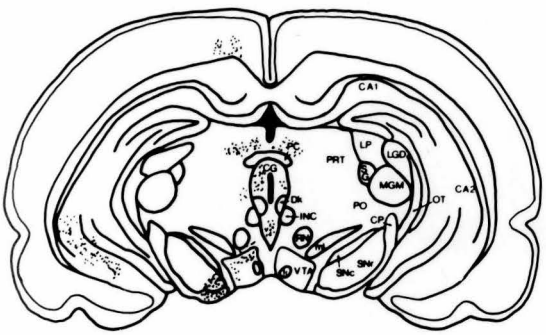
CA1
PRT
LP
LGD
MGM
CA2
PO
CP
OT
VTA
SNc
SNr

H

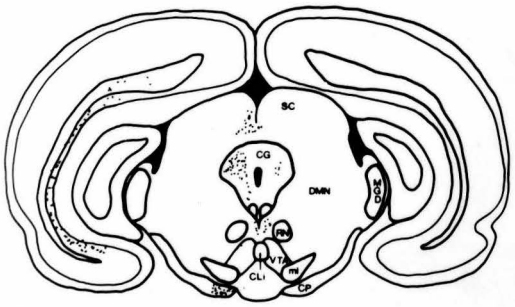
SC
CG
DMN
RN
VTA
CLi
mt
CP

I

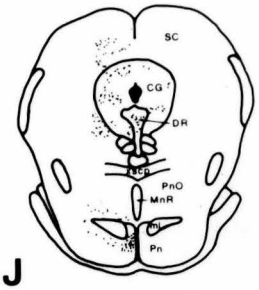
SC
CG
DR
PnO
MnR
Pn

J

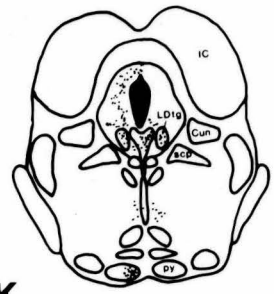
IC
LDtg
Cun
scp
py

K

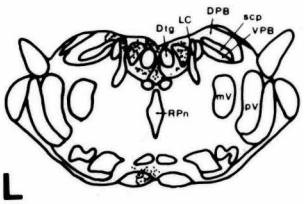
Dtg
LC
DPB
scp
VPB
RPn
mV
DV

L

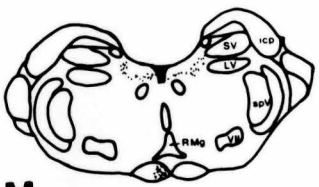
SV
icp
LV
scp
RMg
VII

M

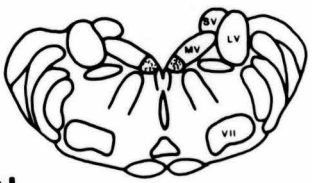
SV
LV
MV
VII

N

Figure 2 cont.

O-S: Rostral-caudal series of coronal outline drawings at 1 mm intervals illustrating the pattern of anterograde labeling seen after a WGA-HRP injection of PL cortex (Figure 1A). Dots represent terminal labeling while lines denote labeled fibers.

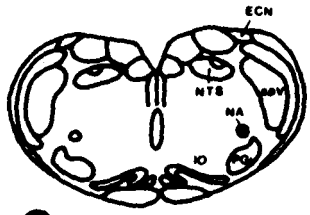
ECN
NTS
mV
NA
IO

O

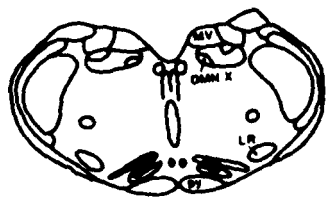
MV
DMN X
LR

P

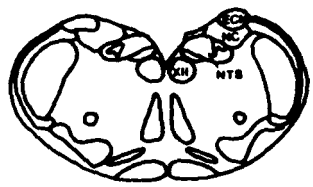
EC
NC
XII
NTS

Q

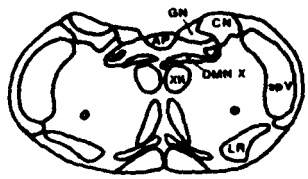
GN
CN
XII
DMN X
mV
LR

R

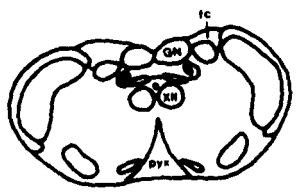
fc
GN
XII
pyx

S

Figure 3.

Darkfield photomicrographs of anterograde labeling observed after a PL injection (Figure 1A). The corresponding line drawing is indicated in parenthesis. A: Anterograde label in the rostral thalamus. Bilateral label can be seen in the parataenial (Pt) and anteromedial (AM) nuclei. The reticular (R) and anteroventral (AV) nuclei also exhibited anterograde labeling. (Figure 2D). B: Anterograde label within the intermediate and ventral portions of the mediodorsal (MD) nucleus. Retrogradely labeled neurons can be seen in the centrolateral (CL) and paracentral (PC) intralaminar nuclei. (Figure 2E). C: Anterograde label in the contralateral basolateral amygdala (BLa). Medial is to the left and dorsal is to the top of the figure. (Figure 2F). D: Anterograde label seen in the ventral hippocampus (CA1) and ventral subiculum. Arrows point to retrogradely labeled pyramidal cells. Medial is to the right, dorsal is to the top. (Figure 2H). Scale bars in A = 250 um; B-D = 100 um.

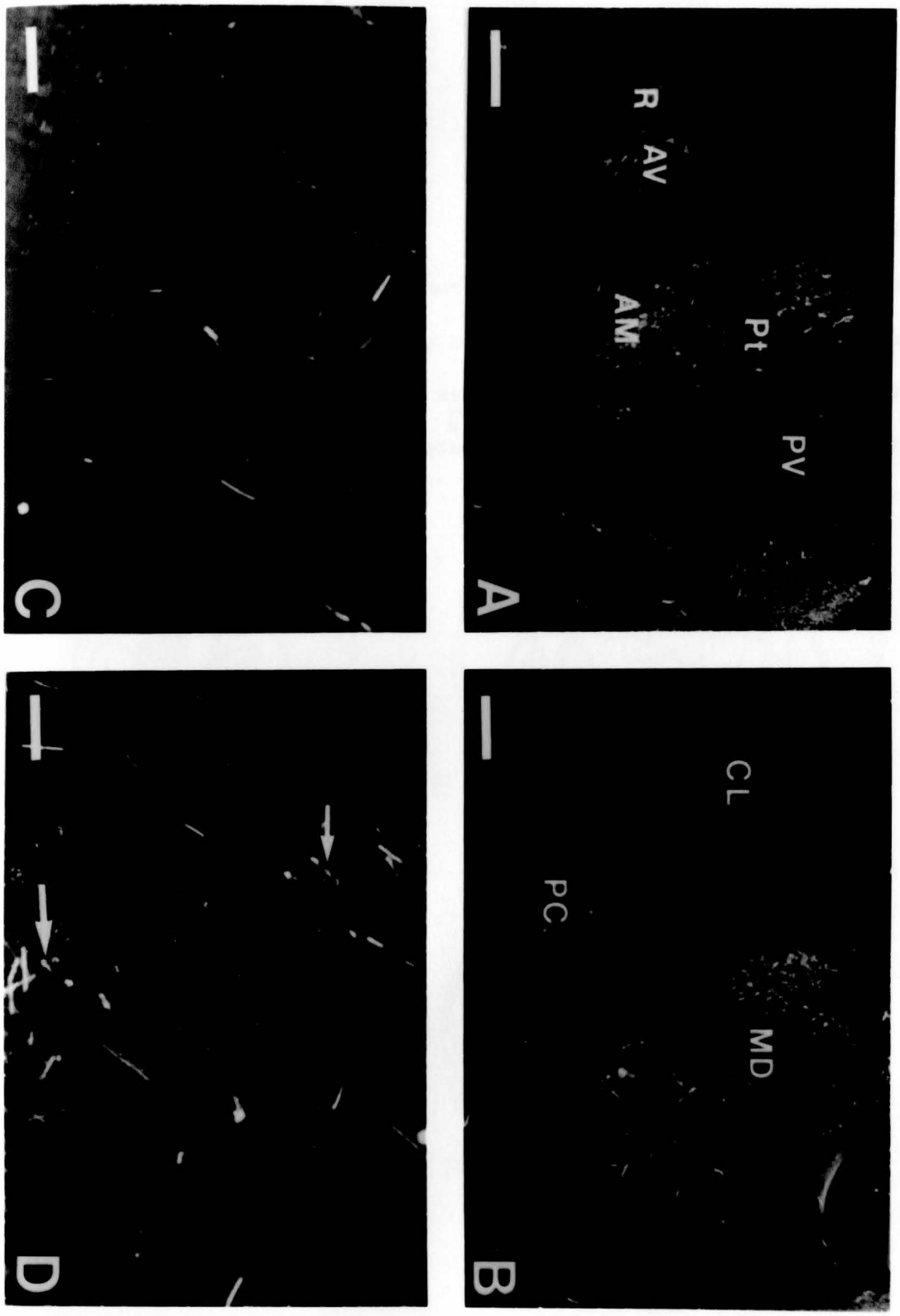
A
Pt
PV
R
AV
AM
B
CL
MD
PC
C
D

Figure 4.

A-F: Rostral-caudal series of coronal outline drawings at 1 mm intervals illustrating the pattern of anterograde labeling seen after a WGA-HRP injection of PL/IL cortex (Figure 1B). Dots represent terminal labeling while lines denote labeled fibers.

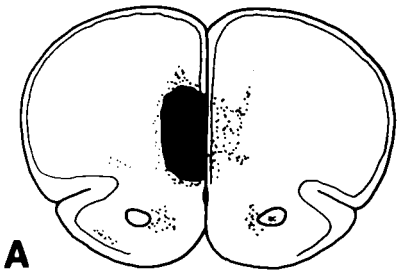
A

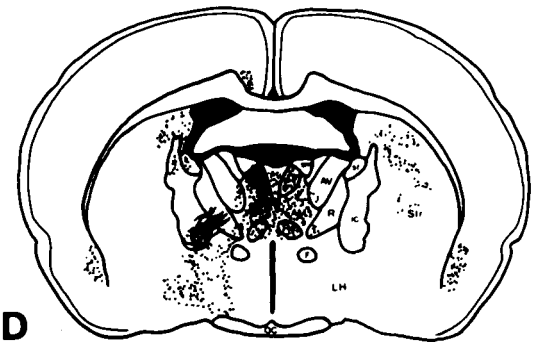
D
LH

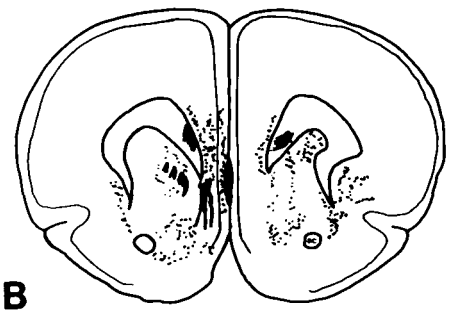
B

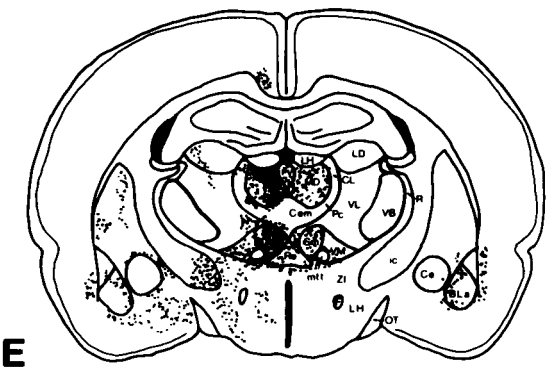
E
LD
VL
VB
Cem
Pc
ZI
LH
OT

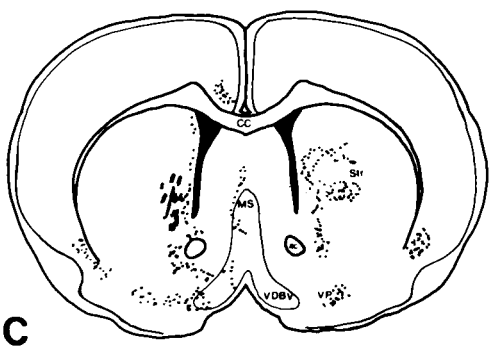
C
CC
MS
VDB
VP

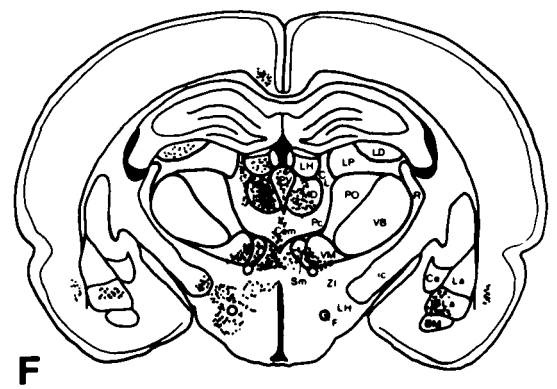
F
LH
LP
LD
PO
VB
Sm
ZI

Figure 4 cont.

G-N: Rostral-caudal series of coronal outline drawings at 1 mm intervals illustrating the pattern of anterograde labeling seen after a WGA-HRP injection of PL/IL cortex (Figure 1B). Dots represent terminal labeling while lines denote labeled fibers.

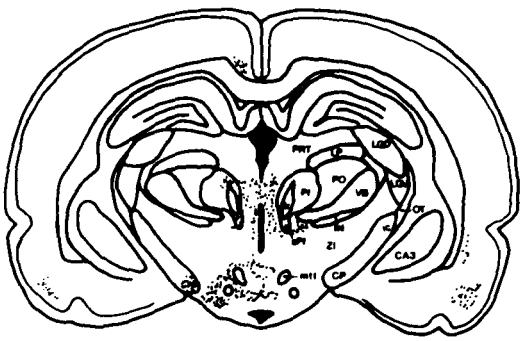
PRT
LDT
PO
VB
ZI
CA3
CP
mlf

G

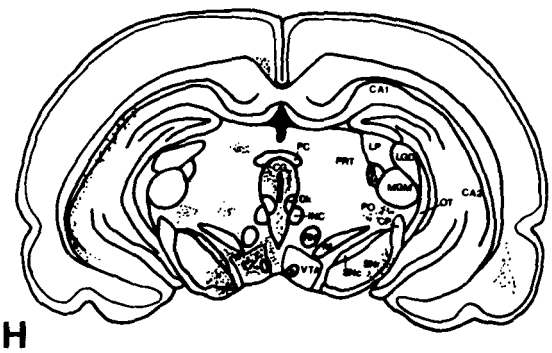
CA1
PC
PRT
LP
LGd
MGM
CA3
LOT
PO
CP
RtC
VTA
SNC

H

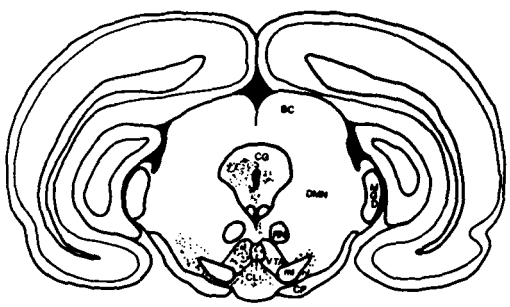
BC
CG
DMN
VTA

I

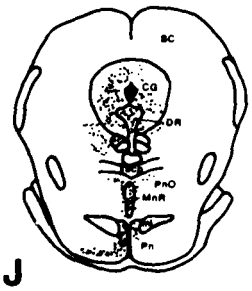
BC
CG
DR
PnO
MnR
Pn

J

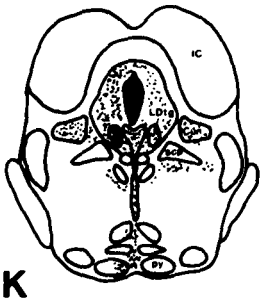
IC
LDTg
PC
PY

K

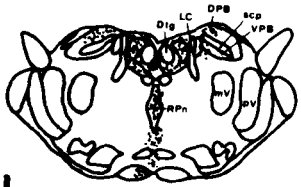
DTg
LC
DPB
scp
VPB
mV
sV
RPn

L

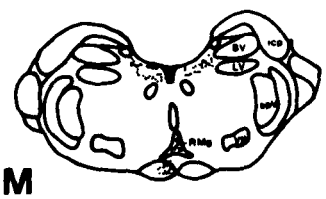
SV
ICP
LV
MVe
RMe

M

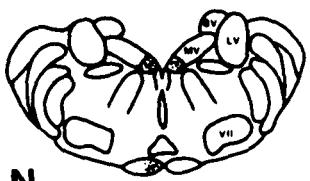
SV
LV
MV
VII

N

Figure 4 cont.

O-S: Rostral-caudal series of coronal outline drawings at 1 mm intervals illustrating the pattern of anterograde labeling seen after a WGA-HRP injection of PL/IL cortex (Figure 1B). Dots represent terminal labeling while lines denote labeled fibers.

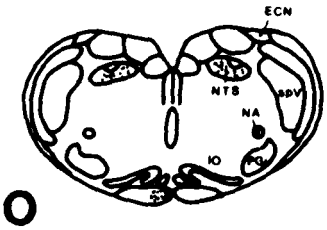
ECN
NTS
NA
spV
IO

O

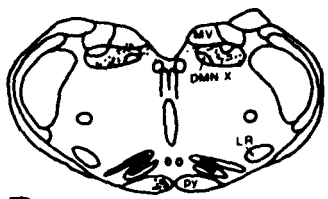
MV
DMN X
LR
Py

P

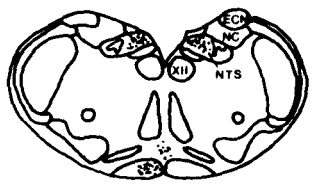
ECN
NC
XII
NTS

Q

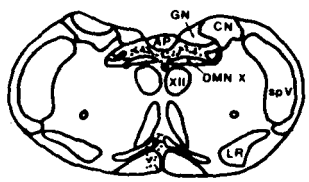
GN
CN
XII
DMN X
spV
LR

R

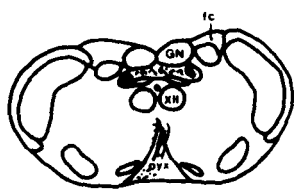
fc
GN
XII

S

Figure 5.

Darkfield photomicrographs of anterograde labeling observed after a PL/IL injection (Figure 1B). The corresponding line drawing is indicated in parenthesis. A: Anterograde label in the rostral thalamus. Bilateral label is seen in the parataenial (Pt) nucleus. The anteromedial (AM) and reticular (R) nuclei also show anterograde labeling. (Figure 4D). B: Anterograde labeling within the rostral mediodorsal (MD) nucleus. Heavy label is seen in the medial segment of MD while the lateral segment has only a moderate amount of label. (Figure 4E). C: Anterograde labeling of the ventral thalamus. Label can be seen in the submedius (Sm), rhomboid (Rh), ventromedian (VM) and reuniens (Re) nuclei. (Figure 4E). D: Anterograde label within the caudal MD nucleus. Again, heavy label can be seen in the medial segment of MD while the lateral segment has only a sparse amount of label. (Figure 4F). Scale bars = 250 um.

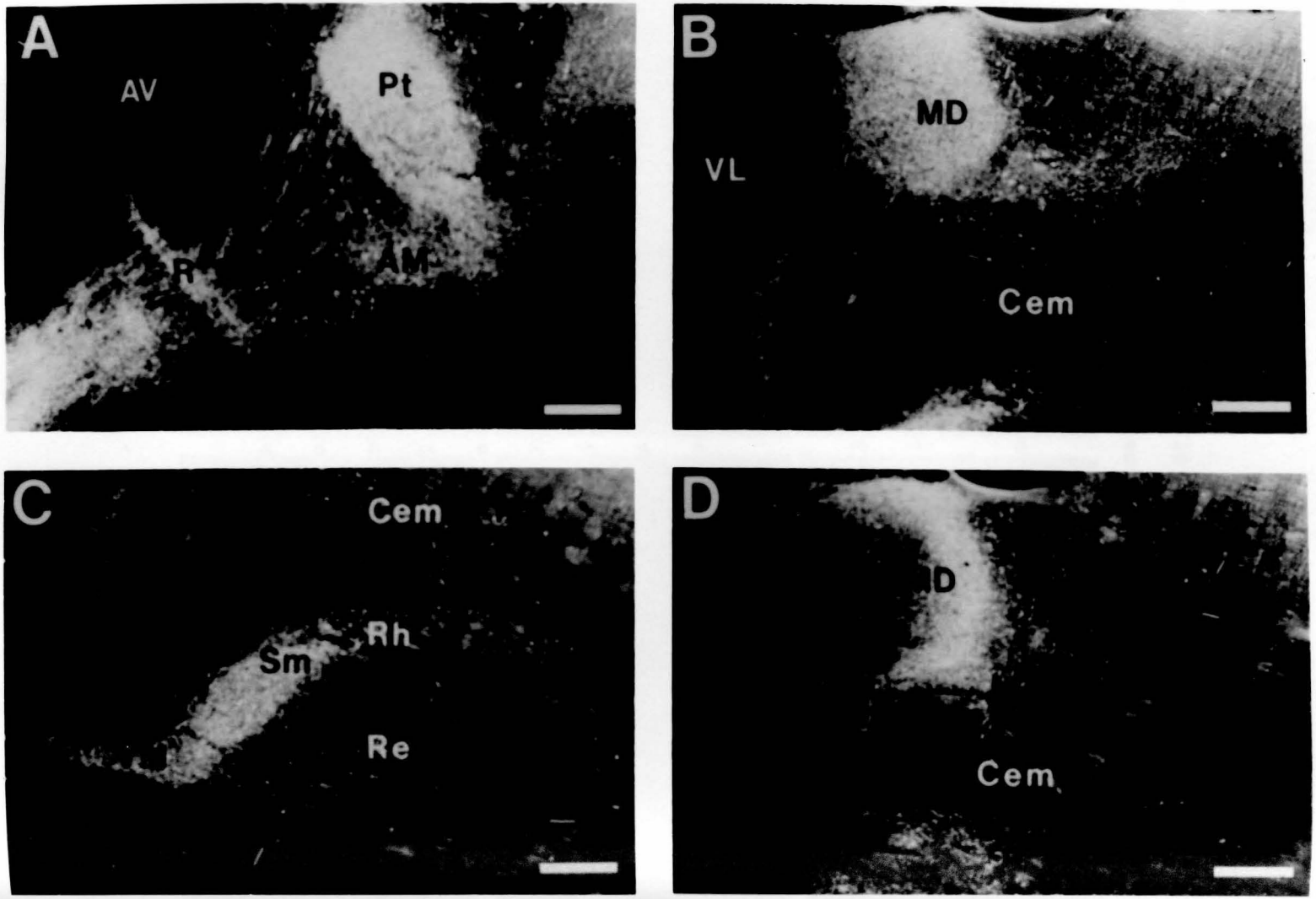
A
AV
Pt
R
M
B
MD
VL
Cem
C
Cem
Rh
Sm
Re
D
D
Cem

Figure 6.

Darkfield photomicrographs of anterograde labeling observed after a PL/IL injection (Figure 1B). The corresponding line drawing is indicated in parenthesis. A: Anterograde label in the ventral portion of the nucleus accumbens (Acc) and light labeling of the olfactory tubercle (OT). Arrows indicate labeling of the cellular bridges between Acc and OT, the unlabeled areas between these cell bridges are portions of the ventral pallidum. (Figure 4B). B: Anterograde label in the central gray (CG). (Figure 4K). C: Anterograde label in the ventral tegmental area (VTA) and the substantia nigra, pars reticulata (SN). (Figure 4H). D: Anterograde label seen in the lateral dorsal tegmental nucleus (LDTg). No label was seen in the dorsal tegmental nucleus of Gudden (DTg). (Figure 4L). E: Anterograde labeling within the pontine nuclei. The label is bilateral, the midline is in the center of the field. (Figure 4J). F: Bilateral anterograde label in the inferior olivary complex. Arrows indicate label within the ventral lateral outgrowth (vlo) and in the Beta subnucleus (B) of the inferior olive. No label can be seen in the medial accessory olive (MAO). (Figure 4R). Scale bar = 250 um.

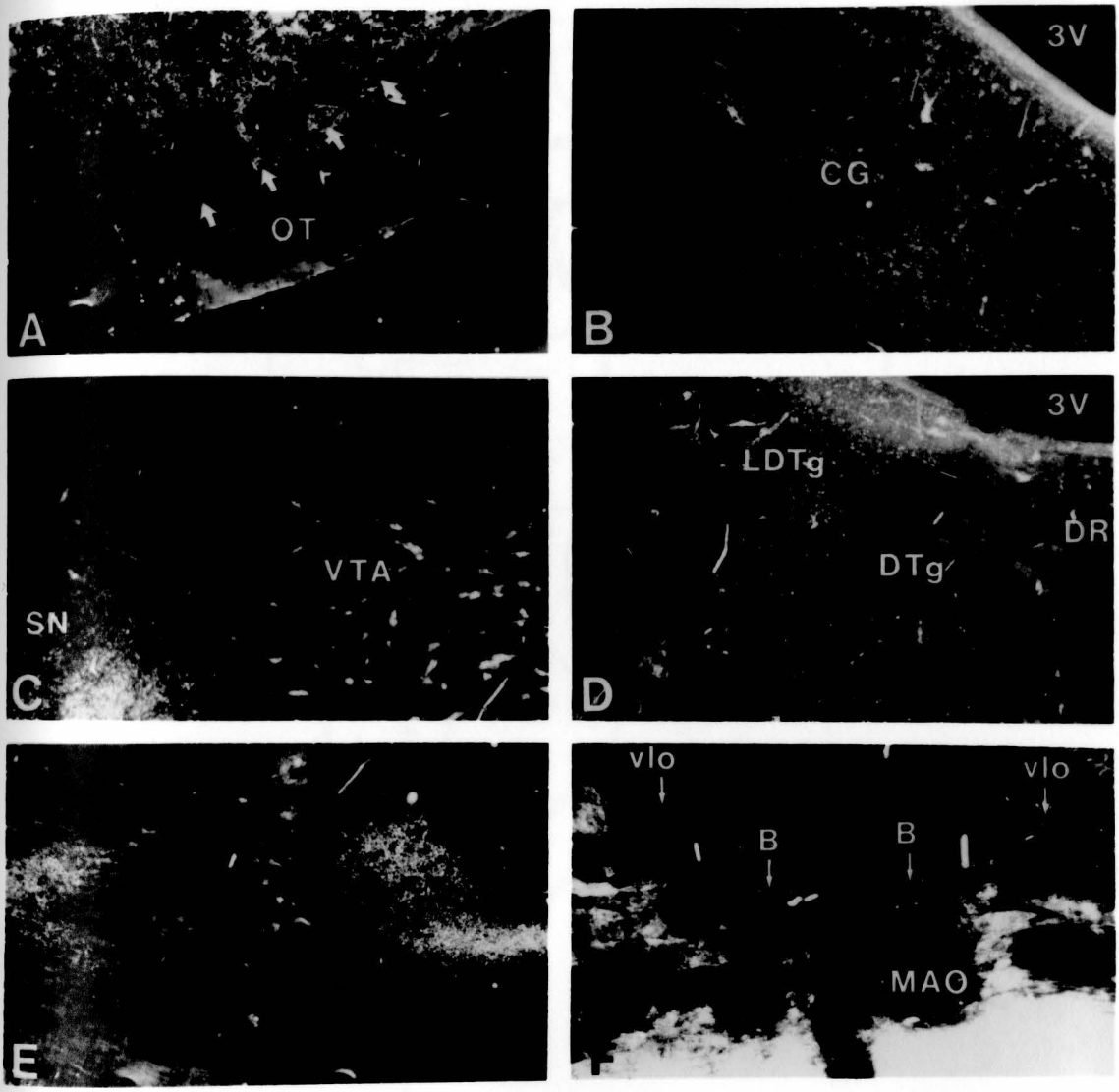
A
OT
B
3V
CG
C
VTA
SN
D
3V
LDTg
DR
DTg
E
vlo
vlo
B
B
MAO

Figure 7.

Line drawing of the anterograde labeling within the rostral NTS (0.9 mm rostral to obex). Insert illustrates the WGA-HRP injection site (hatched area). See text for abbreviations. Scale bar = 200 um.

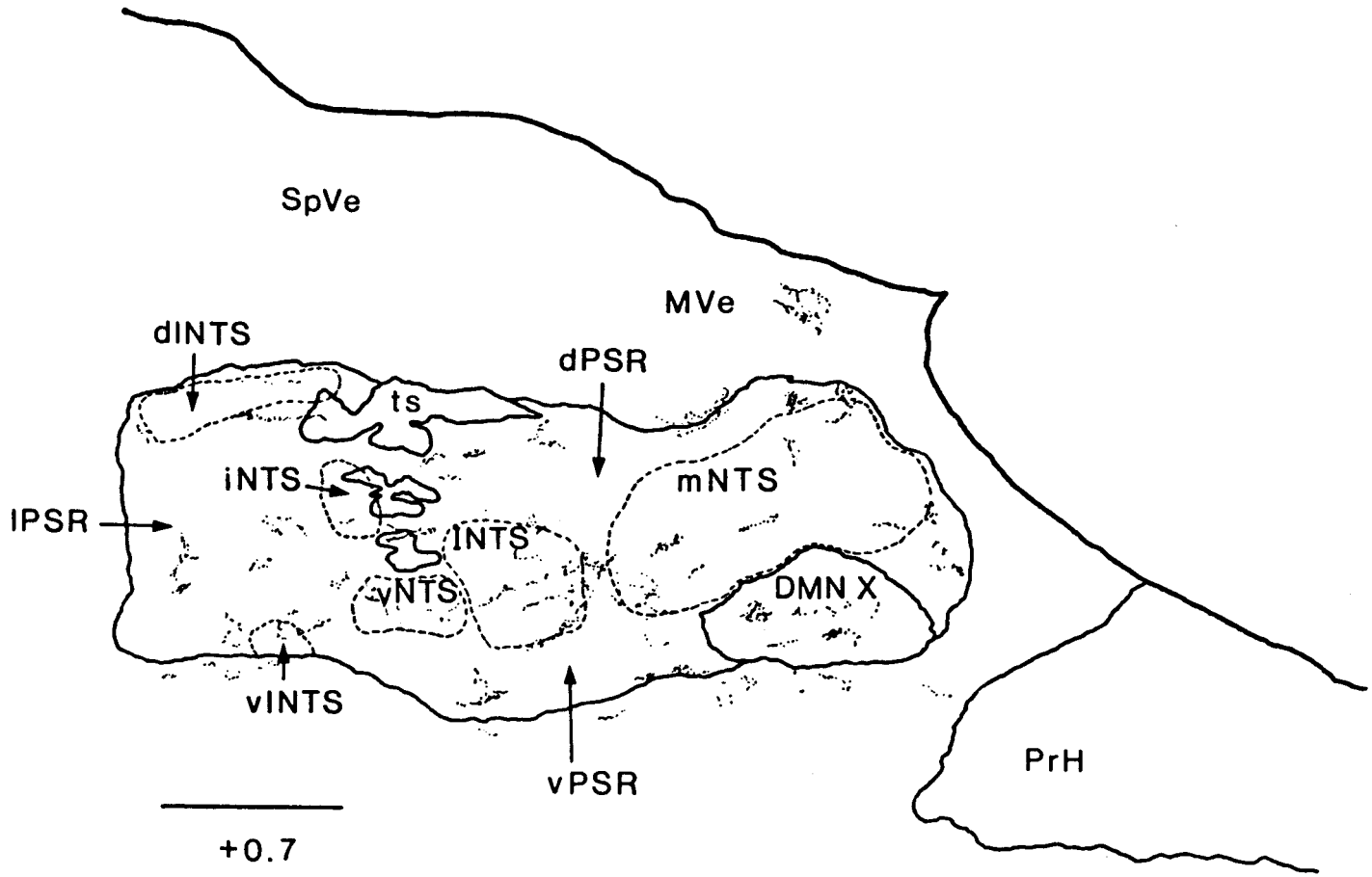
SpVe
MVe
dINTS
dPSR
ts
iNTS
mNTS
lPSR
lNTS
vNTS
DMN X
vINTS
vPSR
PrH
+0.7

Figure 8.

Line drawing of the anterograde labeling within the NTS at the level of the obex. See text for abbreviations. Scale bar = 200 um.

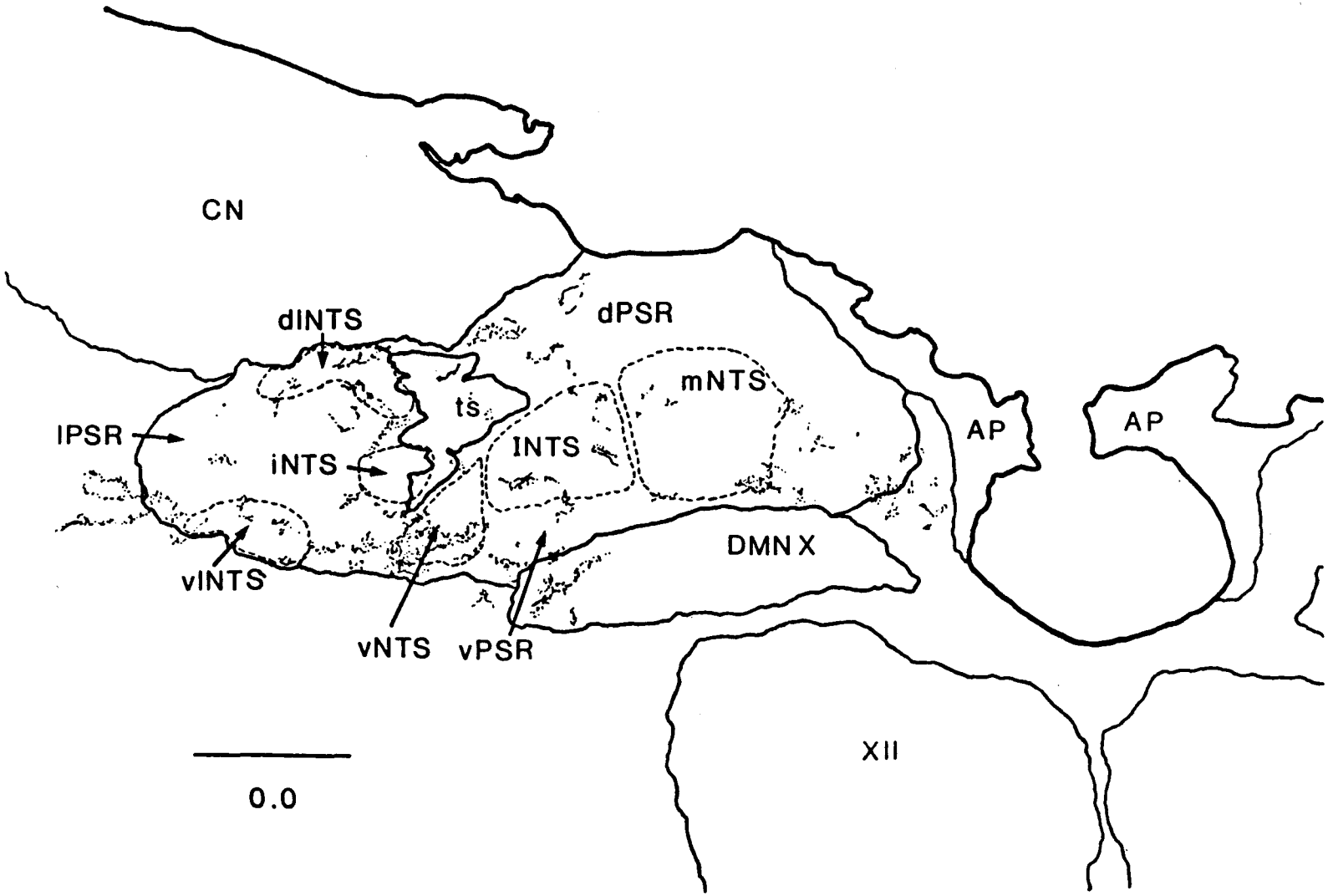
CN
dINTS
dPSR
mNTS
ts
lPSR
iNTS
INTS
AP
AP
DMN X
vINTS
vNTS
vPSR
XII
0.0

Figure 9.

Line drawing of the anterograde labeling within the NTS at a level caudal to obex (0.9 mm caudal to obex). See text for abbreviations. Scale bar = 200 um.

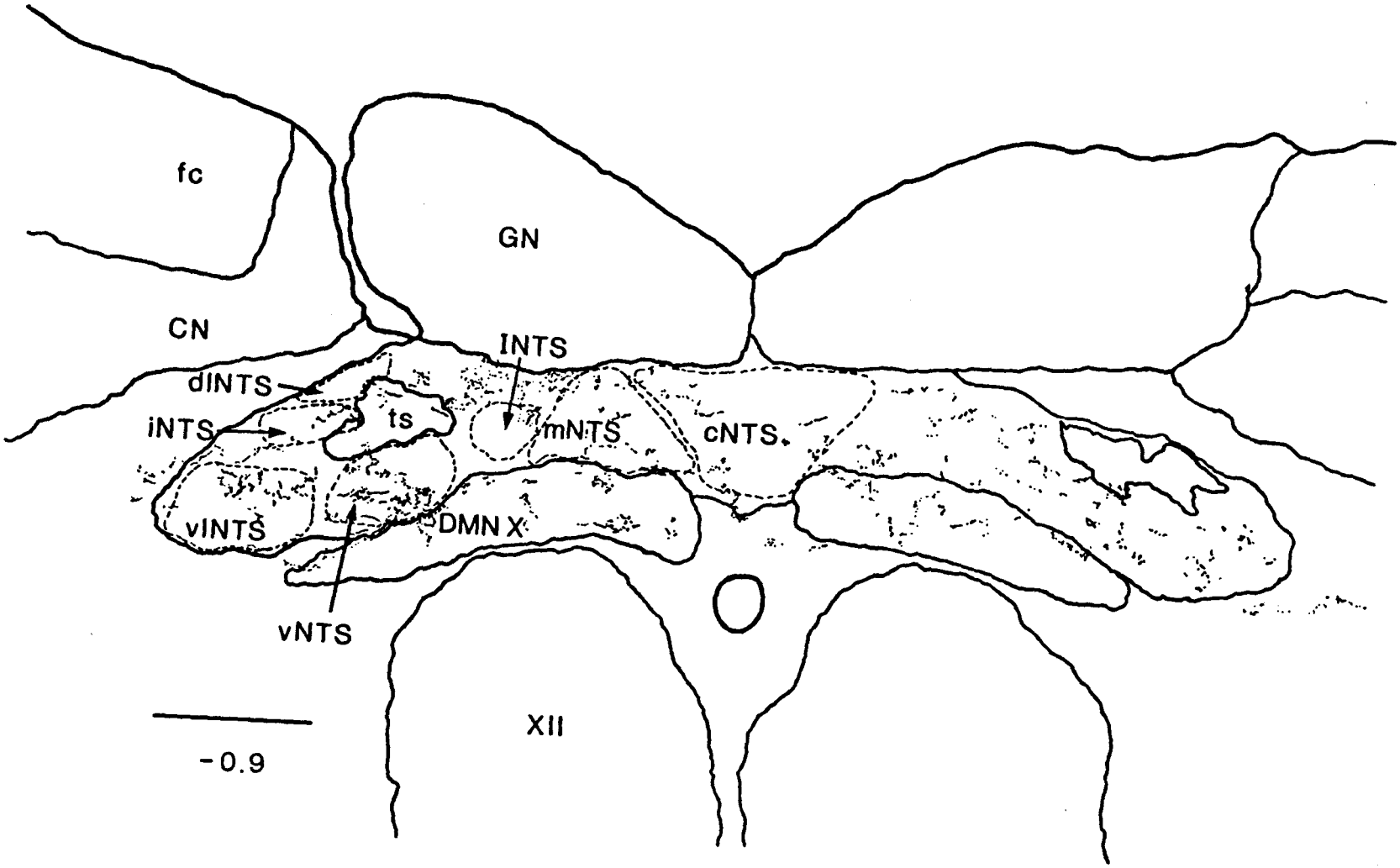
fc
GN
CN
INTS
dINTS
iNTS
ts
mNTS
cNTS
vINTS
DMN X
vNTS
XII
-0.9

Figure 10.

Line drawing of the anterograde labeling within the NTS at an extreme caudal level of the NTS (1.6 mm caudal to obex). See text for abbreviations. Scale bar = 200 um.

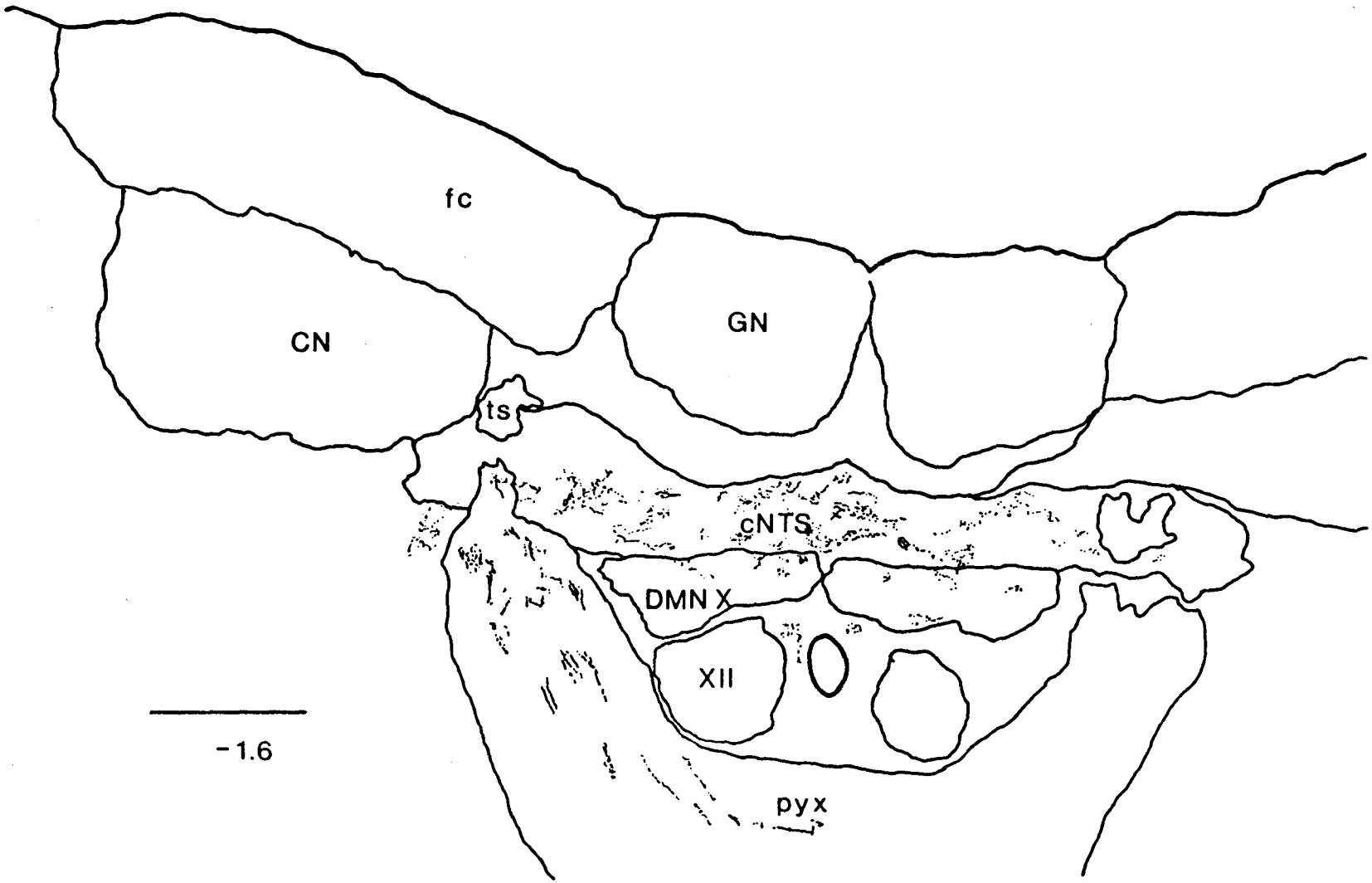
fc
CN
GN
ts
cNTS
DMN X
XII
-1.6
pyx

Figure 11.

A series of darkfield (A,C,E,G) and corresponding brighfield (B,D,F,H) photomicrographs through four levels of the NTS which correspond to the four levels seen in Figures 7-10. The small white arrows in the darkfield photomicrographs indicate the location of terminal anterograde labeling. The two large arrows in G indicate the presence of labeled fibers within the decussating pyramidal tract. See text for abbreviations. Scale bar in H = 250 um.

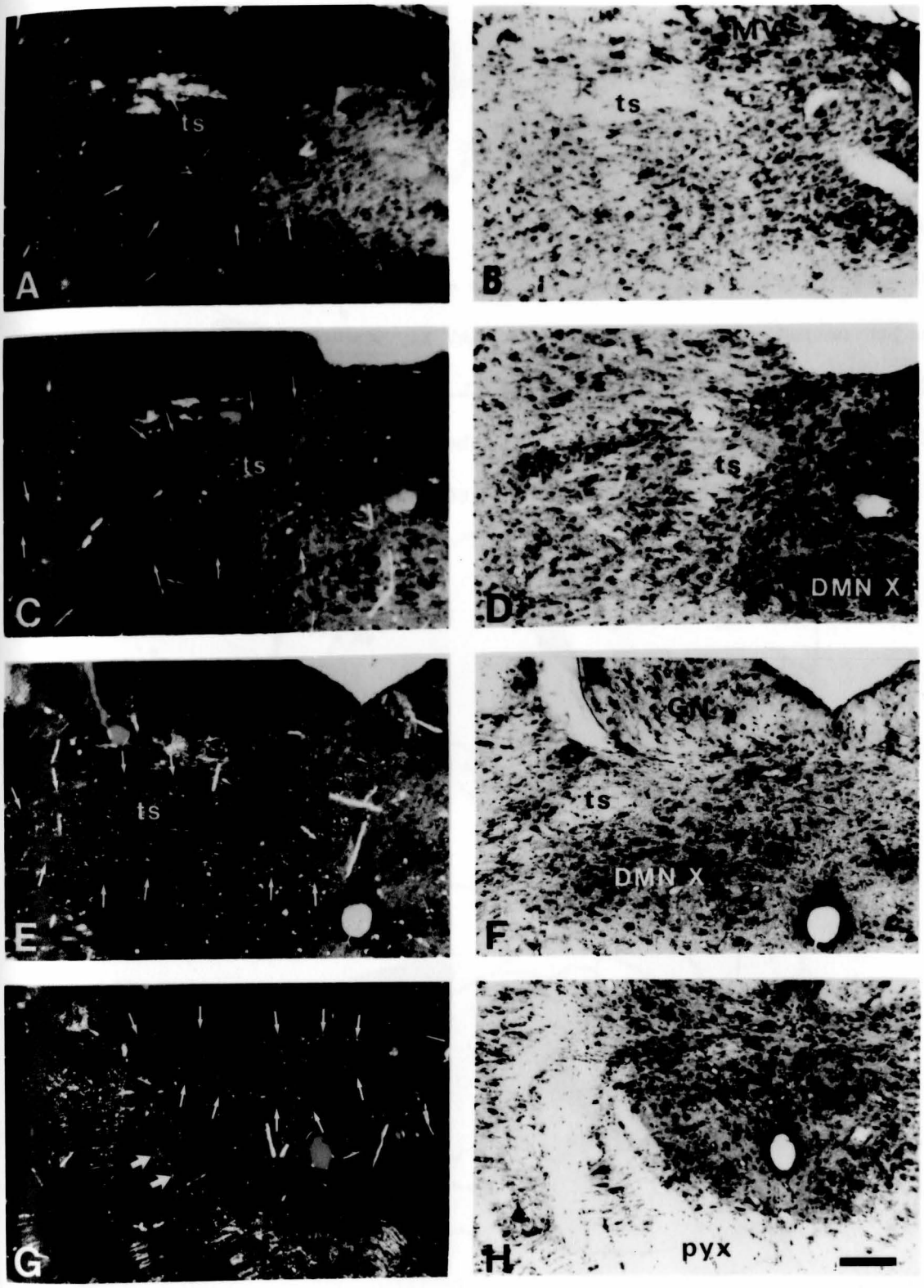
ts
A
MV
ts
B
ts
C
ts
DMN X
D
ts
E
GN
ts
DMN X
F
G
pyx
H

Figure 12.

Schematic drawings of a medial view of the rat brain illustrating the major outputs from the IL cortex. A: Limbic outputs from IL. B: Central motor system outputs from IL. C: Central visceral outputs from IL. Efferent projections to the insular cortex are not illustrated. See text for abbreviations.

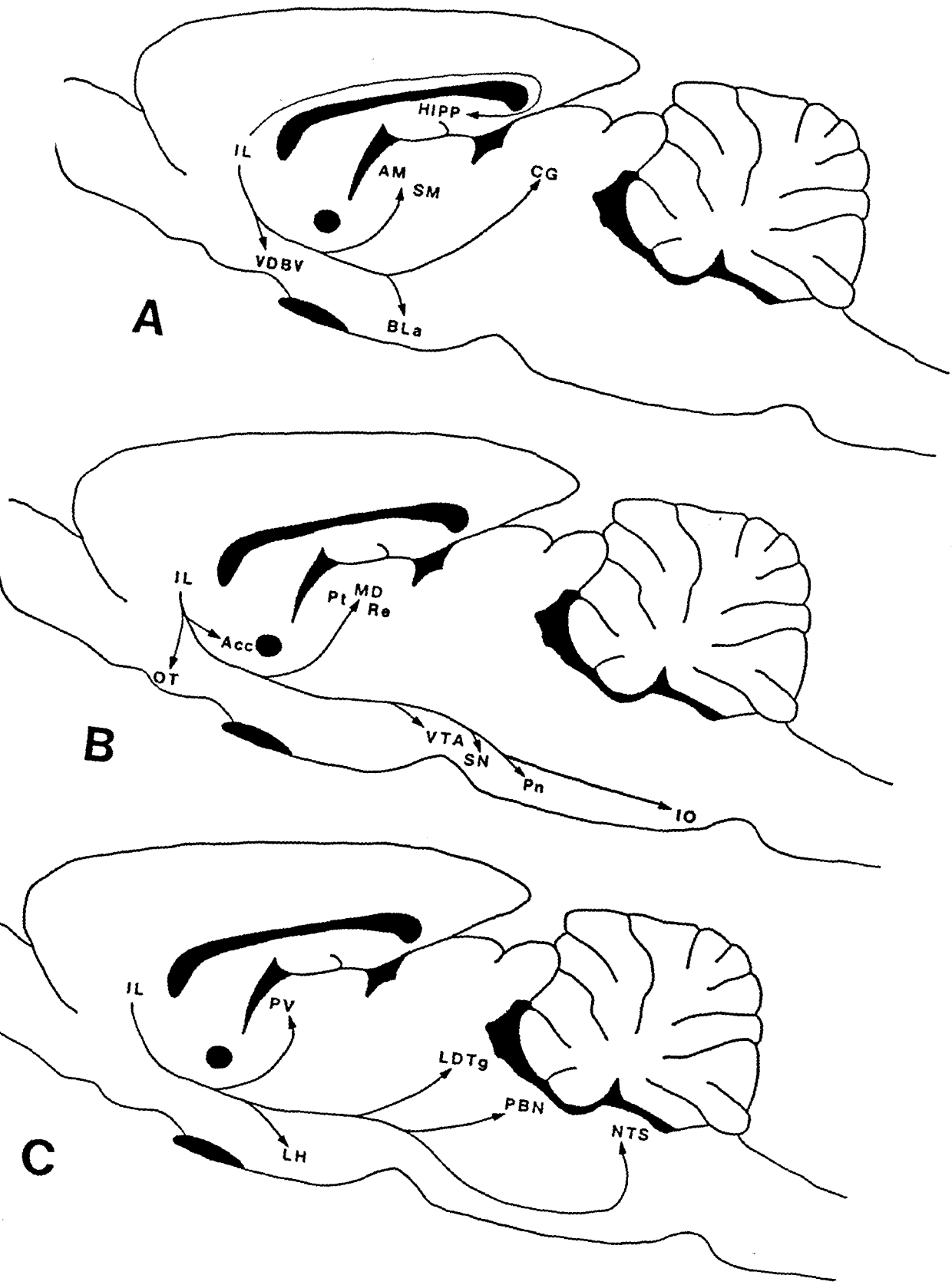
HIPP
IL
AM
SM
CG
VDBV
BLa
A
IL
Pt
MD
Re
Acc
OT
VTA
SN
Pn
IO
B
IL
PV
LDTg
PBN
NTS
LH
C

Figure 13.

Diagram depicting the various components of the ventral striatal system (A) and the dorsal striatal system (B). Modified from Heimer et al. (1982).

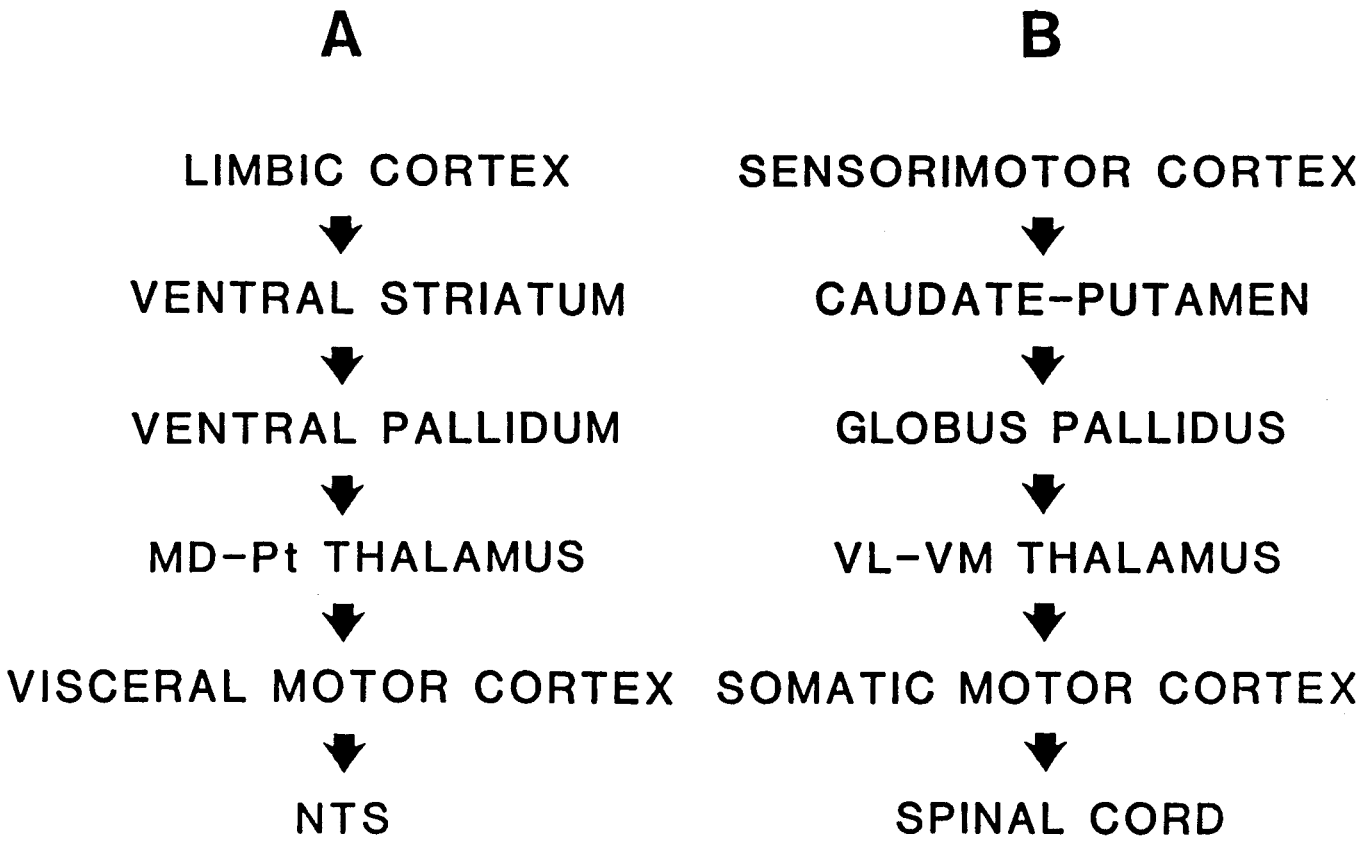
A
LIMBIC CORTEX
VENTRAL STRIATUM
VENTRAL PALLIDUM
MD-Pt THALAMUS
VISCERAL MOTOR CORTEX
NTS
B
SENSORIMOTOR CORTEX
CAUDATE-PUTAMEN
GLOBUS PALLIDUS
VL-VM THALAMUS
SOMATIC MOTOR CORTEX
SPINAL CORD

CHAPTER VI

PHYSIOLOGICAL RESPONSES ELICITED FROM THE RAT MEDIAL FRONTAL CORTEX

ABSTRACT

Low threshold (< 50 uamps) intracortical microstimulation of the infralimbic (IL) region of the rat medial frontal cortex elicited changes in cardiovascular and respiratory activity. The most frequent response elicited was a bradycardia (76%), the second most frequent response seen was a depression of the arterial blood pressure (61%) while the least frequent response was a slowing of respiration. These responses could be abolished with methyl-atropine, bilateral vagotomies or bilateral pyramidotomies. The responses were unaffected by the sympathetic blockers propranolol and phentolamine. These results suggest that the cortically-evoked responses may be mediated via the vagus nerves and that the direct cortico-solitary projection from the IL cortex to the nucleus of the solitary tract may be involved in mediating these responses. The IL cortex appears to function as a "visceral motor cortex," capable of eliciting changes in several autonomic functions.

INTRODUCTION

Autonomic functions can be influenced by virtually every level of the nervous system, including the cerebral cortex. One cortical area frequently associated with autonomic functioning is the anterior cingulate cortex where numerous studies have shown that electrical

stimulation elicits changes in cardiovascular, respiratory and gastric activity (Kaada, 1951, 1960; Lofving, 1961; Henke, 1982; Burns et al., 1983; West and Benjamin, 1983; Neafsey and Hurley, 1984; Burns and Wyss, 1985). The recent finding of a direct projection from the infralimbic (IL) region of the rat medial frontal-anterior cingulate cortex (MFC) to the NTS, specifically to NTS subnuclei which are involved in respiratory and cardiovascular functioning (Chapter V), suggests that this pathway may be responsible for the changes in respiratory and cardiovascular activity evoked by IL stimulation. The present study was designed to investigate the functional characteristics of this direct IL-NTS projection and had three objectives. The first was to systematically map the rat MFC utilizing intracortical microstimulation techniques to determine the specific cortical areas that could elicit changes in blood pressure, heart rate and respiration. These results will then be correlated with the results of our previous anatomical studies. The second objective was to determine if the cardiovascular responses were vagally or sympathetically mediated by blocking vagal or sympathetic activity pharmacologically or by lesions. The third objective was to determine the effects of lesions of the pyramidal tract on the responses elicited by IL stimulation since the IL-NTS projection travels via the pyramidal tract.

MATERIALS AND METHODS

A total of 37 adult long Evans male rats (250-500 gmms) was used in this study. Since both anesthetized and unanesthetized preparations were used in this series of experiments, each will be addressed separately.

Acute Anesthetized Preparation

Physiological Maps

The first experiment in this series was to carefully map the sites from which cardiovascular and/or respiratory responses could be evoked by stimulating the MFC region in the anesthetized rat (n = 26). Animals were anesthetized with Ketamine HCl (100 mg/kg, IP; supplemental doses of one-quarter the initial dose were given to maintain a constant level of anesthesia). A catheter (PE50; filled with 0.9% physiological saline) was inserted into the femoral vein for the administration of supplemental fluids and/or pharmacological agents. A second, heparinized catheter (PE50; 1 part heparin (1000 units/ml): 5 parts 0.9% physiological saline) was inserted into the femoral artery to monitor blood pressure (BP). The BP cannula was attached to a stratham P23 ID pressure transducer and connected to a Grass Model 54 channel polygraph. The BP recording was calibrated at the beginning and end of each experiment. Heart rate recordings were derived from the EKG which was recorded by pin electrodes inserted

through the back and chest musculature and connected to an amplifier. The EKG waveform was displayed on an oscilloscope and fed into a window discriminator; the window's upper and lower levels were carefully monitored and adjusted when necessary to ensure that the EKG signal remained within the window during the stimulation period. The output of the window was sent to a rate meter and this signal was then recorded on the polygraph. A Y-shaped tracheal cannula was inserted to prevent fluid accumulation in the upper respiratory passages, as well as to facilitate artificial respiration, if necessary. The frequency of respiration was monitored using a Grass TCT-1R thermistor device positioned in one of the branches of the tracheal cannula. The thermistor was connected to an amplifier whose output was sent to the polygraph. The animals were then placed into a stereotaxic frame, and a heating pad was used to maintain the animal's body temperature between 36-38 degrees celcius.

Following surgical exposure of the skull and neck musculature, the cisterna magna was opened in order to drain the cerebrospinal fluid and thus prevent cortical swelling. A small, 2x2 mm piece of calvaria just rostral to bregma overlying each MFC was then removed using a low-speed drill. The bone overlying the superior sagittal sinus was then dissected free with the aid of a rongeurs. The dura was removed from the exposed cortex and the cortex bathed in warmed mineral oil. The resulting defect in the calvaria exposed the midline sinus and permitted access to the MFC on either side of the sinus.

A pair of glass-insulated tungsten microelectrodes (Neafsey, 1981) mounted parallel to one another (1.5 mm separation) on a micromanipulator were used to make a series of electrode tracks. The tracks were spaced 0.25-0.5 mm apart, perpendicular to the dorsal cortical surface, with each electrode positioned 0.75 mm lateral to the midline. Electrode penetrations were made in the area 2-4 mm rostral to bregma, and a Kopf 1760/1761 micromanipulator was employed to position and advance the electrodes.

Bilateral electrical stimulation was delivered every 0.5 mm along the 4-5 mm extent of each track using a 10-30 second train of 0.5 msec pulses at 50 Hz and a maximum current of 50 uamps; at least 30 seconds elapsed between stimulation trains. Current intensities began at 25 uamps, and, if a response was noted, the threshold current for the response was determined by progressively lowering the current intensity until the response was no longer elicited. If a response was not elicited with 25 uamps, the stimulating current was progressively increased until a maximum of 50 uamps was reached to determine if that point was responsive or not; non-responsive points are defined as points where 50 uamps of current did not elicit a response. At selected points, small electrolytic lesions (5-10 uamps, DC for 5-10 seconds) were made to facilitate histological reconstruction of the electrode tracks.

At the conclusion of each experiment, the animals were sacrificed by cardiac perfusion with 0.9% saline and 10% buffered formalin, and

the brains removed, placed in a 30% sucrose-formalin solution and allowed to sink (2-3 days). Fifty micron frozen coronal or sagittal sections were cut, mounted and stained with cresyl violet or cyanin R (a myelin stain). Line drawings of each section were made utilizing a Bausch and Lomb projection scope, and the electrode tracks were then reconstructed on these drawings. The cytoarchitectonic region(s) (see Chapter II for review of MFC cytoarchitecture), where low threshold responses could be evoked, were then determined.

Pharmacological Study

In eight of the experiments just described, the effect of various pharmacological agents on the responses was examined. Following the identification of a responsive point, either methyl-atropine, propranolol or phentolamine was administered via the venous catheter in the following doses: methyl-atropine, 0.04 mg/kg; propranalol, 1 mg/kg; phentolamine, 1 mg/kg. Two to five minutes after the administration of the drug, a bilateral stimulus identical to the stimulus which evoked the response was delivered, and the effect of the drug on the response noted. At the conclusion of the experiment, the animals were sacrificed, perfused and the brains processed in the same manner as previously outlined.

Lesion Experiments

In five of the acute experiments the effects of either a vagotomy or pyramidotomy on the responses were tested. The animals in this group underwent identical surgical procedures as the two previous groups. Following the identification of a responsive point, the electrodes were cemented into place using dental acrylic cement, and the animals were then turned over in the stereotaxic frame to expose their ventral surface. Following dissection of the neck musculature, either the vagi or pyramidal tracts were exposed. The vagi were carefully dissected out of the carotid sheaths, with special care taken to avoid excessive manipulation or physical trauma to the nerves. Stimulation of IL was then delivered to confirm that the response was still present. Then the vagus nerve on one side was cut, the stimulation repeated and the response noted. After 2-5 minutes, the other vagus nerve was cut, the stimulation was repeated and the response noted.

The pyramidotomy lesions were performed in the following manner. After dissection of the neck musculature, the trachea and esophagus were ligated and cut; a tracheal cannula was inserted into the proximal end of the trachea to maintain an airway. The basilar portion of the occiput was exposed, and, using a low-speed drill, a small piece of bone was removed from the region of the pyramidal tracts (rostral to the decussation). At this point stimulation was repeated to verify the response still occurred with the pyramids intact. A #11 scalpel blade was used to section the pyramidal tracts,

one side at a time. After sectioning the tract on one side, stimulation was repeated and the response noted; after 2-5 minutes the remaining pyramidal tract was sectioned, stimulation was repeated and the response noted. At the end of these experiments (both vagotomy and pyramidotomy) the animals were perfused and the brains processed for light microscopy as previously described.

Chronic Unanesthetized Preparation

Another series of experiments examined the effects of stimulating the MFC on heart rate in awake, unanesthetized animals. Initially, the rats (n = 11) were anesthetized with Ketamine HCl (100 mg/kg, IP). While anesthetized each animal had two flexible EKG leads embedded into the back and chest musculature. Those leads were then led subcutaneously to the back of the neck where they were fixed to the skull with dental acrylic cement. The animals were then placed into a stereotaxic frame, and a small bilateral craniotomy over the MFC (2-5 mm rostral to bregma) performed. Using a micromanipulator, a single glass-insulated tungsten electrode (Neafsey, 1981) was stereotaxically implanted into each hemisphere (3.0-3.7 mm rostral to bregma, 0.75 mm lateral to the midline, depth of 3.0-4.0 mm down from the cortical surface). The placement of the electrodes was checked by delivering low intensity electric stimulation (< 50 uamps) and eliciting a heart rate (derived from the EKG) response. Once a response was noted the electrodes were cemented in place. The scalp was sutured tightly

around the cement plug, and the animals allowed to recover. Following a 1-2 day recovery period, each animal was placed in a Plexiglas testing chamber. A flexible cable was attached to the stimulating and recording leads on the animal's head; the animal was free to move. Bilateral electrical stimulation was delivered using 5 second trains of negative 0.5 msec pulses at 25-50 Hz with current intensities between 50-300 uamps, with the initial current between 50-100 uamps. In some animals (n=3) the effects of methyl-atropine (0.04 mg/kg IP) on the response was studied. After 2-4 testing sessions, marking lesions were made through the stimulating electrodes (5-10 uamps DC for 5-10 seconds). The animals were then overdosed with sodium pentabarbitol (40 mg/kg, IP) and sacrificed by cardiac perfusion with 0.9% saline and 10% buffered formalin, and the brains removed. Similar histological procedures were followed as described earlier, and the cytoarchitectonic region(s) where low threshold responses were evoked were determined.

RESULTS

Acute Anesthetized Preparation

Of 486 stimulation points explored within the rat MFC, 63% had an effect on either heart rate, blood pressure or respiration. Thirty percent of the responsive points elicited changes in two of the parameters measured, and changes in all three parameters were seen

after bilateral electrical stimulation of 18% of the sites tested. Of the responses seen, the most prevalent type (76%) consisted of bradycardia (Figures 2A-D). This type of response could be elicited with stimulation currents as low as 10 uamps (Figure 2B). These stimulus-evoked changes in heart rate began within 1-2 seconds of stimulus onset, and the heart rate returned to baseline (pre-stimulus level) within 10-15 seconds after stimulus offset. The bradycardia elicited was usually between a 10-20% decrease from the baseline rate with the relatively low current intensities used (< 50 uamps). Larger drops in heart rate could be elicited with higher currents (50-100 uamps), but these higher intensity stimuli were not routinely employed to avoid excessive spread of current.

The second most frequently observed response (61%) was a depressor response of the arterial blood pressure. This depressor effect usually began within 1-2 seconds of stimulus onset (Figures 2A,B,C) and returned to baseline levels within 10-20 seconds after stimulus offset. Figure 2D illustrates another type of depressor response, one where the drop in arterial pressure did not coincide with the heart rate decrease but instead began about 5-10 seconds after stimulus onset and returned to baseline within twenty seconds after stimulus offset. Using a Paired T-test, statistical analysis of these cortically-evoked heart rate and blood pressure responses revealed that, in the 18 animals analyzed, the resposes were statistically significant from the baseline levels at a P value of <

.0005 (Table 1).

Alterations in respiration were the least frequently observed effect of bilateral MFC stimulation (32%). Two different types of respiratory response were seen, the first being a slight slowing of the respiratory frequency, with what appeared to be deeper, slower breaths being taken by the animal (Figures 2A,B,C; it is difficult to appreciate these respiratory effects in these reduced-size tracings at this chart speed, but they can be clearly observed on the original records). The second type of respiratory response consisted of a total cessation of respiration, usually during the expiration phase of the cycle (Figure 2D).

Histological reconstructions of the electrode penetrations indicated that the majority of responsive points were located in the pre- and infralimbic areas of the MFC (see Chapter II for description of cytoarchitecture). The coronal section in Figure 1A illustrates a single electrode tract from experiment ACUTE 19 with a lesion in the taenia tecta. Stimulation of a point 0.5 mm dorsal to this point (Figures 3E,F) produced the responses shown in Figure 2D. Figures 3A,C,E show line drawings of sagittal sections from three experiments in which the electrode tracks have been reconstructed and the stimulation points labeled according to the type of response evoked by stimulation. Although there is some variability from case to case as to the exact location of the responsive areas, it appears that the responsive area is confined to the pre- and infralimbic cortices. The

dorsally located anterior cingulate cortex and ventrally located region taenia tecta were generally non-responsive. Figures 3B,D,F illustrate the threshold intensity of the responses illustrated in Figures 3A,C,E. The solid circles indicate points where the threshold for a response was 25 uamps or less; note that these points were all located in the deeper, infralimbic portions of the MFC.

Effects of Atropine, Propanolol or Phentolamine on Responses

To determine whether or not these inhibitory responses were vagally mediated, the effect of methyl-atropine, propranolol or phentolamine was tested in four animals. Figure 4A illustrates the heart rate, blood pressure and respiratory response evoked by cortical stimulation prior to the administration of methyl-atropine (0.04 mg/kg, IV). Figure 4B illustrates the effect of methyl atropine on subsequent stimulation efficacy in the same animal. Seventy five seconds after the administration of atropine, a 40 uamp stimulus which previously had elicited clear heart rate and slight blood pressure responses (Figure 4A) produced only a slight decrease in heart rate and no obvious effect on blood pressure (Figure 4B). However, the respiratory response (cessation during expiration) was still present and seemed greatly enhanced over the pre-atropine trials (Figure 3B, second and third stimuli). Similar results were seen in the other animals treated with methyl-atropine. The effects of propranolol and phentolamine on the responses were also studied. Figure 4C, from

another experiment, illustrates the pre-propranolol responses evoked by cortical stimulation. Figure 4D illustrates the responses seen one minute, four minutes and five minutes after the administration of propranolol (1 mg/kg, IV). Note that the responses persisted with little or no effect caused by the propranolol. Similar responses were seen in the other animals treated with propranolol, as well as in the animals treated with phentolamine.

Effect of Vagal Lesions

To further investigate the role of the vagus nerve in these responses the effect of unilateral and bilateral vagotomies was tested in three animals. Figure 5A illustrates the depressor response, respiratory response and a slight heart rate decrease in an intact rat. Figure 5B illustrates the effect of sectioning the right cervical vagus on the response to subsequent stimulation in the same animal. The depressor response still appears to be present although the heart rate decrease appears to be slightly less than that seen in the intact animal (Figure 5A). After sectioning the left vagus nerve (Figure 5B, middle panel) the subsequent stimulation appeared to still elicit a depressor response, but the heart rate response was abolished. Figure 5B (third panel) illustrates the responses seen five minutes after the bilateral vagotomy was completed. At this time only a decrease of the respiratory frequency could be elicited from cortical stimulation, while both the BP and HR responses had been

eliminated by the bilateral vagotomy. The vagal lesions in the other two animals had similar effects. (The changed pattern of spontaneous respirations was due to the vagal lesions).

Effect of Pyramidal Tract Lesions

From our earlier anterograde tracing study (see Chapter V), it appeared that the cortico-solitary projections travelled via the pyramidal tract to reach the NTS. To test whether this tract was important in mediating the responses seen after cortical stimulation, unilateral and bilateral pyramidotomies were studied in two animals. Figure 6A illustrates the heart rate and blood pressure responses evoked by cortical stimulation in an intact animal. Higher current intensities (150, 300, or 400 uamps) were necessary to evoke these responses when the animal had been turned over; the reason for this is not known, but it may have been due to a shift in electrode position when the animal was in the new position. The effect of sectioning the left pyramid on subsequent stimulation efficacy in the same animal is shown in Figure 6B. There was some attenuation of the blood pressure depressor response while the heart rate response appeared only slightly affected by the left pyramid lesion. After sectioning the right pyramid and the remaining midline fibers of both pyramids the HR and BP responses were almost entirely abolished (Figure 6C). Figure 6D illustrates the effect of cortical stimulation five minutes after the total pyramidotomy was completed, and it is clear the responses

were still absent. The bilateral pyramidal tract lesion is illustrated in Figure 1C. In the other animal studied the lesion missed the pyramidal tract but did damage the ventrolateral medulla unilaterally. This lesion also abolished the response to IL cortex stimulation.

Chronic Preparation

Of the 11 rats tested, four responded to cortical stimulation with a marked decrease in heart rate (HR), while one animal responded to stimulation with an increase in HR. The remaining six animals exhibited no changes in HR upon electrical stimulation. Histology showed the electrode placements in these six non-responsive animals were in the cortical white matter or the dorsal anterior cingulate cortex, not in the pre- and infralimbic cortices.

The decreases in HR seen in four animals ranged from a 10-30% drop from the baseline rate (Figures 7A,B,8A). These reponses were evoked by current intensities of 150 uamps or less, with 50 uamps being the lowest stimulus current that evoked an appreciable heart rate decrease. The decreases in HR were most obvious when the baseline rate was high (> 500 bpm). When the baseline rate was low (< 400 bpm) the effect of cortical stimulation in one animal was an increase in HR (16% above baseline) with a 50 uamp stimulus (Figures 8C,D). Using a Paired T-test, statistical analysis of these cortically-evoked heart rate (bradycardia) responses revealed that

these drops in heart rate were statistically significant from the baseline levels at a P value of < .01 (Table 2).

Histological reconstructions of the electrode tracks allowed for the localization of responsive points. All responsive points were localized within the infralimbic cortex (IL) (Figure 9); stimulation of points within the more dorsal prelimbic cortex (PL) resulted in smaller and less consistent effects on heart rate.

The effect of methyl-atropine on these HR responses was studied in animals where low threshold responses were obtained (Figures 7C, 8A). Two to five minutes after the administration of methyl-atropine, a stimulus identical to the stimulus which elicited the initial response was given. The result was that the atropine appeared to have completely abolished the response (Figures 7D, 8B).

DISCUSSION

The results of the present study demonstrate that electrical stimulation of the infralimbic (IL) region of the rat medial frontal cortex (MFC) can evoke substantial, short latency decelerations in heart rate, depression of arterial blood pressure and a depression of respiration. The stimulus-evoked HR responses were seen in both anesthetized and non-anesthetized preparations and were completely abolished or greatly attenuated by atropine or bilateral section of the cervical vagus nerves. These results suggest that the heart rate

response is vagally mediated. Pyramidal tract lesions also abolished the responses, but similar effects could also be obtained by lesions of the adjacent ventrolateral medulla, making it difficult to be certain that the central pathway involves the pyramids.

Changes in autonomic parameters evoked by stimulation of the anterior cingulate-medial frontal cortex have been previously reported for several species, including rat (Smith, 1938, 1945; Ward, 1948; Kaada, et al., 1949; Kaada, 1951, 1960; Wall and Davis, 1951; Anand and Dua, 1956; Lofving, 1961; Hoff et al., 1963; Hall et al., 1977; Burns et al., 1983; Burns and Wyss, 1985). However, none of these studies have shown that the cortical autonomic effector area corresponds to the cortex that has direct projections to brainstem autonomic nuclei such as the nucleus of the solitary tract (NTS). The area of the MFC from which low threshold responses were elicited from in the present study, namely the infralimbic cortex, has been shown to project to the NTS (Terreberry and Neafsey, 1983; van der Kooy et al., 1982, 1984), suggesting that this cortico-solitary projection may be functioning in autonomic control of cardiovascular and respiratory activity.

The present data indicate that the responsive cortical area is very discrete, with the lowest thresholds for eliciting these responses seen when the stimulation site is within the IL cortex. Stimulation of the more dorsal prelimbic (PL) cortex also elicits autonomic responses, but the thresholds for these points are higher

than those which elicit responses from the IL cortex. The dorsal anterior cingulate (AC) cortex was generally non-responsive at the current intensities utilized in the present study (< 50 uamps). Recent studies by Burns et al. (1983) and Burns and Wyss (1985) reported BP changes from AC stimulation; however, the stimulating currents used in those studies were 800-200 uamps, respectively. Additionally, Burns and Wyss (1985) reported that pressor responses were elicited from the ventral portion of the IL cortex and the anterior one-third of the AC cortex in the awake rat. In the present experiments only depressor responses were elicted from the MFC of Ketamine-anesthetized rats. The difference in results may be due to the use of anesthesia in our experiments. However, studies by Burns et al. (1983) and Burns and Wyss (1985) reported no alteration in HR during MFC stimulation of the anesthetized or awake rat, in apparent disagreement with the present data. The anesthetic agent may be one explanation for this discrepancy, as their studies employed a-chloralose, urethane or ether anesthesia while the present study employed Ketamine HCl. However, the failure of their studies to find heart rate decreases in the awake rat clearly disagrees with our results. It is possible their electrode placements were too dorsal, since six of our awake rats, with electrodes in the AC cortex, also did not show heart rate decreases. In agreement with our findings, Buchanan and Powell (1984) have reported heart rate decreases following MFC stimulation in awake rabbits.

The pharmacological and vagal lesion data suggest that the responses are primarily vagally mediated. Methyl-atropine acts on cholinergic muscarine synapses, which are characteristic of the vagus nerve. In both the anesthetized and awake rat the administration of methyl-atropine abolishes or markedly attenuates the heart rate responses, while having only a small effect on the depressor response and possibly slightly enhancing the respiratory response (see Figure 4). This data indicates that vagal activity is necessary to elicit the bradycardia effect, but not the blood pressure or respiratory effect. The presence of a slight heart rate decrease after atropine treatment in some animals indicates that there may be some cortical inhibition of sympathetic outflow as part of the response. The vagal lesion data also support the notion of vagal mediation of the cortically evoked autonomic responses. Unilateral vagotomies result in slight attenuation of the responses, while bilateral vagotomies abolish the responses.

Propranolol blocks β-adrenergic sympathetic synapses, while phentolamine blocks α-adrenergic sympathetic synapses. The administration of propranolol or phentolamine had little effect on the cortically evoked bradycardia, BP decrease and respiratory slowing. Thus, the effects of cortical stimulation do not appear to be mediated primarily via the sympathetic component of the autonomic nervous system. However, since in the intact animal, the parasympathetic and sympathetic nervous systems act in concert most of the time, it is

likely that the cortical stimulation is influencing both divisions of the autonomic nervous system to some extent.

Lesions of the pyramidal tracts also eliminated the responses. However, these data must be considered cautiously since in one animal a lesion that abolished the cortically-evoked response damaged a portion of the adjacent ventrolateral medulla and largely spared the pyramids. Electrical stimulation of the ventrolateral medulla elicits strong arterial hypertension and tachycardia responses (Ciriello and Calaresu, 1977; Dampney et al., 1982), and this region has connections with the intermediolateral cell column in the spinal cord (Loewy and McKellar, 1981; Loewy et al., 1981).) The closeness of the pyramids to the ventrolateral medulla makes it difficult to restrict lesions to only the pyramids, and thus, at present, it is not possible to unequivocally state that the effects of IL stimulation are mediated by the pathway to the NTS that travels via the pyramids.

In summary, the present study has demonstrated the existence of a discrete region of the rat MFC where electrical stimulation is capable of eliciting changes in cardiovascular and respiratory function and that this influence may be mediated via a direct projection from the IL cortex to the NTS. The identification of this "visceral motor cortex" provides an important clue for understanding the anatomical and functional organization of the medial frontal cortex in the rat.

Figure 1.

Photomicrographs of Nissl stained sections of acute stimulation experiments. A: Coronal section from experiment ACUTE 19. Dot indicates position of point where the responses seen in Figure 2D were evoked. Asterisk denotes location of marking lesion within the taenia tecta. B: Sagittal section from same brain. The dot indicates location of responsive point seen in Figure 2D, asterisk denotes position of marking lesion within the taenia tecta. C: Coronal section through the medulla from experiment Pt 1. Arrows denote the site and extent of the bilateral pyramidotomy done. See Figure 4 for the effect of this lesion on the responses seen after cortical stimulation. Abbreviations: AC, anterior commissure; cc, corpus callosum. Scale bars = 1 mm.

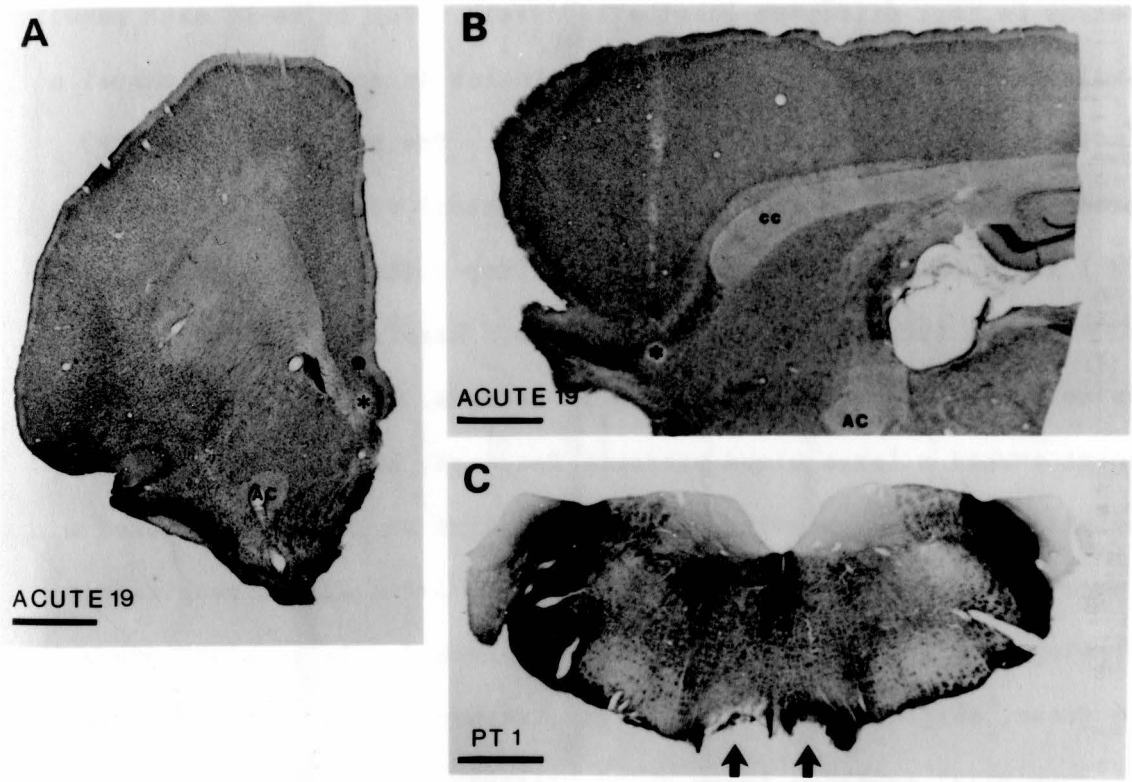
A
AF
ACUTE 19
B
cc
AC
ACUTE 19
C
PT 1

Figure 2.

Physiological responses evoked from stimulation of the medial frontal cortex in four different anesthetized rats. Top trace in each panel indicates the stimulus on/off; the stimulus intensities (in uamps) are indicated at the point of stimulus onset. The blood pressure (BP) trace calibration is 150-0 mm Hg (top-bottom) for A-D. The heart rate (HR) trace calibration is 500-250 bpm (top-bottom) for A and C, 400-300 bpm (top to bottom) for B and D. Respiration (RESP) pattern is on bottom trace. Time scale = 30 seconds. A: Stimulation at this point evoked a large blood pressure decrease, bradycardia, and a slight respiratory slowing. B: Stimulation at this point evoked a large blood pressure decrease, bradycardia and a slight respiratory slowing. C: Stimulation at this point evoked a large blood pressure decrease, slight bradycardia and respiratory slowing. D: Stimulation at this point evoked a large blood pressure decrease that did not correspond exactly with the bradycardia seen and respiration was completely inhibited during the expiratory phase of the respiratory cycle.

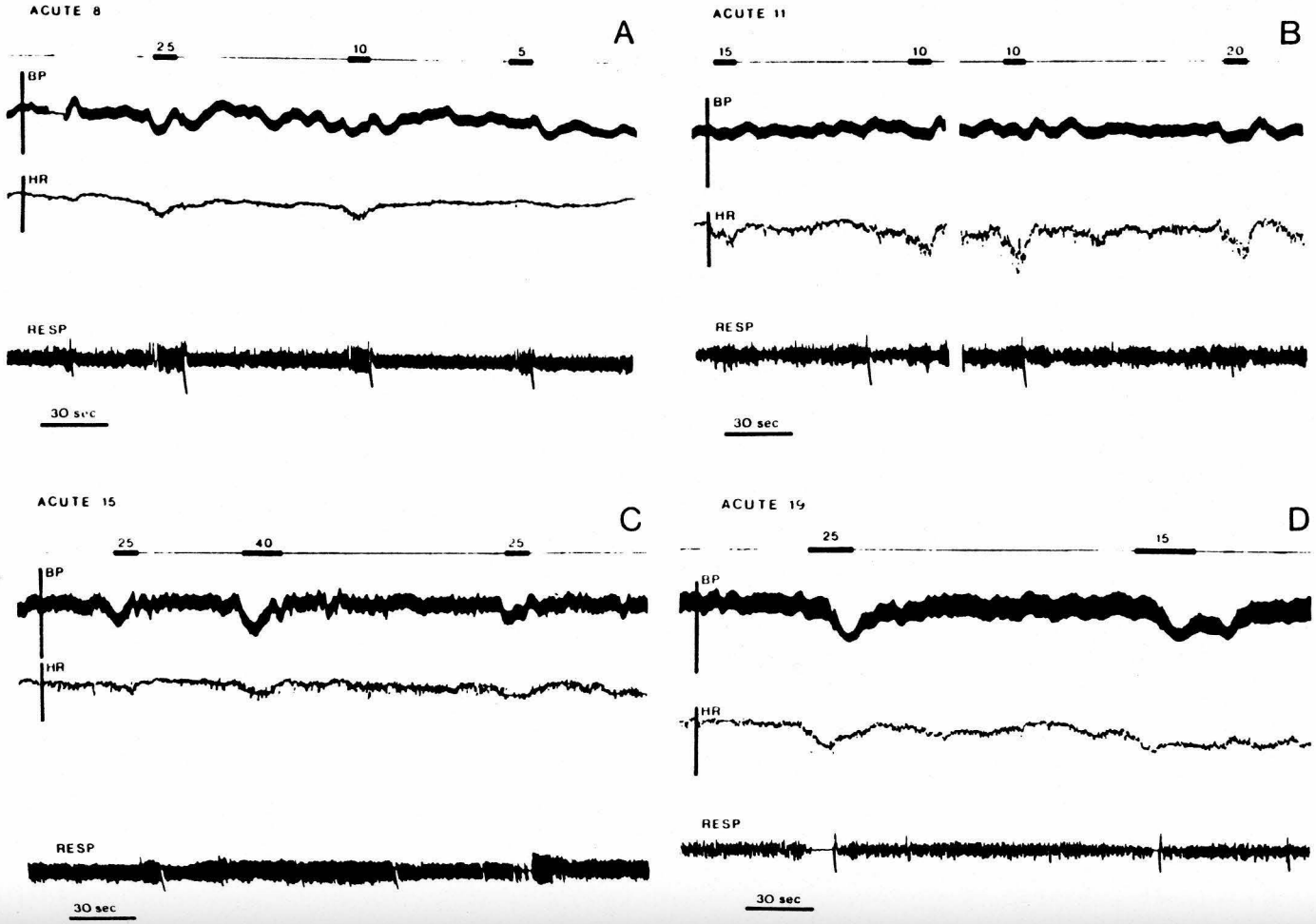
ACUTE 8
A
25
10
5
BP
HR
RESP
30 sec
ACUTE 11
B
15
10
10
20
BP
HR
RESP
30 sec
ACUTE 15
C
25
40
25
BP
HR
RESP
30 sec
ACUTE 19
D
25
15
BP
HR
RESP
30 sec

Figure 3.

Line drawings of sagittal views of the rat brains from three different experiments illustrating the location, variety and thresholds of the responses. The different types of responses are shown in A, C, E. NR, no response; H, heart rate (decrease); P, blood pressure (depressor); R, respiratory response. Figures 3E,F are line drawings of the sagittal section shown in Figure 1B. The asterisk (*) in Figure 3E corresponds to the lesion (denoted by an asterisk) illustrated in both the coronal and sagittal section in Figures 1A,B. The asterisks denote sites where marking lesions were made. The thresholds of the responses are shown in B, D, F. Solid squares (■) denote points where no response was elicited with stimulus intensities of 50 uamps, solid triangles (▲) denote points where responses were elicited with stimulus intensities between 25-50 uamps, solid circles (●) denote low threshold points where responses were elicited with stimulus intensities below 25 uamps. Note that lowest threshold points are in the infralimbic region of the MFC. Abbreviations: AC, anterior commissure; cc, corpus callosum; LV, lateral ventricle.

A

ACUTE 3

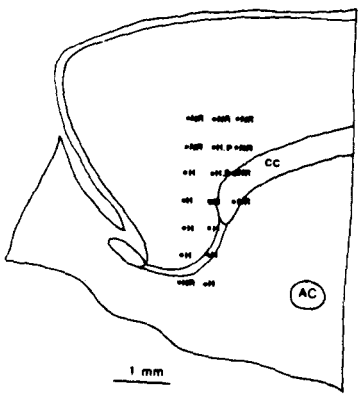

B

ACUTE 3

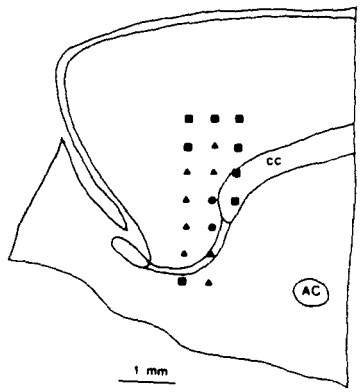

C

ACUTE 18

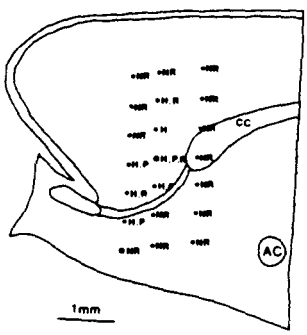

D

ACUTE 18

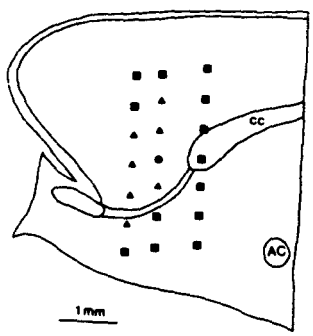

E

ACUTE 19

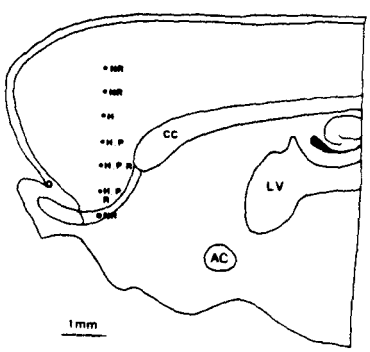

F

ACUTE 19

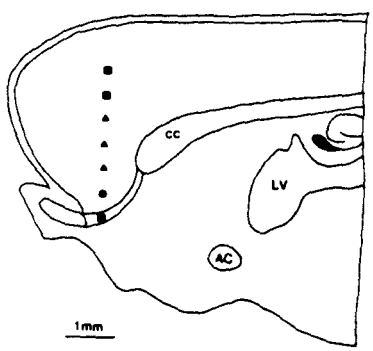

Figure 4.

Pharmacological effects on cortically evoked responses. A: Cortically evoked responses before the administration of methyl-atropine. B: Effects of cortical stimulation after the administration of 0.8 cc (IV) of methyl-atropine (0.04 mg/kg). First stimulus 75 seconds after atropine. Note that the cardiovascular responses (BP and HR) are abolished but the respiratory slowing appears enhanced (arrows) by the administration of methyl-atropine. C: Cortically evoked responses before the administration of propranolol in another experiment. D: Effects of cortical stimulation after the administration (IV) of 0.2 cc of propranolol (1 mg/kg). First stimulus 1 minute after propranolol. For traces A, C, D, blood pressure (BP) calibration is 150-0 mm Hg (top-bottom), heart rate (HR) calibration is 400-300 bpm (top-bottom) the respiration (RESP) trace is on the bottom. For trace B, heart rate (HR) calibration is 500-400 bpm (top-bottom). Time scale = 30 seconds.

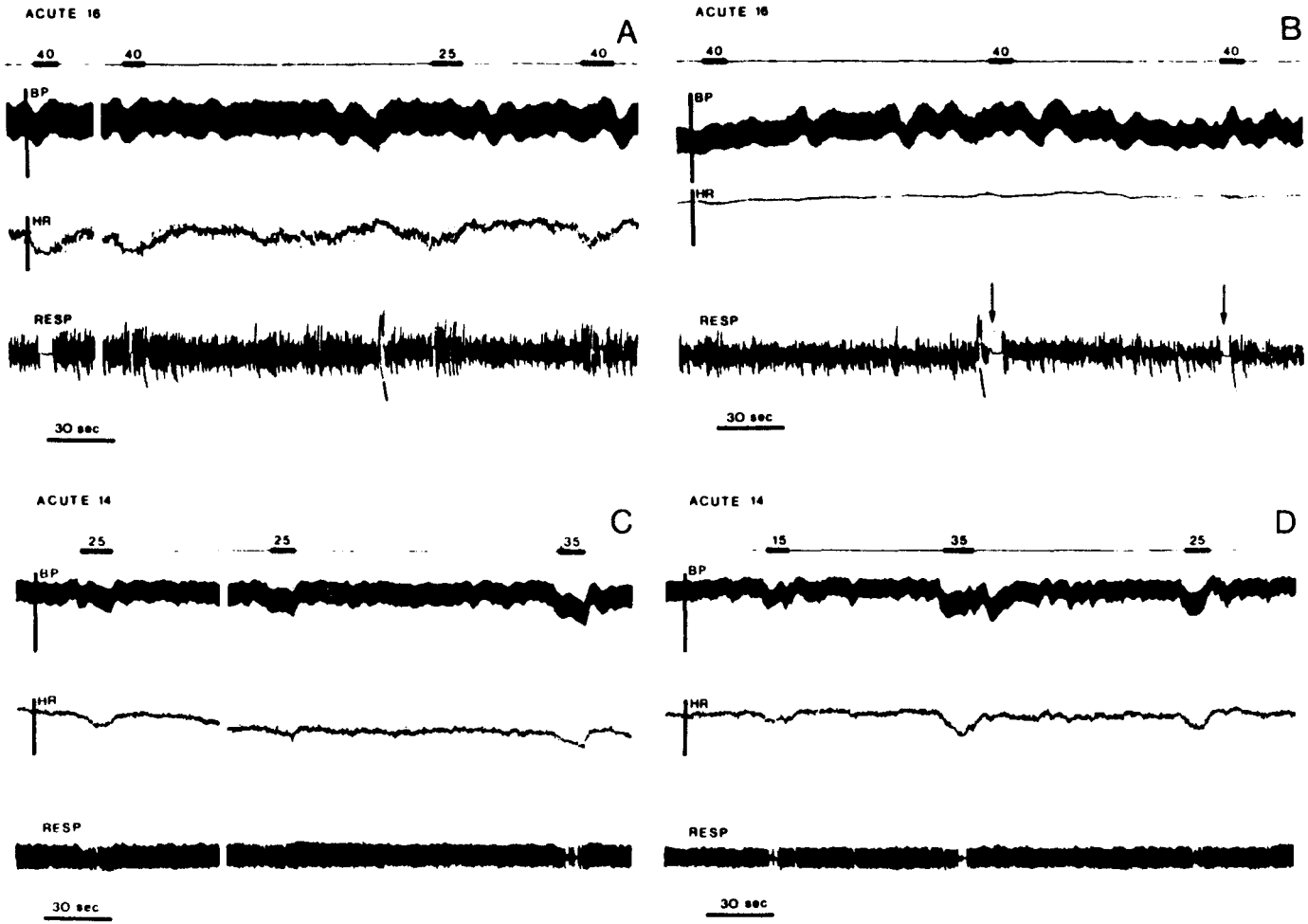
ACUTE 16
A
40
40
25
40
BP
HR
RESP
30 sec
ACUTE 16
B
40
40
40
BP
HR
RESP
30 sec
ACUTE 14
C
25
25
35
BP
HR
RESP
30 sec
ACUTE 14
D
15
35
25
BP
HR
RESP
30 sec

Figure 5.

Effects of unilateral and bilateral vagotomy on cortically evoked responses. A: Cortically evoked responses before vagotomy. B: Left panel illustrates the effect of right cervical vagus transection on the evoked responses. Arrow indicates point of transection. Responses slightly attenuated but still present. Middle panel illustrates the effect of left cervical vagus transection in same animal (thus bilateral vagotomy completed). Arrow indicates point of transection. Note elimination of heart rate response, while the blood pressure response remains. Right panel illustrates the responses seen five minutes after the bilateral vagotomy was completed. For both traces, blood pressure (BP) calibration is 150-0 mm Hg (top-bottom), heart rate (HR) calibration is 400-300 bpm (top-bottom), the respiration (RESP) trace is on the bottom. Time scale = 30 seconds.

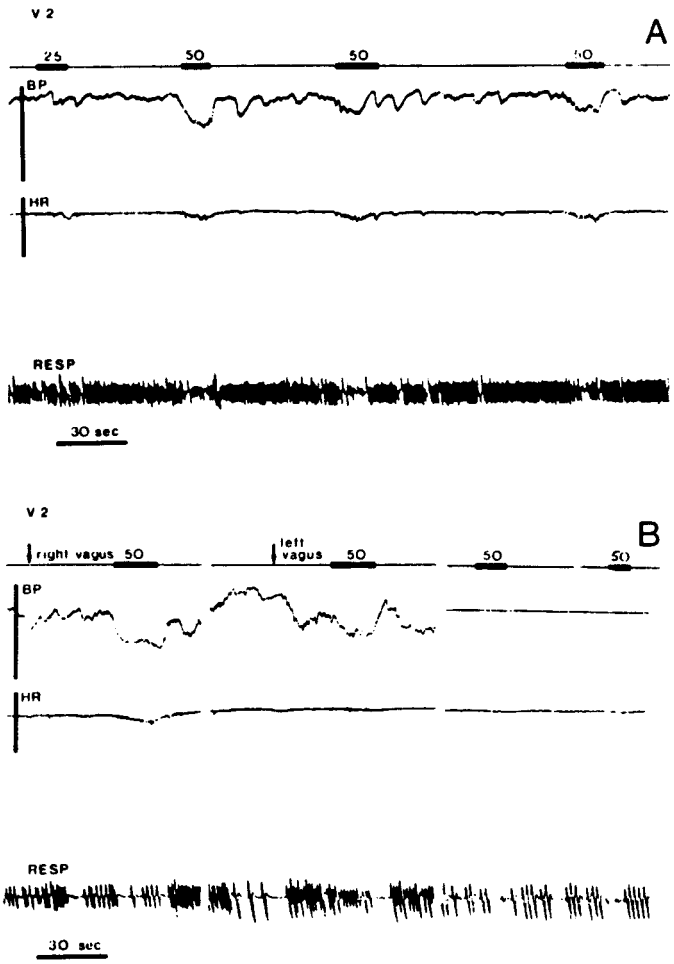
V 2
A
25
50
50
50
BP
HR
RESP
30 sec
V 2
B
right vagus 50
left vagus 50
50
50
BP
HR
RESP
30 sec

Figure 6.

Effect of pyramidal tract (PT) transection on cortical evoked responses. A: Cortically evoked responses before pyramidotomy. B: The effect of left PT transection on the responses in the same animal. Arrows indicate the time the transection was performed. The heart rate response still appeared to be present while the blood pressure response was slightly attenuated. C: Effect of right PT transection, and transection of the remaining midline PT fibers. Arrows indicate the point of transection. Note that some heart rate response still appears to be present after right PT lesion but not after section of midline PT fibers. D: Stimulation of cortex 7.5 and 9.5 minutes after bilateral pyramidotomy completed. Note total abolition of the responses. For all four traces, blood pressure (BP) calibration is 150-0 mm Hg, heart rate (HR) calibration is 400-300 bpm (top-bottom), the respiration (RESP) trace is on the bottom. Time scale = 30 seconds.

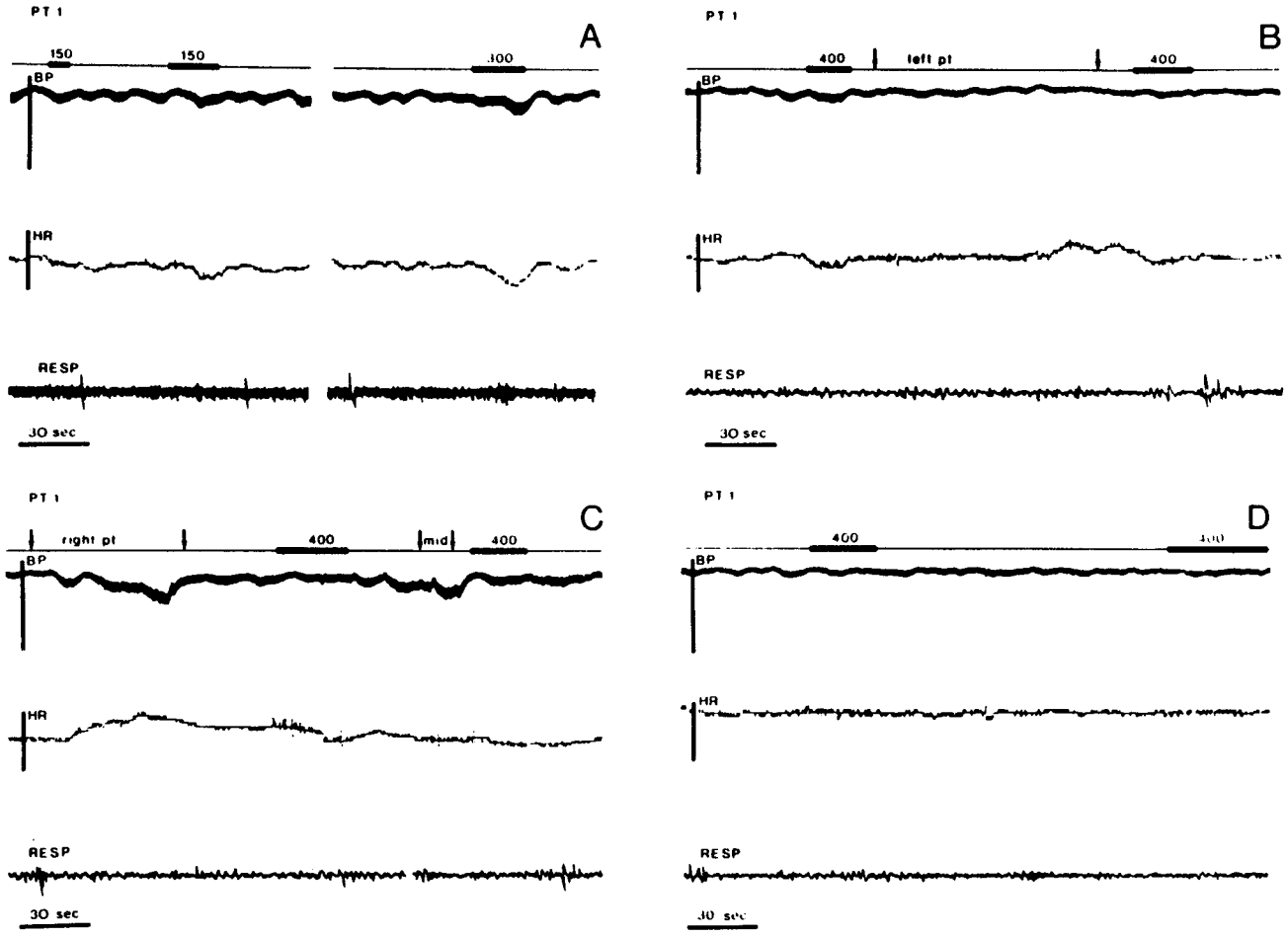
PT 1
A
150
150
300
BP
HR
RESP
30 sec
PT 1
B
400
left pt
400
BP
HR
RESP
30 sec
PT 1
C
right pt
400
mid
400
BP
HR
RESP
30 sec
PT 1
D
400
BP
HR
RESP

Figure 7.

Chronic stimulation results. A: The results of bilateral cortical stimulation in rat #3. Trace is of the resultant heart rate (hr) decrease following bilateral cortical stimulation (s:200 uamps, .5 sec pulses, 50 Hz, 5 sec train); second stimulus was same parameters as the first but with a current intensity of 100 uamps. Time base (t) = 5 seconds; heart rate calibration (hr), 600-300 bpm (top to bottom). B: Same point as illustrated in A, stimulus (s) intensity of 300 uamps. Time base = 1 second; heart rate calibration, 600-300 bpm (top-bottom). C: The results of bilateral cortical stimulation in rat #5 which resulted in a slight slowing of heart rate which persisted for about 5 seconds after stimulus (s) offset. Two traces are superimposed. Arrowhead indicates a missed heart beat seen on the EKG. Stimulus parameters were 50 uamps, .5 sec pulses, 50 Hz, 5 sec train. Time base = 1 second; heart rate calibration, 600-300 bpm (top-bottom). D: Same point as in C to illustrate the effect of methyl-atropine on the response. Two traces are superimposed. The first one was 45 seconds after methyl-atropine administration, and the response was somewhat attenuated with the heart rate returning to the baseline before stimulus (s) offset. The arrow points to the trace of the response to stimulation 2 minutes after methyl-atropine administration when the response was totally abolished. Time base = 2 seconds; heart rate calibrator, 600-300 bpm (top-bottom). w = window discriminator.

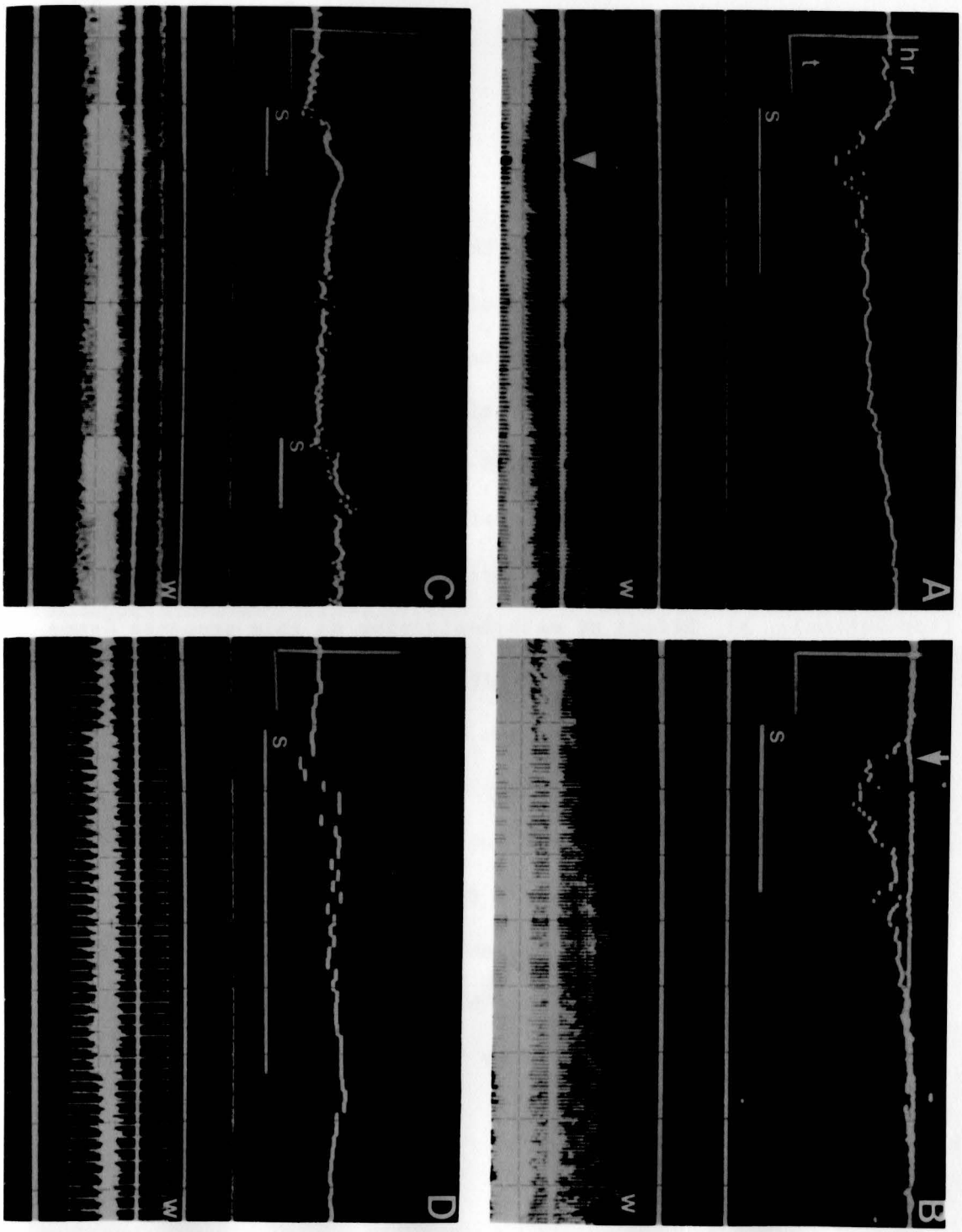
A
hr
t
s
w
B
s
w
C
s
s
w
D
s
w

Figure 8.

Chronic stimulation results. A: The results of bilateral cortical stimulation in rat #10. Trace is of the resultant heart rate (hr) decrease following bilateral cortical stimulation of the MFC (see Figure 9 for histological localization of the stimulation point). Stimulation (s) parameters were 100 uamps, .5 sec pulses, 25 Hz, 5 sec train. Arrowhead indicates a missed heart beat seen on the EKG. Time base (t) = 2 seconds; heart rate calibration, 600-300 bpm (top-bottom). B: Effect of methyl-atropine on this response (same animal as in A). Two traces, the first trace is the pre-atropine trial with a decrease in heart rate. The second trace (indicated by the arrow) is 2 minutes after methyl-atropine administration. C: The results of bilateral cortical stimulation in rat #4. Trace is of the resultant heart rate (hr) increase following bilateral cortical stimulation of the MFC. Stimulation parameters were 100 uamps, .5 sec pulses, 50 Hz, 5 sec. train. Time base = 5 seconds; heart rate calibration, 600-300 bpm. D: Same animal as in C but the time base = 1 second.

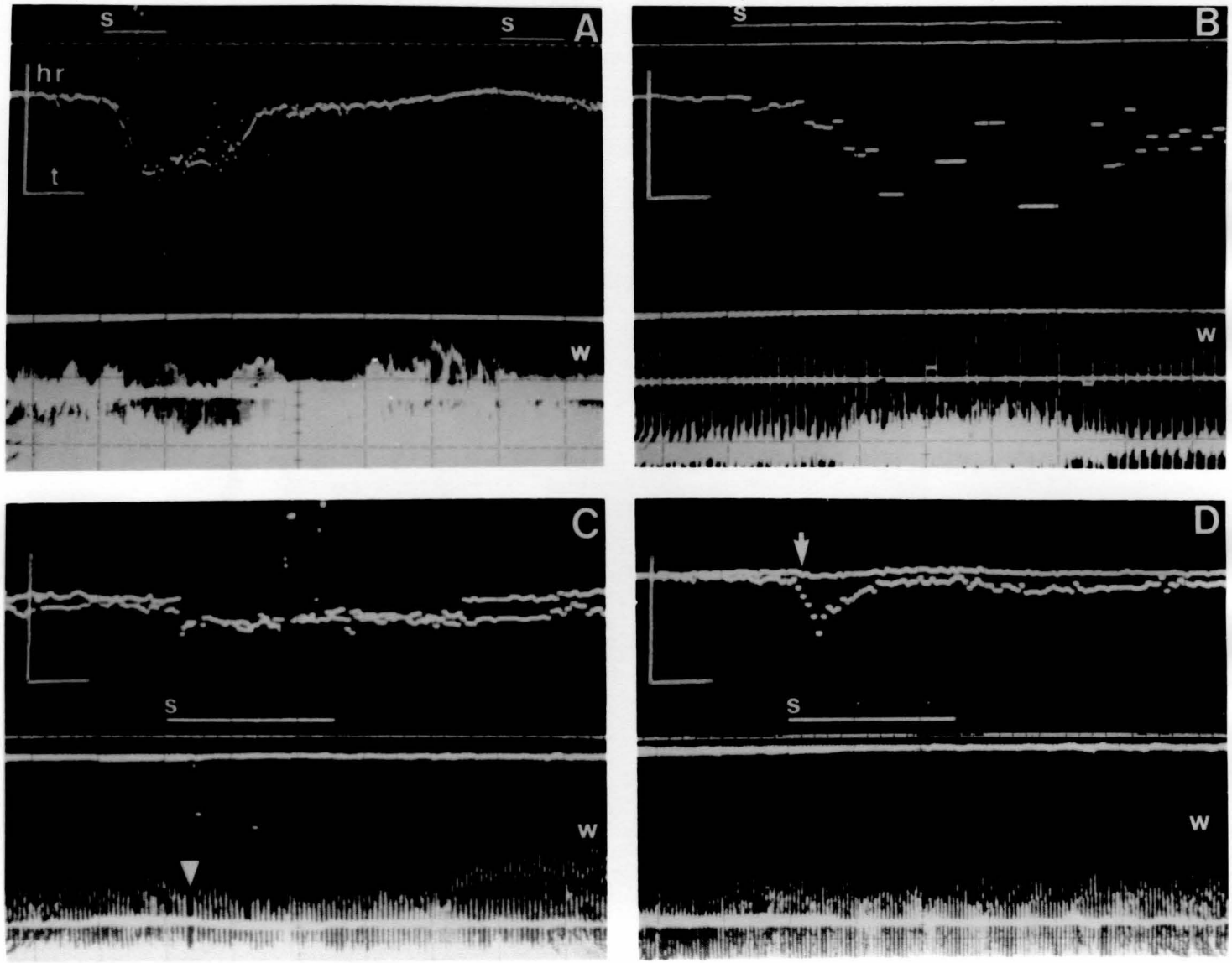
A
s
s
hr
t
w
B
s
w
C
s
w
D
s
w

Figure 9.

Nissl stained coronal section through the MFC of rat #10. The arrows indicate the position within the infralimbic cortex of the responsive point seen in Figures 8A,B which elicited decreases in heart rate upon stimulation. Scale bar = 1 mm.

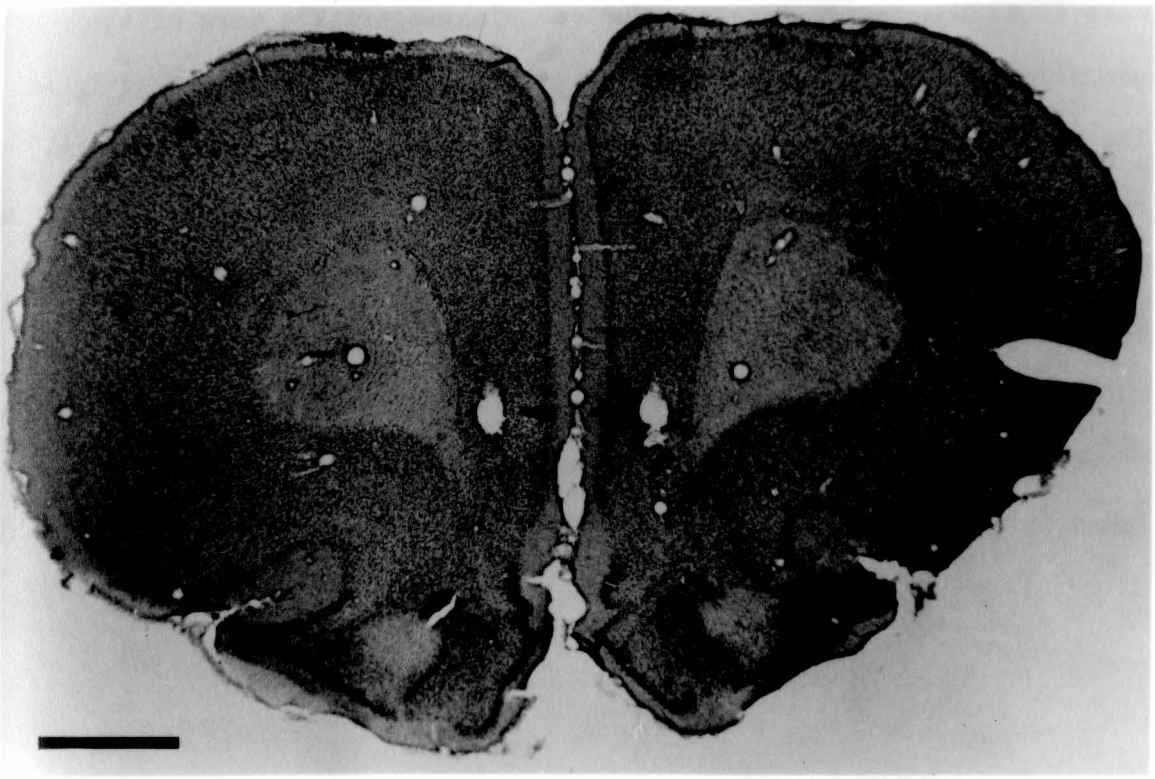

Table 1.

Statistical analysis of the heart rate and blood pressure responses seen in 18 anesthetized rats. The coordinates are the mean of the coordinates of the points that elicited responses at 25 uamps or less. The top value is the rostral-caudal coordinate, with bregma being the zero point. The bottom value is the depth from the cortical surface. Heart rate values are in beats per minute (bpm) while the blood pressure values are in millimeters of mercury (mmHg). Using a Paired T-test, the drops in heart rate and blood pressure (mean during stimulation) were statistically significant from the baseline levels (mean before stimulation), at a P value of <.0005.

ACUTE STIMULATION

(n = 18)

Coordinates (mm)

$$\frac{3.42 \pm 0.28}{3.92 \pm 0.73}$$

Heart Rate (bpm)

(n = 17)

mean HR before stim.	mean HR during stim.	
322.53 ± 11.28	294.53 ± 9.72	P < .0005

Blood Pressure (mmHg)

(n = 9)

mean BP before stim.	mean BP during stim.	
126.22 ± 5.2	104.11 ± 5.95	P < .0005

Table 2.

Statistical analysis of the heart rate responses seen in four unanesthetized rats. The coordinates are the mean of the coordinates of the points that elicited responses at 150 uamps or less. The top value is the rostral-caudal coordinate, with bregma being the zero point. The bottom value is the depth from the cortical surface. Heart rate values are in beats per minute (bpm). Using a Paired T-test, the drops in heart rate (mean during stimulation) were statistically significant from the baseline level (mean before stimulation), at a P value of $<.01$.

CHRONIC STIMULATION

(n = 5)

Coordinates (mm)

$$\frac{3.16 \pm 0.15}{3.68 \pm 0.23}$$

Heart Rate (bpm)

(n = 4)

mean HR before stim.	mean HR during stim.	
532.5 ± 7.5	412.5 ± 25.62	$P < .01$

CHAPTER VII

DISCUSSION

The cytoarchitecture, anatomical connections and physiological role in cardiovascular and respiratory control of the infralimbic (IL) region of the rat medial frontal cortex (MFC) have been studied in this dissertation. IL receives heavy limbic inputs, while its main efferents are to motor and visceral structures. Electrical stimulation of this area results in bradycardia, depressor responses and depression of respiratory activity. These cortically-evoked responses can be abolished by vagal blockade or vagotomies, and were unaffected by sympathetic blockade. These data suggest that the IL cortex functions as a "visceral motor cortex."

The primary inputs to IL are limbic. These include projections from the ventral hippocampus, basolateral amygdala and ventral tegmental area. The primary outputs from IL are to central motor (ventral striatum, pons, inferior olive) or visceral (insular cortex, lateral hypothalamus, NTS) structures. Thus the general scheme of the connections of the IL cortex is:

LIMBIC ⟶ IL ⟶ VISCERAL/MOTOR.

This pairing of limbic and visceral structures through the IL cortex suggests that MacLean's (1949) original definition of the limbic system as the "visceral brain" is still valid, despite recent doubts about this association.

The IL cortex may be classified as a "visceral motor" cortex based on the following criteria. The IL cortex is agranular and its position adjacent to the somatic motor cortex and frontal eye fields

places it in the cortical motor system category, and its projections to the inferior olive and pontine gray indicate that this cortical area can influence somatic and visceral motor activity through the cerebellar system. Another observation that suggests that the IL cortex functions as a motor structure is that IL sends projections to the ventral striatum proposed by Heimer and Wilson (1975) and Heimer et al. (1982). Additionally, IL, along with the insular cortex, is the cortical target of the ventral striatal-pallidal system via projections from the ventral pallidum to the mediodorsal, parataenial an paraventricular thalamic nuclei, which, in turn project to IL and insular cortex. This ventral striatal-pallidal system parallels the classical dorsal striatal system, and, although the function of the ventral striatum remains unknown at this time, suggestions have been made that this is an area where limbic inputs may influence motor activity (Mogenson et al., 1980; Newman and Winans, 1980a; Heimer et al., 1982). This suggests that perhaps the ventral striatum functions, at least in part, as a "visceral striatum."

If IL is considered as a visceral motor region, an interesting topographical organization becomes evident when one looks at a coronal view of the rat frontal and parietal cortex (Figure 1). From medial to lateral, the following cortical areas are found: visceral motor, frontal eye fields, somatic motor, somatic sensory, visceral sensory and olfactory sensory (piriform cortex). This pattern suggests that the neocortex is bounded at its medial and lateral edges by visceral

cortex, an observation that may have relevance to theories of cortical evolutionary development and to our understanding of "association areas" of the cerebral cortex.

In conclusion, there is an extensive and important cortical visceral representation in the infralimbic and insular cortices. This should not be suprising since Hughlings Jackson's notion of "re-representation" of functions at all levels of the CNS has been accepted for over 100 years. However, there has been a certain reluctance to attribute a "visceral" function to the cortex since the cortex is thought to be associated with "higher" functions of intelligence and thought. Nonetheless, the evidence from this study and others is clear and suggests that other cortical "association" regions may also be mislabeled due to our ignorance of their fundamental sensorimotor relations.

Figure 1.

Schematic diagram of tographical organization of the rat medial frontal cortex (MFC). Arrow heads indicate the borders between the functional subdivisions of the MFC; which are visceral motor, frontal eye fields, somatic motor, somatic sensory, visceral sensory and olfactory sensory. The visceral motor area is made up of the pre- and infralimbic cortices, while the anterior cingulate and agranular medial areas constitute the frontal fields. The AgL region corresponds to the somatic motor or primary motor cortex. The somatic sendory cortex is comprised of the primary and secondary somatosensory cortices. The insular cortex comprises the visceral sensory region, and the olfactory sensory piriform cortex and olfactory tubercle occupy the ventral surface of the brain. Abbreviations: AC, anterior cingulate cortex; Acb, nucleus accumbens; AgM, agranular medial cortex; AgL, agranular lateral cortex; Cl, claustrum; CP, caudate-putamen; DPC, doarsal peduncular cortex; Gr (SI), primary somatosensory cortex; Gr (SII), secondary somatosensory cortex; IL, infralimbic cortex; Ins, insular cortex; Pir, piriform cortex; PL, prelimbic cortex; tt, taenia tecta.

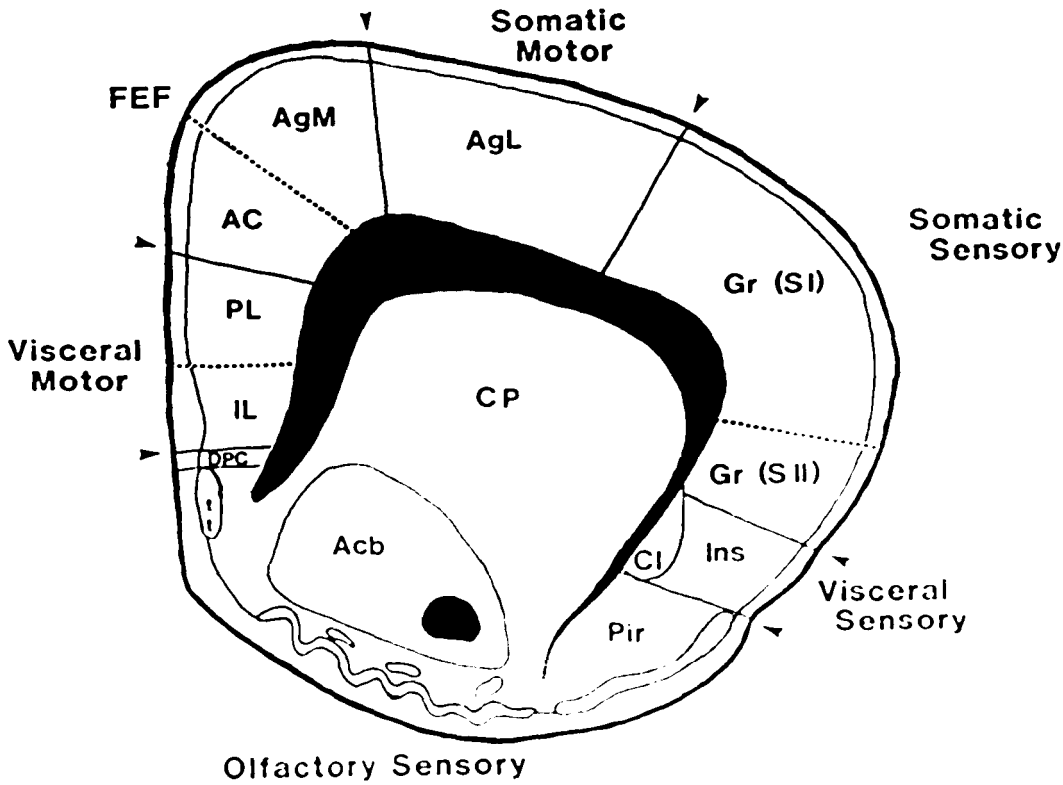
Somatic
Motor
FEF
AgM
AgL
AC
Somatic
Sensory
Gr (SI)
PL
Visceral
Motor
CP
IL
DPC
Gr (S II)
Acb
Cl
Ins
Visceral
Sensory
Pir
Olfactory Sensory

CHAPTER VIII

SUMMARY AND CONCLUSIONS

The findings of this study were:

1. The infralimbic (IL) cortex located on the medial surface of the cerebral hemisphere appears to receive heavy inputs from "limbic" structures, including the hippocampus, amygdala and ventral tegmental area. IL also receives numerous visceral inputs from the insular cortex, lateral hypothalamus, parabrachial nuclei and the lateral dorsal tegmental nucleus. Thus, the IL cortex may serve to integrate limbic and visceral information suggesting that MacLean's (1949) definition of the limbic system as the "visceral brain" is still valid.

2. The primary efferent projections from the infralimbic (IL) region of the MFC are those to central motor structures (ventral striatum, pontine nuclei, inferior olive) and central visceral structures (insular cortex, lateral hypothalamus, lateral dorsal tegmental nucleus, nucleus of the solitary tract). The label in the NTS was localized within cardiovascular and respiratory subnuclei of the NTS. These data suggest that the IL cortex may function as a "visceral motor" cortex, involved in CNS control of several visceral or autonomic functions.

3. Low threshold (< 50 uamps) intracortical microstimulation of the infralimbic (IL) region of the rat medial frontal cortex elicited

bradycardia, decreases in blood pressure and depression of respiratory activity. The most frequent response seen was a bradycardia (76%), the second most frequent response was a depression of the arterial blood pressure (61%) while the least frequent (32%) response was a slowing of respiration.

4. These low threshold cortically-evoked responses could be abolished with methyl-atropine, bilateral vagotomies or bilateral pyramidotomies. The responses were unaffected by the sympathetic blockers propranolol and phentolamine. These results suggest that the cortically-evoked responses may be mediated via the vagus nerves and that the direct cortico-solitary projection from the IL cortex to the nucleus of the solitary tract may be involved in mediating these responses.

BIBLIOGRAPHY

LITERATURE CITED

Achari, N.K., and C.B.B. Downman (1970) Autonomic effector responses to stimulation of nucleus fastigius. J Physiol 210: 637-650.

Al-Senawi, D.E.A.-.H., and C.B.B. Downman (1983) Cardiac arrhythmic response evoked by stimulation of fastigial nuclei in the anesthetized cat. J Autonomic Nervous Syst 8: 15-24.

Anand, B.K., and S. Dua (1956) Circulatory and respiratory changes induced by electrical stimulation of limbic system (visceral brain). J Neurophysiol 19: 393-400.

Babkin, B.P., and T.J. Speakman (1950) Cortical inhibition of gastric motility. J Neurophysiol 13: 55-63.

Bailey, P., and W.H. Sweet (1940) Effects on respiration, blood pressure and gastric motolity of stimulation of orbital surface of frontal lobe. J Neurophysiol 3: 276-281.

Bailey, P., G. von Bonin, H.W. Garol, and W.S. McCulloch (1943) Functional organization of temporal lobe of monkey (Macaca mulatta) and chimpanzee (Pan satyrus). J Neurophysiol 6: 121-128.

Baumgarten, R., and S. Nakayama (1964) Spontane und reizbedingte Anderungen der antidromen Erregbarkeit von bulbaren respiratorischen Nervenzellen der Katze. Pflugers Arch 281: 245-258.

Beckstead, R.M. (1976) Convergent thalamic and mesencephalic projections to the anterior medial cortex in the rat. J Comp Neurol 166: 403-416.

Beckstead, R.M. (1979) An autoradiographic examination of corticocortical and subcortical projections of the mediodorsal-projection (prefrontal) cortex in the rat. J Comp Neurol 184: 43-62.

Beckstead, R.M., V.B. Domesick, and W.J.H. Nauta (1979) Efferent connections of the substantia nigra and ventral tegmental area in the rat. Brain Res 175: 191-217.

Benjamin, R.M., and K. Akert (1959) Cortical and thalamic areas involved in taste discrimination in the albino rat. J Comp Neurol 111: 231-259.

Benjamin, R.M., and C. Pfaffman (1955) Cortical localization of taste in albino rat. J Neurophysiol 18: 56-64.

Bisset, G.W., W. Feldberg, P.G. Guertzenstein, and M. Rocha e Silva (1975) Vasopressin release by nicotine: the site of action. BJP 54: 463-474.

Brodal, A. (1981) Neurological Anatomy in Relation to Clinical Medicine. New York and Oxford: Oxford University Press, pp. 689-690.

Brodal, P., E. Dietrichs, J.G. Bjaalie, T. Nordby, and F. Walberg (1983) Is lectin-coupled horseradish peroxidase taken up and transported by undamaged as well as by damaged fibers in the central nervous system?. Brain Res 278: 1-9.

Brodmann, K. (1909) Vergleichende Lokalisationslehre der Grobhirnrinde in ihren Prinzipien dargestellt auf Grund des Zellenbaus. Leipzig: J.A. Barth, pp. 1-324.

Brown, J.T., V. Chan-Palay, and S.L. Palay (1977) A study of afferent inputs to the inferior olivary complex in the rat by retrograde axonal transport of horseradish peroxidase. J Comp Neurol 176: 1-22.

Buchanan, S.L., D.A. Powell, and J. Valentine (1984) Cardiovascular adjustments elicited by electrical stimulation of frontal cortex in conscious rabbits. Soc Neurosci Abst 10: 614.

Bunney, B.S., and G.K. Aghajanian (1976) The precise localization of nigral afferents in the rat as determined by a retrograde tracing technique. Brain Res 117: 423-435.

Bunt, A.H., A.E. Hendrickson, J.S. Lund, R.D. Lund, and A.F. Fuchs (1975) Monkey retinal ganglion cells: morphometric analysis and tracing of axonal projections, with a consideration of the peroxidase technique. J Comp Neurol 164: 265-286.

Burns, S.M., E.E. Geisert, S.R. Winternitz, and J.M. Wyss (1983) The role of the cingulate gyrus in cardiovascular functioning. Anat Rec 205: 28A.

Burns, S.M., and J.M. Wyss (1985) The involvement of the anterior cingulate cortex in blood pressure control. Brain Res 340: 71-77.

Calaresu, F.R., and J. Ciriello (1980) Projections to the hypothalamus from buffer nerves and nucleus tractus solitarius in the cat. Am J Physiol 239: R130-R136.

Chapman, W.P., R.B. Livingston, K.E. Livingston, and W.H. Sweet (1950) Possible cortical areas involved in arterial hypertension. ResPubl Ass Res Nerv Ment 29: 775-798.

Chung, J.M., K. Chung, and R.D. Wurster (1975) Sympathetic preganglionic neurons of the cat spinal cord: horseradish peroxidase study. Brain Res 91: 126-131.

Ciriello, J., and F.R. Calaresu (1977) Lateral reticular nucleus: a site of somatic and cardiovascular integration in the cat. Am J Physiol 233: R100-R109.

Ciriello, J., and F.R. Calaresu (1980) Role of paraventricular and suproptic nuclei in central cardiovascular regulation in the cat. Am J Physiol 239: R137-R142.

Clark, G., K.L. Chow, C.G. Gillaspy, and D.A. Klotz (1949) Stimulation of anterior limbic region in dogs. J Neurophysiol 12: 459-463.

Cohen, M.I. (1979) Neurogenesis of respiratory rhythm in the mammal. Physiol Rev 59: 1105-1173.

Conrad, L.C.A., C.M. Leonard, and D.W. Pfaff (1974) Connections of the median and dorsal raphe nuclei in the rat: an autoradiographic and degeneration study. J Comp Neurol 156: 179-206.

Conrad, L.C.A., and D.M. Pfaff (1976) Efferents from the medial basal forebrain and hypothalamus in the rat. II. An autoradiography study of the anterior hypothalamus. J Comp Neurol 169: 211-262.

Contreras, R.J., R.M. Beckstead, and R. Norgren (1982) The central projections of the trigeminal, facial, glossopharyngeal and vagus nerves: an autoradiographic study in the rat. J Autonomic Nervous Syst 6: 303-322.

Craig, A.D., and H. Burton (1981) Spinal and medullary lamina I projection to nucleus submedius in medial thalamus: a possible pain center. J Neurophysiol 45: 443-466.

Dahlstrom, A., and K. Fuxe (1964) Evidence for the existence of monoamine-containing neurons in the central nervous system. I. Demonstration of monoamines in the cell bodies of brain stem neurones. Acta Physiol Scand 62 S232: 1-55.

Dampney, R.A.L., A.K. Goodchild, L.G. Robertson, and W. Montgomery (1982) Role of ventrolateral medulla in vasomotor regulation: a correlative anatomical and physiological study. Brain Res 249: 223-235.

Danilewsky, B. (1875) Experimentelle Beitrage zur Physiologie des Gehirns. Pflugers Arch 11: 128-138.

Davies, R.O., and M. Kalia (1981) Carotid sinus nerve projections to the brain stem of the cat. Brain Res Bull 6: 531-541.

Delgado, J.M.R., and R.B. Livingston (1948) Some respiratory, vascular and thermal responses to stimulation of orbital surface of frontal lobe. J Neurophysiol 11: 39-55.

Domesick, V.B. (1969) Projections from the cingulate cortex in the rat. Brain Res 12: 296-320.

Domesick, V.B. (1972) Thalamic relationships of the medial cortex in the rat. Brain Behav Evol 6: 457-483.

Donoghue, J.P., and C. Parham (1983) Afferent connections of the lateral agranular field of the rat motor cortex. J Comp Neurol 217: 390-404.

Donoghue, J.P., and S.P. Wise (1982) The motor cortex of the rat: cytoarchitecture and microstimulation mapping. J Comp Neurol 212:

76-88.

Dunsmore, R.H., and M.A. Lennox (1950) Stimulation and strychninization of supracallosal anterior cingulate gyrus. J Neurophysiol 13: 207-214.

Dursteler, M.R., C. Blakemore, and L.J. Garey (1977) Uptake of horseradish peroxidase by geniculo-cortical axons in the golden hamster: analysis by computer reconstruction. Exp Brain Res 29: 487-500.

Fallon, J.H., and R.Y. Moore (1978a) Catecholamine innervation of the basal forebrain. III. Olfactory bulb, anterior olfactory nuclei, olfactory tubercle and piriform cortex. J Comp Neurol 180: 533-544.

Fallon, J.H., and R.Y. Moore (1978b) Catecholamine innervation of the basal forebrain. IV. Topography of the dopamine projection to the basal forebrain and neostriatum. J Comp Neurol 180: 545-580.

Feldberg, W. (1976) The ventral surface of the brain stem: a scarcely explored region of pharmacological sensitivity. Neuroscience 1: 427-441.

Fibiger, H.C. (1982) The organization and some projections of cholinergic neurons of the mammalian forebrain. Brain Res Rev 4: 327-388.

Finch, D.M., E.L. Derian, and T.L. Babb (1984) Afferent fibers to rat cingulate cortex. Exp Neurol 83: 468-485.

Folkow, B., and E. Neil (1971) Circulation. New York: Oxford Univ. Press, pp. 307-363.

Fukuda, Y., W.R. See, and Y. Honda (1980) H+-sensitivity and pattern of discharge of neurons in the chemosensitive areas of the ventral medulla of rat in vitro. Pflugers Arch 388: 53-61.

Fulton, J.F. (1949) Physiology of the Nervous System. New York: Oxford Univ. Press.

Fulwiler, C., and C. Saper (1984) Subnuclear organization of the efferent connections of the parabrachial nucleus in the rat. Brain Res Rev 7: 229-259.

Galeno, T.M., and M.J. Brody (1983) Hemodynamic responses to amygdaloid stimulation in spontaneously hypertensive rats. Am J Physiol 245: R281-R286.

Galosy, R.A., L.K. Clarke, M.R. Vasko, and I.L. Crawford (1981) Neurophysiology and neuropharmacology of cardiovascular regulation and stress. Neurosci Biobehav Rev 5: 137-175.

Geis, G.S., and R.D. Wurster (1980a) Horseradish peroxidse localization of cardiac vagal preganglionic somata. Brain Res 182: 19-30.

Gerfen, C.R., and R.M. Clavier (1979) Neural inputs to the prefrontal agranular insular cortex in the rat: horseradish peroxidase study. Brain Res Bull 4: 347-353.

Gibson, A.R., D.I. Hansma, J.C. Houk, and F.R. Robinson (1984) A sensitive low artifact TMB procedure for the demonstration of WGA-HRP in the CNS. Brain Res 298: 235-241.

Goldschmidt, R.B., and L. Heimer (1980) The rat olfactory tubercle: its connections and relation to the strio-pallidal system. Soc Neurosci Abst 6: 271.

Gonatas, N.K., C. Harper, T. Mizutani, and J.O. Gonatas (1979) Superior sensitivity of conjugates of horseradish peroxidase with wheat germ agglutinin for studies of retrograde axonal transport. J Histochem Cytochem 27: 728-734.

Greatrex, R.M., and O.T. Phillipson (1982) Demonstration of synaptic input from prefrontal cortex to the habenula in the rat. Brain Res 238: 192-197.

Groenewegen, H.J., and W.J.H. Nauta (1982) Afferent and efferent connections of the mediodorsal thalamic nucleus in the rat. Neurosci Lett Supp 10: S217.

Groenewegen, H.J., and C.A. Van Dijk (1984) Efferent connections of the dorsal tegmental region in the rat, studied by means of anterograde transport of the lectin Phaseolus vulgaris-leucoagglutinin (PHA-L). Brain Res 304: 367-371.

Guertzenstein, P.G., and S. Silver (1974) Fall in blood pressure produced from discrete region on the ventral surface of the medulla by glycine and lesions. J Physiol 242: 489-503.

Guldin, W.O., and H.J. Markowitsch (1983) Cortical and thalamic afferent connections of the insular and adjacent cortex of the rat. J Comp Neurol 215: 135-153.

Guldin, W.O., M. Pritzel, and H.J. Markowitsch (1981) Prefrontal cortex of the mouse defined as cortical projection area of the thalamic mediodorsal nucleus. Brain Behav Evol 19: 93-107.

Haberly, L.B., and J.L. Price (1978) Association and commissural fiber systems of the olfactory cortex of the rat. J Comp Neurol 181: 781-808.

Hall, R.D., and E.P. Lindholm (1974) Organization of motor and somatosensory neocortex in the albino rat. Brain Res 66: 23-38.

Hall, R.E., R.B. Livingston, and C.M. Bloor (1977) Orbital cortical influences on cardiovascular dynamics and myocardial structure in conscious monkeys. J Neurosurg 46: 638-647.

Hamilton, R.B., H. Ellenberger, D. Liskowsky, and N. Schneiderman (1981) Parabrachial area as mediator of bradycardia in rabbits. J Autonomic Nervous Syst 4: 261-281.

Hardy, S.G.P. (1985) Analgesia elicited by prefrontal stimulation. Brain Res 339: 281-284.

Hardy, S.G.P., and G.R. Leichnetz (1981) Frontal cortical projections to the periaqueductal gray in the rat: A retrograde and orthograde horseradish peroxidase study. Neurosci Lett 23: 13-17.

Heimer, L., R.D. Switzer, and G.W. van Hoesen (1982) Ventral striatum and ventral pallidum. Components of the motor system?. Trends in

Neurosci 5: 83-87.

Heimer, L., and R.D. Wilson (1975) Golgi Centennnial Symposium. New York: Raven Press, pp. 177-193.

Heinemann, H., G. Stock, and H. Schaeffer (1973) Temporal correlation of responses in blood pressure and motor reaction under electrical stimulation of limbic structures in the unanesthetized cat. Pflugers Arch 343: 27-40.

Henke, P.G., and R.J. Savoie (1982) The cingulate cortex and gastric pathology. Brain Res Bull 8: 489-492.

Herkenham, M. (1978) The connections of the nucleus reuniens thalami: evidence for a direct thalamo-hippocampal pathway in the rat. J Comp Neurol 177: 589-610.

Herkenham, M. (1979) The afferent and efferent connections of the ventromedial thalamic nucleus in the rat. J Comp Neurol 183: 487-518.

Herkenham, M., and W.J.H. Nauta (1977) Afferent connections of the habenular nuclei in the rat. A horseradish peroxidase study with a note on the fiber-of-passage problem. J Comp Neurol 173: 123-146.

Higgins, G.A., and J.S. Schwaber (1983) Somatostatinergic projections from the central nucleus of the amygdala to the vagal nuclei. Peptides 4: 1-6.

Hilton, S.M. (1966) Hypothalamic regulation of the cardiovascular system. Br Med Bull 22: 243-248.

Hilton, S.M., and A.W. Zbrozyna (1963) Amygdaloid region for defense reactions and its efferent pathway to the brain stem. J Physiol 165: 160-173.

Hodes, R., and H.W. Magoun (1942) Pupillary and other responses from stimulation of the frontal cortex and basal telencephalon of the cat. J Comp Neurol 76: 461-473.

Hoff, E.C., J.F. Kell, and M.N. Carr (1963) Effects of cortical stimulation and lesions on cardiovascular function. Physiol Rev 43: 68-114.

Hoffman, B.L., and T. Rasmussen (1953) Stimulation studies of insular cortex of Macaca mulatta. J Neurophysiol 16: 343-351.

Hopkins, D.A., and G. Holstege (1978) Amygdaloid projections to the mesencephalon, pons and medulla oblongata in the cat. Exp Brain Res 32: 529-547.

Irle, E., and H.J. Markowitsch (1984) Basal forebrain efferents reach the whole cerebral cortex of the rat. Brain Res Bull 12: 493-512.

Jackson, J.H. (1875) Clinical and physiological researches on the nervous system. I. On the anatomical and physiological localization of movements in the brain. London: Low, Churchill, p. 37 pp.

Jayaraman, A. (1985) Functional compartments in the cat striatum. Soc Neurosci Abst 11: 199.

Jones, B.E., and R.Y. Moore (1977) Ascending projections of the locus coeruleus in the rat. II. Autoradiographic study. Brain Res 127: 23-53.

Jones, E.G. (1975) Possible determinants of the degree of retrograde neuronal labeling with horseradish peroxidase. Brain Res 85: 249-253.

Jones, E.G., and R. Leavitt (1974) Retrograde axonal transport and the demonstration of non-specific to the cerebral cortex and striatum from thalamic intralaminar nuclei in the rat, cat and monkey. J Comp Neurol 154: 349-378.

Kaada, B.R. (1951) Somato-motor, autonomic and electrocorticographic responses to electrical stimulation of 'rhinencephalic' and other structures in primates, cat and dog. Acta Physiol Scand 24 S83: 1-285.

Kaada, B.R. (1960) Cingulate, posterior orbital, anterior insular and temporal pole cortex. In S.R. Geiger (ed): Handbook of Physiology.

Baltimore: Williams and Wilkins Co., pp. 1345-1372.

Kaada, B.R. (1972) Stimulation and regional ablation of the amygdaloid complex with reference to functional representation. In B.E. Eleftherion (ed): The Neurobiology of the Amygdala. New York: Plenum Press, pp. 205-281.

Kaada, B.R., and H. Jasper (1952) Respiratory responses to stimulation of temporal pole, insula, and hippocampal and limbic gyri in man. Arch Neurol Psychiat 68: 609-619.

Kaada, B.R., K.H. Pribram, and J.A. Epstein (1949) Respiratory vascular responses in monkeys from temporal pole, insula, orbital surface and cingulate gyrus. J Neurophysiol 12: 347-356.

Kabat, H., H.W. Magoun, and S.W. Ranson (1935) Electrical stimulation of points in the forebrain and midbrain. Arch Neurol Psychiat 34: 931-955.

Kalia, M. (1981a) Anatomical organization of central respiratory neurons. Ann Rev Physiol 43: 105-120.

Kalia, M. (1981b) Brain stem localization of vagal preganglionic neurons. J Autonomic Nervous Syst 3: 451-481.

Kalia, M., K. Fuxe, T. Hokfelt, O. Johansson, R. Lang, D. Ganten, C. Cuello, and L. Terenius (1984) Distribution of neuropeptide immunoreactive nerve terminals within the subnuclei of the nucleus of the tractus solitarius of the rat. J Comp Neurol 222: 409-444.

Kalia, M., and M. Kropilak (1982) Brain stem projections of sensory and motor innervation of the left atrium of the cat. Circulation 66: 291-311.

Kalia, M., and M.-.M. Mesulam (1980a) Brain stem projections of sensory and motor components of the vagus complex in the cat: I. The cervical vagus and nodose ganglion. J Comp Neurol 193: 435-465.

Kalia, M., and M.-.M. Mesulam (1980b) Brain stem projections of sensory and motor components of the vagus complex in the cat: II. Laryngeal, traheobronchial, pulmonary, cardiac, and

gastrointestinal branches. J Comp Neurol 193: 467-508.

Kalia, M., and J.M. Sullivan (1982) Brainstem projections of sensory and motor components of the vagus nerve in the rat. J Comp Neurol 211: 248-264.

Kalia, M., and R.V. Welles (1980) Brain stem projections of the aortic nerve in the cat: a study using tetramethyl benzidine as the substrate for horseradish peroxidase. Brain Res 188: 23-32.

Karplus, J.P., and A. Kreidl (1910) Gehirn und Sympathicus. III. Mitteilung. Sympathicusleitung im Gehirn und Halsmark. Pflugers Arch 143: 109-127.

Kelley, A.E., and L. Stinus (1984) The distribution of the projection from the parataenial nucleus of the thalamus to the nucleus accumbens in the rat: An autoradiographic study. Exp Brain Res 54: 499-512.

Kita, H., and Y. Oomura (1981) Reciprocal connections between the lateral hypothalamus and the frontal cortex in the rat: electrophysiological and anatomical observations. Brain Res 213: 1-16.

Kita, H., and Y. Oomura (1982b) An HRP study of the afferent connections to rat lateral hypothalamic region. Brain Res Bull 8: 63-71.

Kolb, B. (1984) Functions of the frontal cortex of the rat: A comparative review. Brain Res Rev 8: 65-98.

Kremer, W.F. (1947) Autonomic and somatic reactions induced by stimulation of the cingular gyrus in dogs. J Neurophysiol 10: 371-379.

Krettek, J.E., and J.L. Price (1977a) The cortical projections of the mediodorsal nucleus and adjacent thalamic nuclei in the rat. J Comp Neurol 171: 157-192.

Krettek, J.E., and J.L. Price (1977b) Projections from the amygdaloid complex to the cerebral cortex and thalamus in the rat and cat. J

Comp Neurol 172: 687-722.

Krettek, J.E., and J.L. Price (1977c) Projections from the amygdaloid complex and adjacent olfactory structures to the entorhinal cortex and to the subiculum in the rat and cat. J Comp Neurol 172: 723-752.

Krettek, J.E., and J.L. Price (1978a) Amygdaloid projections to subcortical structures within the basal forebrain and brainstem in the rat and cat. J Comp Neurol 178: 225-254.

Krettek, J.E., and J.L. Price (1978b) A description of the amygdaloid complex in the rat and cat with observations on intra-amygdaloid axonal connections. J Comp Neurol 178: 255-280.

Lamour, Y., P. Dutar, and A. Jobert (1982) Topographic organization of basal forebrain neurons projecting to the rat cerebral cortex. Neurosci Lett 34: 117-122.

Lamour, Y., P. Dutar, and A. Jobert (1984) Cortical projections of the nucleus of the diagonal band of Broca and of the substantia innominata in the rat: an anatomical study using the anterograde transport of a conjugate of wheat germ agglutinin and horseradish peroxidase. Neuroscience 12: 395-408.

LaVail, J.H., and M.M. LaVail (1972) Retrograde axonal transport in the central nervous system. Science 176: 1416-1418.

Leichnetz, G.R., R.F. Spencer, and D.J. Smith (1983) A retrograde study of prefrontal projections to the superior colliculus, paramedian pontine reticular formation and oculomotor complex demonstrates some overlap in areas of origin. Anat Rec 205: 111A.

Leonard, C.M. (1969) The prefrontal cortex of the rat. I. Cortical projection of the mediodorsal nucleus. II. Efferent connections. Brain Res 12: 321-343.

Lewis, V.A., and G.F. Gebhart (1977) Evaluation of the periaqueductal central gray (PAG) as a morphine-specific locus of action and examination of morphine-induced and stimulation induced analgesia at coincident PAG loci. Brain Res 124: 283-303.

Liberson, W.T., W.B. Scoville, and R.H. Dunsmore (1951) Stimulation studies of the prefrontal lobe and uncus in man. Electroenceph Clin Neurophys 3: 1-8.

Lind, R.W., L.W. Swanson, and P.E. Sawchenko (1985) Anatomical evidence that neural circuits related to the subfornical organ contain angiotensin II. Brain Res Bull 15: 79-82.

Lindvall, O., A. Bjorklund, R. Moore, and U. Stenevi (1974) Mesencephalic dopamine neurons projecting to neocortex. Brain Res 81: 325-331.

Livingston, R.B., W.P. Chapman, and K.E. Livingston (1948) Stimulation of orbital surface of man prior to frontal lobotomy. ResPubl Ass Res Nerv Ment 27: 421-437.

Llamas, A., C. Avendano, and F. Reinoso-Suarez (1977) Amygdaloid projections to prefrontal and motor cortex. Science 195: 794-796.

Loeschcke, H.H., J. de Lattre, M.E. Schlafke, and C.O. Trouth (1970) Effects on respiration and circulation of electrically stimulating the ventral surface of the medulla oblongata. Resp Physiol 10: 184-197.

Loewy, A.D. (1981) Descending pathways to sympathetic and parasympathetic preganglionic neurons. J Autonomic Nervous Syst 3: 265-275.

Loewy, A.D., and H. Burton (1978) Nuclei of the solitary tract: efferent projections to the lower brain stem and spinal cord of the cat. J Comp Neurol 181: 421-450.

Loewy, A.D., and S. McKellar (1981) Serotonergic projections from the ventral medulla to the intermediolateral cell column in the rat. Brain Res 211: 146-152.

Loewy, A.D., C.B. Saper, and R.P. Baker (1979) Descending projections from the pontine micturition center. Brain Res 172: 533-538.

Loewy, A.D., J.H. Wallach, and S. McKellar (1981) Efferent connections of the central medulla oblngata in the rat. Brain Res Rev 3: 63-80.

Lofving, B. (1961) Cardiovascular adjustments induced from the rostral cingulate gyrus. Acta Physiol Scand 53 S184: 1-82.

Loughlin, S.E., and J.H. Fallon (1984) Substantia nigra and ventral tegmental area projections to cortex: topography and collateralization. Neuroscience 11: 425-435.

Macchi, G., M. Bentivoglio, P. Rossini, and E. Tempesta (1978) The basolateral amygdaloid projections to the neocortex in the cat. Neurosci Lett 9: 347-351.

MacLean, P.D. (1949) Psychosomatic disease and the "visceral brain". Recent developments bearing on the Papez theory of emotion. Psychosom Med 11: 338-354.

MacLean, P.D. (1952) Some psychiatric implication of physiological studies on frontotemporal portions of limbic system (visceral brain). Electroenceph Clin Neurophys 4: 407-418.

Markowitsch, H.J., and W.O. Guldin (1983) Heterotopic interhemispheric cortical connections in the rat. Brain Res Bull 10: 805-810.

Markowitsch, H.J., E. Irle, R. Bang-Olsen, and P. Flindt-Egebak (1984) Claustral efferents to the cat's limbic cortex studied with retrograde and anterograde tracing techniques. Neuroscience 12: 409-425.

Merker, B. (1983) Silver staining of cell bodies by means of physical development. J Neurosci Methods 9: 235-241.

Mesulam, M.-.M. (1978) Tetramethyl benzidine for horseradish peroxidase neurohistochemistry: a non-carcinogenic blue reaction product with superior sensitivity for visualizing neural afferents and efferents. J Histochem Cytochem 26: 106-117.

Mesulam, M.-.M. (1982) Principles of horseradish peroxidase neurohistochemistry and their applications for tracing neural pathways - axonal transport, enzyme histochemistry and light microscopic analysis. In M.-.M. Mesulam (ed): Tracing Neural Connections with Horseradish Peroxidase. Chichester: John Wiley,

pp. 1-151.

Mesulam, M.-.M., and E.J. Mufson (1980) The rapid anterograde transport of horseradish peroxidase. Neuroscience 5: 1277-1286.

Mesulam, M.-.M., E.J. Mufson, A.I. Levey, and B.H. Wainer (1983) Cholinergic innervation of cortex by the basal forebrain: cytochemistry and cortical connections of the septal area, diagonal band nuclei, nucleus basalis (substantia innominata), and hypothalamus in the Rhesus monkey. J Comp Neurol 214: 170-197.

Milaihoff, G.A., C.B. McArdle, and C.E. Adams (1981) The cytoarchitecture, cytology, and synaptic organization of the basilar pontine nuclei in the rat. I. Nissl and Golgi studies. J Comp Neurol 195: 181-201.

Mitchell, R.A., H.H. Loeschcke, J.W. Severinghaus, B.W. Richardson, and W.H. Massion (1963) Regions of respiratory chemosensitivity on the surface of the medulla. Ann NY Acad Sci 109: 661-681.

Miura, M., and D.J. Reis (1969) Cerebellum: a pressor response elicited from the fastigial nucleus and its efferent pathway in brainstem. Brain Res 13: 595-599.

Miura, M., and D.J. Reis (1970) A blood pressure response from fastigial nucleus and its relay pathway in brainstem. Am J Physiol 219: 1330-1336.

Miura, M., and D.J. Reis (1972) The role of the solitary and paramedian reticular nuclei in mediating cardiovascular reflex responses from carotid baro- and chemoreceptors. J Physiol 223: 525-548.

Mogenson, G.J., and F.R. Calaresu (1973) Cardiovascular responses to electrical stimulation of the amygdala in the rat. Exp Neurol 39: 166-180.

Mogenson, G.J., D.L. Jones, and C.-.Y. Yim (1980) From motivation to action: functinal interface between the limbic system and motor system. Prog Neurobiol 14: 69-97.

Mraovitch, S., M. Kumada, and D.J. Reis (1982b) Role of the nucleus parabrachialis in cardiovascular regulation in cat. Brain Res 232: 57-75.

Mraovitch, S., D.A. Ruggiero, C.A. Ross, and D.J. Reis (1982a) Direct projections to autonomic centers of forebrain and brainstem from a cortical vasopressor area in rat. Soc Neurosci Abst 8: 77.

Nauta, W.J.H. (1972) The central visceromotor system: A general survey. In C.H. Hockman (ed): Limbic System Mechanisms and Autonomic Functions. Springfield: C.C. Thomas, pp. 21-33.

Neafsey, E.J. (1981) A simple method for glass insulating tungsten microelectrodes. Brain Res Bull 6: 95-96.

Neafsey, E.J., and K.M. Hurley (1984) Effects of stimulation of rat medial frontal infralimbic cortex on gastric motility. Soc Neurosci Abst 10: 831.

Neafsey, E.J., and C. Sievert (1982) A second forelimb motor area exists in rat frontal cortex. Brain Res 232: 151-156.

Newman, R., and S.S. Winans (1980a) An experimental study of the ventral striatum of the golden hamster. I. Neuronal connections of the nucleus accumbens. J Comp Neurol 191: 167-192.

Newman, R., and S.S. Winans (1980b) An experimental study of the ventral striatum of the golden hamster. II. Neuronal connections of the olfactory tubercle. J Comp Neurol 191: 193-212.

Nitecka, L., L. Amerski, and O. Narkiewicz (1981) Interamygdaloid connections in the rat studied by the horseradish peroxidase method. Neurosci Lett 26: 1-4.

Norgren, R. (1978) Projections from the nucleus of the solitary tract in the rat. Neuroscience 3: 207-218.

Norgren, R., and C.M. Leonard (1973) Ascending central gustatory connections. J Comp Neurol 150: 217-238.

Price, J.L. (1981) The efferent projections of the amygdaloid complex in the rat, cat and monkey. In Y. Ben-Ari (ed): The Amygdaloid Complex INSERM Symposium No. 20. New York: Elsevier, pp. 121-132.

Ranck, J.B. (1975) Which elements are excited in electrical stimulation of mammalian central nervous system: a review. Brain Res 98: 417-440.

Reep, R.L. (1983) Afferent connections of anterior cingulate cortex in the hamster, Mesocricetus auratus. Anat Rec 205: 158A.

Reep, R.L., J.V. Corwin, A. Hashimoto, and R.T. Watson (1984) Afferent connections of medial precentral cortex in the rat. Neurosci Lett 44: 247-252.

Reep, R.L., and S.S. Winans (1982a) Afferent connections of dorsal and ventral agranular insular cortex in the hamster, Mesocricetus auratus. Neuroscience 7: 1265-1288.

Reep, R.L., and S.S. Winans (1982b) Efferent connections of dorsal and ventral agranular insular cortex in the hamster, Mesocricetus auratus. Neuroscience 7: 2609-2635.

Reis, D.J., and M.C. Oliphant (1964) Bradycardia and tachycardia following electrical stimulation of the amygdala region. J Neurophysiol 27: 893-912.

Ricardo, J.A., and E.T. Koh (1978) Anatomical evidence of direct projections from the nucleus of the solitary tract to the hypothalamus, amygdala, and other forebrain structures in the rat. Brain Res 153: 1-26.

Rogers, R.C., H. Kita, L.L. Butcher, and D. Novin (1980) Afferent projections to the dorsal motor nucleus of the vagus. Brain Res Bull 5: 365-373.

Rose, J.E., and C.N. Woolsey (1948) Structure and relations of limbic cortex and anterior thalamic nuclei in rabbit and cat. J Comp Neurol 89: 279-347.

Norgren, R., and G. Wolf (1975) Projections of thalamic gustatory and lingual areas in the rat. Brain Res 92: 123-129.

Oldfield, B.J., and E.M. McLachlan (1981) An analysis of sympathetic preganglionic neurons projecting from the upper thoracic spinal roots of the cat. J Comp Neurol 196: 329-345.

Ottersen, O.P. (1981) The afferent connections of the amygdala of the rat as studied with retrograde transport of horseradish peroxidase. In Y. Ben-Ari (ed): The Amygdaloid Complex INSERM Symposium No. 20. New York: Elsevier, pp. 91-104.

Ottersen, O.P. (1982) Connections of the amygdala of the rat. IV. Corticoamygdaloid and intraamygdaloid connections as studied with axonal transport of horseradish peroxidase. J Comp Neurol 205: 30-48.

Ottersen, O.P., and Y. Ben-Ari (1979) Afferent connections to the amygdaloid complex of the rat and cat. I. Projections from the thalamus. J Comp Neurol 187: 401-424.

Papez, J.W. (1937) A proposed mechanism of emotion. Arch Neurol Psychiat 38: 725-743.

Paxinos, G., and C. Watson (1982) The Rat Brain in Stereotaxic Coordinates. New York: Academic Press Inc..

Phillipson, O.T. (1979c) Afferent projections to the ventral tegmental area of Tsai and interfascicular nucleus: a horseradish peroxidase study in the rat. J Comp Neurol 187: 117-144.

Pitts, R.F., M.G. Larrabee, and D.W. Bronk (1941) An analysis of hypothalamic cardiovascular control. Am J Physiol 134: 359-384.

Pool, J.L., and J. Ransohoff (1949) Autonomic effects on stimulating rostral portion of cingulate gyri in man. J Neurophysiol 12: 385-392.

Powell, T.P.S., and W.M. Cowan (1954) The connexions of the midline and intralaminar nuclei of the thalamus of the rat. J Anat 88: 307-319.

Rose, M. (1927) Gyrus limbicus anterior und regio retrosplenialis (Cortex holoprotoptychos quinquestratificatus). J Psychol Neurol (Leipzig) 35: 65-173.

Rosene, D.L., and M.-.M. Mesulam (1978) Fixation variables in horseradish peroxidase neurohistochemistry I. The effects of fixation time and perfusion procedures upon enzyme activity. J Histochem Cytochem 26: 28-39.

Ross, C.A., D.A. Ruggiero, and D.J. Reis (1981) Afferent projections to cardiovascular portions of the nucleus of the tractus solitarius in the rat. Brain Res 223: 402-408.

Royce, G.J. (1982) Laminar origin of cortical neurons which project upon the caudate nucleus: a horseradish peroxidase investigation in the cat. J Comp Neurol 205: 8-29.

Sachs, E., S.J. Brendler, and J.F. Fulton (1949) The orbital gyri. Brain 72: 227-240.

Saper, C.B. (1982a) Convergence of autonomic and limbic connections in the insular cortex of the rat. J Comp Neurol 210: 163-173.

Saper, C.B. (1982b) Reciprocal parabrachial-cortical connections in the rat. Brain Res 242: 33-40.

Saper, C.B. (1984) Organization of cerebral cortical afferent systems in the rat. II. Magnocellular basal nucleus. J Comp Neurol 222: 313-342.

Saper, C.B., and A.D. Loewy (1980) Efferent connections of the parabrachial nucleus in the rat. Brain Res 197: 291-317.

Saper, C.B., A.D. Loewy, L.W. Swanson, and W.M. Cowan (1976) Direct hypothalamo-autonomic connections. Brain Res 117: 305-312.

Sarter, M., and H.J. Markowitsch (1983) Convergence of basolateral amygdaloid and mediodorsal thalamic projections in different areas of the frontal cortex in the rat. Brain Res Bull 10: 607-622.

Sarter, M., and H.J. Markowitsch (1984) Collateral innervation of the medial and lateral prefrontal cortex by amygdaloid, thalamic, and brain-stem neurons. J Comp Neurol 224: 445-460.

Schafer, H. (1960) Central control of cardiac function. Physiol Rev 40 S4: 213-231.

Schiff, M. (1875) Untersuchungen uber die motorischen Functionen des Grosshirns. Arch exptl Path Pharmokol 3: 171-179.

Schlafke, M.E., W.R. See, and H.H. Loeschcke (1970) Ventilatory responses to alterations of H+ ion concentration in small areas of the ventral medullary surface. Resp Physiol 10: 198-212.

Schwaber, J.S., B.S. Kapp, and G. Higgins (1980) The origin and extent of direct amygdala projections to the region of the dorsal motor nucleus of the vagus and the nucleus of the solitary tract. Neurosci Lett 20: 15-20.

Schwaber, J.S., B.S. Kapp, G.A. Higgins, and P.R. Rapp (1982) Amygdaloid and basal forebrain direct connections with the nucleus of the solitary tract and the dorsal motor nucleus. J Neuroscience 2: 1424-1438.

Seifert, W. (1983) Neurobiology of the Hippocampus. New York: Academic Press.

Shapiro, R.E., and R.R. Miselis (1983) Orgainzation of gastric efferent and afferent projections within the dorsal medulla oblongata in rat. Anat Rec 205: 182A.

Shipley, M.T. (1982) Insular cortex projection to the nucleus of the solitary tract and brainstem visceromotor regions in the mouse. Brain Res Bull 8: 139-148.

Shipley, M.T., and Y. Geinisman (1984) Anatomical evidence for convergence of olfactory, gustatory, and visceral afferent pathways in mouse cerebral cortex. Brain Res Bull 12: 221-226.

Shipley, M.T., and M.S. Sanders (1982) Special senses are really special: evidence for a reciprocal, bilateral pathway between

insular cortex and nucleus parabrachialis. Brain Res Bull 8: 493-501.

Showers, M.J.C., and E.C. Crosby (1958) Somatic and visceral responses from the cingulate gyrus. Neurology 8: 561-565.

Simon, H., M. Le Moal, and A. Calas (1979) Efferents and afferents of the ventral tegmental-A10 region studied after local injection of [3H]leucine and horseradish peroxidase. Brain Res 178: 17-40.

Sinnamon, H.M., and B.S. Galer (1984) Head movements elicited by electrical stimulation of the anteromedial cortex of the rat. Physiol Behav 33: 185-190.

Smith, O.A., S.J. Jabbur, R.F. Rushmer, and E.P. Lasher (1960) Role of hypothalamic structures in the cardiac control. Physiol Rev 40 S4: 136-141.

Smith, W.K. (1938) The representation of respiratory movements in the cerebral cortex. J Neurophysiol 1: 55-68.

Smith, W.K. (1944) The results of stimulation of the uncus and adjacent portions of the hippocampal gyrus. Fed Proc 3: 43.

Smith, W.K. (1945) The functional significance of the rostral cingular cortex as revealed by its responses to electrical excitation. J Neurophysiol 8: 241-255.

Speakman, T.J., and B.P. Babkin (1949) Effect of cortical stimulation on respiratory rate. Am J Physiol 159: 239-246.

Spencer, W.G. (1895) The effect produced upon respiration by faradic excitation of the cerebrum in the monkey, dog, cat and rabbit. Phil Trans Roy Soc London, 185: 609-657.

Steindler, D.A. (1982) Differences in the labeling of axons of passage by wheat germ agglutinin after uptake by cut peripheral nerve versus injections within the central nervous system. Brain Res 250: 159-167.

Swanson, L.W. (1981) A direct projection from Ammon's horn to prefrontal cortex in the rat. Brain Res 217: 150-154.

Swanson, L.W. (1983) The hippocampus and the concept of the limbic system. In W. Seifert (ed): Neurobiology of the Hippocampus. New York: Academic Press, pp. 3-19.

Swanson, L.W., and W.M. Cowan (1977) An autoradiographic study of the organization of the efferent connections of the hippocampal formation in the rat. J Comp Neurol 172: 49-84.

Swenson, R.S., and A.J. Castro (1983) The afferent connections of the inferior olivary complex in rats: A study using the retrograde transport of horseradish peroxidase. Am J Anat 166: 329-341.

Terreberry, R.R., and E.J. Neafsey (1983) Rat medial frontal cortex: a visceral motor region with a direct projection to the solitary nucleus. Brain Res 278: 245-249.

Terreberry, R.R., and E.J. Neafsey (1984) The effects of medial prefrontal cortex stimulation on heart rate in the awake rat. Soc Neurosci Abst 10: 614.

Torvik, A. (1956) Afferent connections to the sensory trigeminal nuclei, the nucleus of the solitary tract, and adjacent structures. J Comp Neurol 106: 51-141.

Tower, S.S. (1936) Extrapyramidal action from the cat's cerebral cortex: Motor and inhibitory. Brain 59: 408-444.

Trojanowski, J.Q., J.o. Gonatas, and N.K. Gonatas (1981) Conjugates of horseradish peroxidase (HRP) with cholera toxin and wheat germ agglutinin are superior to free HRP as orthogradely transported markers. Brain Res 223: 381-385.

Tulloch, I.F., G.W. Arbuthnott, and A.K. Wright (1978) Topographical organization of the striatonigral pathway revealed by anterograde and retrograde neuroanatomical tracing techniques. J Anat 127: 425-441.

van der Kooy, D., L.Y. Koda, J.F. McGinty, C.R. Gerfen, and F.E. Bloom (1984) The organization of projections from the cortex, amygdala, and hypothalamus to the nucleus of the solitary tract in rat. J Comp Neurol 224: 1-24.

van der Kooy, D., J.F. McGinty, L.Y. Koda, C.R. Gerfen, and F.E. Bloom (1982) Visceral cortex: a direct connection from prefrontal cortex to the solitary nucleus in rat. Neurosci Lett 33: 123-127.

Vogt, B.A., and A. Peters (1981) Form and distribution of neurons in rat cingulate cortex: areas 32, 24, and 29. J Comp Neurol 195: 603-625.

von Euler, C., J.N. Hayward, I. Marttila, and R.J. Wyman (1973) Respiratory neurons of the ventrolateral nucleus of the solitary tract of the cat: Vagal input, spinal connections and morphological identification. Brain Res 61: 1-22.

von Euler, U.S., and B. Folkow (1958) The effect of stimulation of autonomic areas in the cerebral cortex upon the adrenaline and noradrenaline secretion from the adrenal gland in the cat. Acta Physiol Scand 42: 313-320.

Wall, P.D., and G.D. Davis (1951) Three cerebral cortical systems affecting autonomic functions. J Neurophysiol 14: 507-517.

Ward, A.A. (1948) The cingular gyrus: area 24. J Neurophysiol 11: 13-23.

West, C.H.K., and R.M. Benjamin (1983) Effects of stimulation of the mediodorsal nucleus and its projection cortex on heart rate in the rabbit. J Autonomic Nervous Syst 9: 547-557.

Wong-Riley, M.T.T. (1974) Demonstration of geniculocortical and callosal projection neurons in the squirrel monkey by means of retrograde axonal transport of horseradish peroxidase. Brain Res 79: 267-272.

Wree, A., K. Zilles, and A. Schleicher (1983) A quantitative approach to cytoarchitectonics. VIII. The areal pattern of the cortex of the albino mouse. Anat Embryol 166: 333-353.

Wyss, J.M., and R. Goldstein (1976) Lesion artifact in brain stimulation experiment. Physiol Behav 16: 387-389.

Wyss, J.M., and K. Sripanidkulchai (1983) The induseum griseum and anterior hippocampal continuation in the rat. J Comp Neurol 219: 251-272.

Wyss, J.M., and K. Sripanidkulchai (1984) The topography of the mesencephalic and pontine projections from the cingulate cortex of the rat. Brain Res 293: 1-15.

Yamamoto, T. (1984) Taste responses of cortical neurons. Prog Neurobiol 23: 273-315.

Yamamoto, T., R. Matsuo, and Y. Kawamura (1980) Localization of cortical gustatory area in rats and its role in taste discrimination. J Neurophysiol 44: 440-455.

Yasui, Y., K. Itoh, M. Takada, A. Mitani, T. Kaneko, and N. Mizuno (1985) Direct cortical projections to the parabrachial nucleus in the cat. J Comp Neurol 234: 77-86.

Young, W.S., G.F. Alheid, and L. Heimer (1984) The ventral pallidal projection to the mediodorsal thalamus: a study with fluorescent retrograde tracers and immunohistofluorescence. J Neuroscience 4: 1626-1638.

Zilles, K., B. Zilles, and A. Schleicher (1980) A quantitative approach to cytoarchitectonics. VI. The areal pattern of the cortex of the albino rat. Anat Embryol 159: 335-360.

APPROVAL SHEET

The dissertation submitted by Robert R. Terreberry has been read and approved by the following committee:

Dr. Edward J. Neafsey, Director
Associate Professor, Anatomy, Loyola

Dr. Thackery S. Gray
Assistant Professor, Anatomy, Loyola

Dr. Robert D. Wurster
Professor, Physiology, Loyola

Dr. C.C.C. O'Morchoe
Director, College of Medicine
Urbana-Champaign, Illinois

Dr. Rand S. Swenson
Professor, Anatomy
National College of Chiropractic
Lombard, Illinois

The final copies have been examined by the director of the dissertation and the signature which appears below verifies the fact that any necessary changes have been incorporated and the dissertation is now given final approval by the committee with reference to content and form.

The dissertation is therefore accepted in partial fulfillment of the requirements for the degree of Doctor of Philosophy.

Oct. 17, 1985
Date

E. J. Neafsey
Director's Signature